12-2018

Insights Into The Reactivation, Regulation And Essentiality Of Oxidative Protein Folding Pathways In Actinobacteria

Belkys Sanchez

INSIGHTS INTO THE REACTIVATION, REGULATION AND ESSENTIALITY OF OXIDATIVE PROTEIN FOLDING PATHWAYS IN ACTINOBACTERIA

by

Belkys Cecilia Sánchez Martinez, M.S.

APPROVED:

Hung Ton-That, Ph.D.
Advisory Professor

Barbara Murray, M.D.

Kevin Morano, Ph.D.

William Margolin, Ph.D.

Jeffrey Actor, Ph.D.

APPROVED:

Dean, The University of Texas
MD Anderson Cancer Center UTHealth Graduate School of Biomedical Sciences

INSIGHTS INTO THE REACTIVATION, REGULATION AND ESSENTIALITY OF OXIDATIVE PROTEIN FOLDING PATHWAYS IN ACTINOBACTERIA

A

DISSERTATION

Presented to the Faculty of

The University of Texas

MD Anderson Cancer Center UTHealth

Graduate School of Biomedical Sciences

in Partial Fulfillment

of the Requirements

for the Degree of

DOCTOR OF PHILOSOPHY

by

Belkys Cecilia Sánchez Martinez, M.S.

Houston Texas

December, 2018

DEDICATION

To Jordana

May my actions and achievements be an example of determination, show you that everything is possible and empower you to pursue your dreams.

ACKNOWLEDGEMENTS

I would like to thank my advisor Dr. Hung Ton-That for his guidance throughout my scientific development. I appreciate his support and encouragement to improve and reach my full potential. Under his supervision I developed determination and learned to be resilient and independent, which I know will help me to continue achieving my professional goals in the future. Additionally, I thank him for supporting my career goals and explorations of diverse aspects of science.

The guidance and advice of the members of my advisory committee Dr. Barbara Murray, Dr. Kevin Morano, Dr. William Margolin and Dr. Jeffrey Actor have been critical for my dissertation research and my development as a scientist. I will always be grateful for your encouragement. Special acknowledgments to Dr. Kevin Morano for your constant support and the many reference letters that you wrote for scholarship and award applications.

I would like to thank Dr. Julie Chang, who is the lab manager and heart of the Ton-That Lab. I deeply appreciate the mentorship and training she provided me since I arrived for my lab rotation. Her help over the years has also been important to my success. In addition, I appreciate the support during my laboratory endeavors provided by my excellent lab mates, Truc Luong, Chenggang Wu and Amar Al Mamun. Thank you for your technical expertise and helpful suggestions. I am especially grateful to have shared my bench with Sara Siegel. Thank you for always being open to talk about science and life, and all your assistance editing my written work.

I would like to thank the most important people in my world, my family. I am so blessed to have supporting parents, who have always encouraged me to pursue my dreams, and improve academically and personally. Mom and dad, I would not be here without your constant support and love. I will be forever grateful to have you as parents. Thank you to my brother Nestor, who makes me laugh when I need it the most. I appreciate the support of my aunt and uncle, Marielis and Wilmer for welcoming into their home when I first arrived to Houston. Finally, I would like to thank my husband Gregorio. It has definitely not been an easy road, but your constant support kept me going. Thank you understanding and supporting me during the ups and downs of my graduate career. I am so blessed to share my life with you. You have given me the most precious gifts in my life, our little doggies Bruno and Grace, and our daughter Jordana. I love you and the family we have built so much!

Last but not least, thank you God for providing me the strength to achieve this goal and always being on my side.

INSIGHTS INTO THE REACTIVATION, REGULATION AND ESSENTIALITY OF OXIDATIVE PROTEIN FOLDING PATHWAYS IN ACTINOBACTERIA

Belkys Cecilia Sánchez Martinez, M.S.

Advisory Professor: Hung Ton-That, Ph.D.

Accurate disulfide bond formation is important for proper folding, stability and function of exported proteins. The process of disulfide bond formation, termed oxidative protein folding, is catalyzed by thiol-disulfide oxidoreductase enzymes. Oxidative protein folding pathways influence processes essential for bacterial physiology and pathogenicity. In the Gram-positive actinobacterial pathogens *Actinomyces oris* and *Corynebacterium diphtheriae* oxidative protein folding is catalyzed by the primary thiol-disulfide oxidoreductase MdbA. MdbA is required for assembly of adhesive pilus, which mediate receptor-dependent bacterial interactions, or coaggregation, in *A. oris.* In the first part of this dissertation, I identify components of the electron transport chain (ETC) required for pilus assembly, by characterizing *A. oris* Tn5 transposon mutants defective in coaggregation. Analyses of non-polar deletion mutants of *nuo* genes, encoding the NADH-dehydrogenase subunits, and *ubiE*, a menaquinone C-methyltransferase encoding-gene, confirmed defects in reactivation of MdbA. Our findings indicate these ETC components are biochemically linked to pilus assembly via oxidative protein folding.

Because deletion of *mdbA* causes a temperature-sensitive growth and cell division defect in *C. diphtheriae,* it was postulated that additional oxidoreductase enzymes compensate for the loss of *mdbA* at the permissive temperature. The second part of this dissertation focuses on the characterization of an alternate oxidoreductase denominated TsdA. I found that Δ*mdbA* compensatory mutants overexpressing TsdA harbor a mutation that creates a sigma factor σ^A extended promoter thereby resulting in increased promoter strength. I determined that expression of this oxidoreductase is induced at 40°C, suggesting a novel role for an oxidoreductase in resistance to heat stress. Last, I investigated the requirement of MdbA for oxidative folding of cell division factors *in C. diphtheriae.* Penicillin binding proteins (PBPs) synthesize the bacterial cell wall and are key components of the cell division machinery. I demonstrated that overexpression of corynebacterial PBPs predicted to have disulfide bonds significantly rescues the morphology defects of the Δ*mdbA* strain. Furthermore, MdbA was found to be required for PBP stability and function. Overall this dissertation provides insights into novel aspects of the reactivation, regulation and requirement for growth of the oxidative protein folding pathways in the actinobacterial pathogens *A. oris* and *C. diphtheriae.*

TABLE OF CONTENTS

LIST OF ILLUSTRATIONS

LIST OF TABLES

CHAPTER 1. Introduction

1.1. Gram-positive Actinobacteria and their role in human health

The phylum *Actinobacteria* is constituted by Gram-positive bacteria with high (≥50%) content of guanine and cytosine (G+C) nucleotides in their chromosomal DNA. Thus, Actinobacteria are commonly referred to as the high G+C Gram-positives. The phylum *Actinobacteria* is large and complex and most of its constituents have irregular rod-shape morphology and aerobic or facultative metabolism. Most Actinobacteria are free-living microorganisms inhabiting the soil; nonetheless human, animal and plant pathogens are also classified within this group [1]. Important actinobacterial human pathogens include *Actinomyces* species, *Corynebacterium diphtheriae* and *Mycobacterium tuberculosis* [2].

The preferred habitat of *Actinomyces* species are mucosal surfaces including the human oral cavity [1, 2]. The essential contributions of *Actinomyces* species, including *Actinomyces oris* (formerly *A. naeslundii* genospecies 2*),* to formation of oral biofilm, caries and periodontal disease have been widely characterized [3-7]. In fact, *A. oris* is frequently found in dental plaque [8]. *Actinomyces* express hair-like surface structures called pili that interact with host and microbial molecules. Type I pili bind to salivary proline-rich proteins [9], and are important for early attachment of *Actinomyces* to the salivary pellicle on the tooth surface [4, 10]. Associations of *Actinomyces* with other bacterial species within the oral biofilm through coaggregation is mediated by type II pili [11-13]. Interactions mediated by *Actinomyces* pili are required for formation of a multi-species biofilm with a compact structure [14]. Accumulation of a multi-species biofilm on the enamel surface (i.e. dental plaque) is an essential step in the development of dental caries and periodontal

infections [2]. These oral diseases are highly prevalent worldwide and cause a significant public health and economic burden [15, 16].

C. diphtheriae is the causative agent of diphtheria in humans, a disease mediated by a toxin that results in formation of an inflammatory pseudomembrane in the upper respiratory tract and potentially death. *C. diphtheriae* is transmitted by direct contact, coughing or sneezing [17]. Once *C. diphtheriae* enters the host, initial adhesion to the upper respiratory tract epithelium is mediated by covalently linked SpaA-type pili on the bacterial surface [18]. *C. diphtheriae* SpaA-type pili are key virulence factors constituted by SpaA, SpaB and SpaC pilin subunits [19]. SpaA is the main shaft pilin, while SpaB and SpaC are minor pilin subunits that mediate binding to human pharyngeal cells [19-21]. Another key virulence factor of *C. diphtheriae* is the potent diphtheriae toxin, encoded by the prophage corynephage beta which is integrated into the chromosome of *C. diphtheriae* toxigenic strains [22]. Diphtheriae toxin is an AB toxin, constituted by the catalytic domain A and the receptor-binding domain B [23]. The B domain binds to the heparin-binding EGF-like growth factor (HB-EGF) on human epithelial cells and facilitates toxin internalization into the cell by receptor-mediated endocytosis [24]. Once in the cytoplasm, the catalytically active domain A inhibits protein synthesis by ADPribosylating translation elongation factor 2 (EF-2) which results in cell death [24, 25]. Furthermore, diphtheria toxin can enter the systemic circulation damaging distant organs such as the heart and the central nervous system [17]. *C. diphtheriae* infections have decreased dramatically worldwide after widespread use of Diphtheria-toxoid based immunization established in 1974. However, outbreaks of respiratory diphtheria continue to emerge

in countries with poor vaccination coverage where a mortality rate exceeding 10% has been reported (www.who.int). Importantly, *C. diphtheriae* can also cause cutaneous infections [17], and an increased emergence in invasive infections such as endocarditis and osteomyelitis caused by non-toxigenic *C. diphtheriae* has been observed in the past years [26].

1.2. Oxidative protein folding pathways in bacteria

Disulfide bonds are covalent linkages between two thiol groups of cysteine (Cys) residues, and are important for function of many proteins by contributing to the structural stability of their active conformations [27]. Disulfide bond formation is an oxidative process, thus is commonly referred to as oxidative protein folding [28]. Due to the importance of disulfide bonds for protein activity, eukaryotic and prokaryotic cells encode specialized machineries that efficiently catalyze disulfide bond formation [27]. Eukaryotic cells catalyze disulfide bond formation in the oxidizing environment of the endoplasmic reticulum [29-31]. Similarly, disulfide bond formation in prokaryotes rarely occurs in the cytoplasm but localizes to the oxidizing cell envelope where proteins with disulfide bonds can be integrated into the cell envelope or secreted outside of the cell [32, 33].

In Gram-negative bacteria the Dsb thioredoxin-like enzymes mediate folding of proteins emerging from the SecYEG secretory machinery into the periplasm [34]. Dsb proteins catalyze oxidation reactions that result in native disulfide bonds, as well as reduction reactions to correct misformed disulfide bonds [35]. The periplasmic protein DsbA is the major thiol-disulfide oxidoreductase enzyme in Gram-negative bacteria

[36], and catalyzes disulfide bond formation by donating a reactive disulfide bond within its catalytic CysXXCys (CxxC) motif through a thiol-disulfide exchange reaction [37]. The disulfide bond formation reaction removes electrons from consecutive pairs of cysteines in unfolded substrates, leading to formation of a covalent bond between the sulfur atoms of the cysteine residues [34, 38]. This process generates a reduced and inactive DsbA. The membrane protein DsbB catalyzes the reoxidation of DsbA to restore the active state after disulfide bond formation [32, 39]. DsbB achieves this by transferring electrons produced from the DsbA reoxidation reaction to ubiquinone under aerobic conditions and menaquinone under anaerobic conditions [40-43]. These co-factors can then transfer electrons to final acceptors maintaining the disulfide bond-forming machinery in an active state [44, 45]. Because DsbA catalyzes disulfide bond formation in unfolded polypeptides as they emerge from the secretory SecYEG machinery, incorrect disulfide bonds can form in proteins that have more than two cysteines and include nonconsecutive disulfide bonds [34]. The isomerization pathway, constituted by DsbC, DsbG and DsbD in *Escherichia coli,* corrects non-native disulfide bonds [46]. DsbC is a periplasmic thioredoxin-like homodimer with thiol-disulfide bond isomerase/reductase activity that promotes rearrangement of non-native disulfide bonds [47]. In contrast to DsbA, DsbC is active in its reduced form and is maintained in the reduced state by its redox partner DsbD [38, 48].

Gram-positive bacteria differ in that Firmicutes generally avoid exporting disulfide bond-containing proteins (70% of their secretome is devoid of cysteine residues), while Actinobacteria favor export of proteins that have even numbers of cysteine

residues and likely form disulfide bonds [49]. Gram-positive Firmicutes express enzymes implicated in oxidative folding of specific substrates and are often encoded within an operon with genes encoding these substrates [50, 51]. On the other hand, Gram positive Actinobacteria including *Actinomyces, Corynebacterium* and *Mycobacterium* encode disulfide bond forming machineries with broad substrate specificity and their deletion results in growth defects [52-54].

The oxidative protein folding machinery in the Gram-positive Actinobacteria *A. oris, C. diphtheriae* and *Corynebacterium matruchotii* includes homologs of the thiol-disulfide oxidoreductase MdbA (Monoderm disulfide bond-forming) [52, 55, 56]. Actinobacterial MdbAs are transmembrane proteins with little sequence similarity to *E. coli* DsbA, but present characteristic features of DsbA family proteins including a thioredoxin-like fold, an extended α-helical domain, and a CxxC motif in the active site [52, 56-58]. In contrast to the prototypical *E. coli* DsbA, which is a periplasmic enzyme, MdbA is predicted to have a transmembrane domain and is detected in membrane fractions in cell fractionation experiments [55]. Similarly, the *M. tuberculosis* oxidoreductase Mt-DsbA is also predicted to be anchored in the cell membrane [59].

Reoxidation of *A. oris* MdbA is mediated by VKOR, a homolog of human vitamin K epoxide reductase, which does not share sequence homology with *E. coli* DsbB [55, 60]. VKOR is a transmembrane protein with 5 membrane-spanning domains and two extra-cytoplasmic pairs of cysteine residues that mediate MdbA reoxidation [60]. The 4 cysteine residues located at the exoplasmic loops of VKOR form redox-reactive disulfide bonds implicated in electron shuffling from MdbA to VKOR, which is

necessary for reactivation of reduced MdbA after oxidative protein folding [60]. An *A. oris* Δ*vkor* mutant accumulates reduced MdbA that can be detected by alkylation of reduced cysteine residues of the CxxC motif with Mal-PEG, which results in a mobility shift of MdbA [55]. It is proposed that electrons resulting from the MdbA reoxidation reaction are transferred to components of the electron transport chain which is shown in **Chapter 3** of this dissertation to be required for reoxidation of *A. oris* MdbA. A VKOR homolog is also proposed to mediate reoxidation of *M. tuberculosis* Mt-DsbA because these enzymes are encoded in an operon and VKOR-derived peptides interact with Mt-DsbA *in vitro* [59]. However, the role of *M. tuberculosis* VKOR in disulfide bond formation has not been explored *in vivo.* On the other hand, the *C. diphtheriae* MdbA redox partner has not been yet identified.

1.3. Roles of oxidative protein folding in bacterial physiology

Disulfide bond containing proteins have diverse functions in bacteria. Consequently, thiol-disulfide oxidoreductases play a role in many important cellular processes such as cell division, energy generation, transport of molecules, adaptation to environmental conditions, assembly of surface structures and pathogenesis. Further details on the role of oxidative protein folding pathways in bacterial processes relevant to this dissertation are described below.

1.3.1. Cell viability

Disulfide bond formation and isomerization are not essential for growth in Gram-negative bacteria, since both *dsbA* and *dsbC* deletion mutants are viable [36, 61]. Furthermore, a triple mutant lacking the main oxidoreductase DsbA and the disulfide isomerases DsbC and DsbG is also viable [61]. This strongly suggests that oxidoreductase pathways are dispensable for folding of essential growth factors in *E. coli*. Nonetheless, it has been observed that growth of *E. coli* disulfide mutants is affected under certain conditions. For example, cells lacking DbsA show a slow growth phenotype in nutrient-restricted minimal media [62], and cannot grow in anaerobic conditions [63]. In contrast, oxidative protein folding is essential for growth in the Actinobacteria *Actinomyces* and *Corynebacterium* [52, 55]. Deletion mutants of *mdbA* have not been obtained in *A. oris* or *C. matruchotii* despite many attempts, however a conditional *mdbA* deletion mutant is viable in *A. oris* [52, 55]. *C. diphtheriae* cells lacking *mdbA* have a temperature-sensitive phenotype and show a strong growth and cell division defect when incubated at the non-permissive temperature [56]. It is thought that Mt-DsbA and VKOR are also essential in *M. tuberculosis*, however these conjectures are based on growth phenotypes observed in transposon-insertion mutants of these genes and disruption of VKOR activity by the inhibitor warfarin [53, 54]. The study of non-polar in-frame *dsbA* and *vkor* deletion mutants of *M. tuberculosis* is warranted to accurately define the essentiality of oxidative protein folding pathways in this important human pathogen. Thus far the essentiality of oxidative protein folding pathways in Actinobacteria is not completely understood. In

chapter 5 of this dissertation, I characterize the role of MdbA in oxidative folding of cell division factors in *C. diphtheriae.*

1.3.2. Resistance to environmental stress

Adaptation of bacteria to modifications of their environment are essential for cell survival. Disulfide isomerase enzymes have been demonstrated to be involved in resistance to oxidative stress exerted by DTT, H_2O_2 and copper [64-66]. Consequently, it has been shown that mutants of DsbC-family enzymes are more sensitive to killing in the presence of DTT, H_2O_2 and copper compared to wild-type strains [64-66]. Interestingly, the disulfide isomerase DsbD, involved in cytochrome biogenesis, is also required for bacterial growth above 42°C [48].

1.3.3. Pathogenicity

The importance of disulfide bond forming pathways in bacterial pathogenicity has been extensively described across Gram-negative bacteria and has been recently studied by our group in Gram-positive Actinobacteria. Gram-negative pathogens including multiple pathogenic *E. coli* strains, *Salmonella enterica*, *Shigella flexneri, Yersinia pestis, Vibrio cholerae, Pseudomona aeruginosa and Bordetella pertussis* secrete virulence factors that contain disulfide bonds, and mutations in disulfide bond forming enzymes frequently result in attenuation of virulence in infection models [28]. Similarly, Gram-positive pathogens such as *Bacillus anthracis* and *C. diphtheriae* require disulfide bond forming pathways to cause disease [50, 67]. It is thought that the stability conferred by disulfide bonds is important for resistance

of secreted virulence factors to proteases and harsh environmental conditions within the host [68]. Disulfide bonds are required for correct folding of adherence factors, motility proteins, secretion machineries and toxins involved in different stages of infection [65].

Adhesive pili are essential for bacterial adhesion, initial colonization and establishment of disease. Correct folding of pilin subunits by DsbA contributes to adherent phenotypes of the Gram-negative uropathogens *Proteus mirabilis* and Uropathogenic *E. coli* (UPEC) [28]. In the Actinobacterium *A. oris,* MdbA is required for assembly og type I and type II pilus that mediate bacterial interactions with host proteins and biofilm formation, respectively [55]. Similarly, the SpaA shaft pilin subunit of *C. diphtheriae* contains a C-terminal disulfide bond essential for protein stability and pilus biogenesis [56]. SpaA-type pilus is a virulence factor that mediates adhesion to the respiratory epithelium [21], and mutants devoid of pili are highly attenuated for virulence in a guinea pig model of diphtheria [56].

After successful colonization, bacterial propagation and survival depends on manipulation of the host. This is in many cases achieved by host killing mediated by bacterial toxins. The prototypic AB toxin, diphtheria toxin, contains two disulfide bonds; the N-terminal disulfide bond covalently links the catalytic domain A and the receptor-binding domain B [69]. Disruption of this disulfide bridge by the reducing environment of the cytoplasm is important for cytotoxic activity [69]. Thus, a *C. diphtheriae* mutant lacking the major oxidoreductase MdbA, which is deficient in toxin production, is highly attenuated for virulence [56]. In Gram-negative bacteria, DsbA is required for folding and activity of clinically important AB toxins including cholera

toxin of *V. cholerae* and heat-labile enterotoxin of enterotoxigenic *E. coli* [65]. Even though some known virulence factors in Gram-positive Firmicutes contain disulfide bonds, oxidoreductases are not generally important for virulence in this bacterial group [50]. One exception is *B. anthracis;* nonetheless effects of the disulfide bond forming pathways in virulence of this pathogen seem to be indirect. *B. anthracis* mutants lacking the thiol-disulfide oxidoreductase CcdA overexpress the master virulence regulator AtxA, resulting in increased production of anthrax toxin [70].

1.4. Insights into the regulation of oxidative protein folding in bacteria

Little is known about the regulation of oxidative protein folding pathways in bacteria. Reports available suggest that factors influencing the regulation of disulfide bond forming enzymes differ depending on their physiological role. It has been shown that activation of the Cpx two-component system in *E. coli* induces a 5- to 10-fold increase in DsbA transcription and synthesis [71]. The Cpx-envelope stress response system is comprised of the membrane-bound CpxA sensor kinase, the cytosolic CpxR response regulator and the periplasmic inhibitor CpxP [72]. It is proposed that regulation of *dsbA* by the Cpx system is mediated by direct binding of the phosphorylated response regulator CpxR upstream of the *dsbA* transcriptional start site [71]. Regulation of *dsbA* by the Cpx system seems logical, as the Cpx system responds to misfolded proteins in the cell envelop and is constitutively activated by disruption of the disulfide isomerization pathways [72, 73]. Cell envelope stress caused by pH changes and metal ions, which induces the Cpx system, is commonly encountered by bacterial pathogens during infection [72, 74].

Nutrient limitation encountered by pathogens within the host [74], has also been shown to affect expression of oxidoreductases [75, 76]. In *Campylobacter jenuni*, the *dsb* genes are organized in two different operons that are regulated by iron availability. Expression of the oxidoreductases DsbA1 and DsbA2 is downregulated in iron-restricted conditions in a ferric uptake regulator (Fur)-dependent manner [75]. It was suggested that proteins involved in iron metabolism are substrates of the Dsb system, and regulation of the oxidative folding pathways can control their abundance in different environmental conditions [75]. Since Fur contributes to the regulation of pathogenicity in many bacteria [77, 78], these results also emphasize the importance of oxidative protein folding pathways in virulence of *C. jejuni.* Regulation of DsbA by nutrient limitation was also observed in adherent-invasive *E. coli* [76]. DsbA expression was upregulated in bacterial cells growing in acidic and nutrient-limited media mimicking environmental conditions encountered within the phagocytic vacuole of macrophages [76].

Oxidoreductase enzymes have also been found to be differentially expressed in some bacterial species that alternate between different life cycle stages. The Dsb system is upregulated in stationary and cyst phases of the intracellular pathogen *Legionella pneumophila.* Increased expression of DsbA2 is explained by the requirement of disulfide bond formation for proper folding of the Dot/Icm type IVb secretion system (T4SS) which is involved in virulence of the cyst-like form [79]. Similarly, expression of the thiol-disulfide oxidoreductase StoA is required for activity of the sporulation-specific penicillin binding protein SpoVD, which mediates biosynthesis of the cortex peptidoglycan layer during endospore formation in *Bacillus*

subtilis [80-82]. StoA transcription is governed by the developmental sigma factors σ^E and σ^G, which control gene expression in the mother cell and the forespore during the sporulation process [83, 84]. The studies described in **Chapter 4** of this dissertation deepen our understanding of the regulation of oxidative folding pathways as I investigate a novel mechanism regulating expression of an alternate thiol-disulfide oxidoreductase in *C. diphtheriae.*

1.5. Significance of these studies

The studies described in this dissertation expand our understanding of diverse aspects of the oxidative protein folding pathways in Actinobacteria, which are essential for activity of proteins involved in many important cellular processes. In the first part of this dissertation, I investigate the link between the oxidative protein folding machinery and the electron transport chain, as well as the requirement of the latter for reoxidation of MdbA in *A. oris*.

In contrast to Gram-positive Firmicutes and Gram-negative bacteria, the disulfide bond forming machinery is essential for growth in Actinobacteria. In the second part of this dissertation, I studied the regulation of an alternate oxidoreductase that seems to be required for viability of *C. diphtheriae* in the absence of MdbA. Finally, in chapter 5 I investigate MdbA substrates involved in cell division, which provides further insights into the requirement of this machinery for bacterial growth.

The β-lactam antibiotic penicillin is the drug of choice to treat *C. diphtheriae* infections. However, *C. diphtheriae* resistance to penicillin and other antibiotics has been reported in many countries [85]. Another clinically important Actinobacterium, multi-drug resistant *M. tuberculosis*, is a major public health issue world-wide [86].

Development of new antimicrobial strategies or enhancement of currently used antibiotics is crucial for treatment of multi-drug resistant pathogens. Knowledge provided by this dissertation is valuable to develop antimicrobials that can inhibit the disulfide bond forming pathways and thus disrupt virulence and cell growth. Since the oxidative protein folding machinery is conserved in Actinobacteria, studies in *Actinomyces* and *Corynebacterium* have direct contributions to the understanding of disulfide bond formation in other actinobacterial pathogens that are difficult to genetically manipulate and grow like *M. tuberculosis.*

CHAPTER 2. Materials and Methods.

This chapter is based in part upon work published in the journal mBio entitled "Electron Transport Chain Is Biochemically Linked to Pilus Assembly Required for Polymicrobial Interactions and Biofilm Formation in the Gram-Positive Actinobacterium Actinomyces oris". mBio. ***2017****: 8: e00399-17. Belkys C. Sánchez is co-first author of this publication (****Belkys C. Sanchez****, Chungyu Chang, Chenggang Wu, Bryan Tran, Hung Ton-That) and was responsible for preparing the original manuscript and conducted the majority of experiments described. Copyright of all material published in mBio remains with the authors.*

For additional information about ASM's permission policies associated with commercial reuse of mBio content, see http://mbio.asm.org/site/misc/reprints.xhtml

2.1. Bacterial strains, plasmids, media, and cell growth

The bacterial strains and plasmids used in this study are listed in Table 2.1. *A. oris* cells were grown in heart infusion broth (HIB) or on heart infusion agar (HIA) plates at 37°C with 5% CO_2. *Streptococcus oralis* cells were grown in HIB containing 1% glucose in a Coy anaerobic chamber. *C. diphtheriae* were grown in HIB or HIA plates at 30ºC or 37ºC. *E. coli* DH5α, BL-21 and S17-1 used for molecular cloning, recombinant protein expression and gene deletions, respectively, were grown in Luria Broth (LB) at 37ºC. When required, kanamycin or ampicillin was added to the bacterial cultures at a final concentration of 35, 50 or 100 μg mL^{-1}. Polyclonal antibodies were raised against Pbp1A and Pbp1B by Cocalico Biologicals using recombinant proteins provided by our laboratory. Diphtheria toxin A antibody (7F2) was purchased from Invitrogen. Reagents were purchased from Sigma unless indicated otherwise.

2.2. Construction of recombinant plasmids

Recombinant vectors using pCWU10. The *nuo* promoter and the *nuoA* coding sequence were PCR-amplified with *A. oris* MG1 genomic DNA as a template using the primers Pnuo-F-KpnI/PnuoA-R and nuoA-F/nuoA-R-HindIII (Table 2.2), respectively, and Phusion DNA polymerase (New England Biolabs; NEB). Overlapping PCR was employed to fuse the two sequences accordingly [87]. The fused fragment was cloned into the pCW10 vector [87], and the generated plasmid was electroporated into an *A. oris nuoA* deletion strain. Similarly, an *ubiE*

complementing plasmid was generated and electroporated into an *ubiE* deletion strain (Table 2.1).

pP^{tsdA}-GFP and pP^{T2G}-GFP. The *tsdA* promoter was PCR-amplified with *C. diphtheriae* NCTC13129 genomic DNA or Δ*mdbA*-S1 genomic DNA as a template using the primers PtsdA-HindIII-F and PtsdA-GFP-R (Table 2.2) and Phusion DNA polymerase (NEB). Similarly, the GFP coding sequence was PCR-amplified with pBsk-GFP (Addgene) [88] plasmid DNA as a template using the primers GFP-F and GFP-BamHI-R (Table 2.2). Overlapping PCR was employed to fuse the two sequences. The fused fragment was cloned into the pCGL0243 vector [89], and the generated plasmid was electroporated into *C. diphtheriae* Δ*tsdA.*

Recombinant vectors using pMCSG7. To generate recombinant, His-tagged Pbp1A, Pbp1B and TsdA-C129S proteins, primers (Table 2.2) were designed to amplify the extracellular-coding regions of each *C. diphtheriae* protein. The PCR products were cloned into pMCSG7 using ligation-independent cloning [90]. The resulting plasmids were transformed in *E. coli* DH5α and then introduced into *E. coli* BL21 (DE3) for protein expression.

2.3. Gene deletion in *A. oris*

All *A. oris* nonpolar, in-frame deletion mutants were generated using a *galK* counter-selection method described previously [91]. In this method, 1-Kb fragments up- and downstream of a targeted gene were amplified using appropriate primers (Table 2.2) and fused using overlapping PCR. The 2-Kb fragment was then cloned into the integrative plasmid pCWU2 (Table 2.1), and the resulting plasmid was

electroporated into the *A. oris* strain CW1, which lacks the *galK* gene [92]. Co-integrants resulting from a single cross-over event were selected on kanamycin-containing HIA plates. Loss of the recombinant plasmid by a second cross-over event resulting in wild-type and mutant alleles was selected using media containing 0.2% 2-deoxygalactose (2-DG). Generated mutants were identified by PCR. For double mutants, such as Δ*nuoAJ* and Δ*nuoAG*, single mutants were used as a starting strain.

2.4. Gene deletions in *C. diphtheriae*

C. diphtheriae in-frame deletion mutants were generated using a SacB counter-selection protocol previously described [19]. Briefly, 1-Kb fragments up- and downstream of a targeted gene were amplified using appropriate primers (Table 2.2) and fused using overlapping PCR. The 2-Kb fragment was then cloned into the integrative plasmid pK19mobsacB (Table 2.1) expressing *kanamycin* resistance and *sacB* genes [93]. The resulting plasmid was introduced into *E. coli* S17-1 for conjugation with *C. diphtheriae*. Co-integrates resulting from a single cross-over event were selected for growth on kanamycin (50 μg mL^{-1}) and nalidixic Acid (35 μg mL^{-1}) plates. Loss of the recombinant plasmid by a second cross-over event resulting in wild-type and mutant alleles were selected for growth on HI agar plates containing 10% sucrose. Deletion mutants were identified by PCR.

2.5. Identification of *A. oris* coaggregation-defective mutants by Tn*5* transposon mutagenesis

Following a published protocol [91], a library of approximately 6,200 kanamycin-resistant Tn*5* mutants was generated from the parental MG1 strain. This

library was used to screen for *A. oris* mutants defective in coaggregation with *S. oralis* using a cell-based screen in 96-well plates as previously reported [55]. Coaggregation was ranked from 1 to 4, largely based on the scoring system described by Cisar and colleagues [94], with the coaggregation phenotypes of *A. oris* MG1 and *S. oralis* So34 considered as 4 and the Δ*fimA* mutant and *S. oralis* So34 as 1; the coaggregation scores 2 and 3 were designated for small and larger clumps of aggregates, respectively.

Consequently, 33 coaggregation-defective mutants were obtained, and TAIL-PCR was employed to map Tn5 insertion sites in these mutants, detailed in our published procedures [91, 92]. In brief, two sequential PCR reactions were performed; the first reaction started with a colony of Tn5 mutants suspended in reaction buffer containing primers Tn5-1 and AD-1 (Table 2.2) and Apex™ Taq DNA Polymerase (Genesee Scientific). The product of this PCR reaction was used for the next one with primers Tn5-2 (Table 2.2) and AD-1. Finally, the obtained product of this reaction was gel-purified and submitted for DNA sequencing using the primer Tn5-3 (Table 2.2). The resulting DNA sequences were blasted against the MG1 genome, http://www.homd.org/, to identify the Tn5 insertion sites.

2.6. Electron microscopy

Immunogold labeling of *A. oris* cells was performed as previously described with some modifications [95]. Cells were washed once and suspended in 0.1 M NaCl. Seven microliters of bacterial cell suspensions were placed on carbon-coated nickel grids and then samples were washed with PBS containing 1% BSA (PBS/1% BSA), followed by blocking with 0.1% gelatin in PBS/1% BSA. Adhered cells were stained

with primary antibodies diluted in PBS-1% BSA (1:100 for α-FimA; 1:50, α-CafA; and 1:1,000, α-Type 1), followed by staining with IgG antibodies conjugated to 18-nm gold particles (Jackson Immunoresearch Laboratories). Finally, samples were washed with water, stained with 1% uranyl acetate, and analyzed using a JEOL JEM-1400 electron microscope. Electron microscopy analysis of *C. diphtheriae* cells was performed following a similar procedure. The results are representative of three independent experiments that the reported phenotypes were observed at least 95% in the fields of view.

2.7. Coaggregation assays

Coaggregation assays were performed as previously described with some modifications [95, 96]. Briefly, stationary phase cultures of *A. oris* and *S. oralis* 34 strains were harvested by centrifugation and suspended in TBS buffer (200 mM Tris-HCl, pH 7.4, 150 mM NaCl, 0.1 mM $CaCl_2$). Equivalent cell numbers of *A. oris* and *S. oralis* strains, based on OD_{600}, were mixed for a few minutes, and bacterial aggregates were imaged using an AlphaImager.

2.8. Biofilm assays

In vitro biofilm formation assays were performed according to a published protocol [87]. Briefly, overnight *A. oris* cell cultures were used to inoculate fresh cultures (1:100 dilution) in 1.5 mL of HIB containing 1% sucrose and kanamycin in 24-well plates. After incubation in a CO_2 incubator at 37°C for 48 hours, the biofilms were gently washed with PBS and dried before staining with 1% crystal violet. After washing the unbound dye, the stained biofilms were subject to ethanol treatment

before quantified by absorbance measurement at 580 nm by a Tecan M1000 microplate reader.

2.9. Cell growth assays

Cell growth of *A. oris* strains was monitored by a plate assay and optical density (OD_{600}) in HIB cultures as previously described [87]. For the plate assay, the MG1 strain and the Δ*ubiE* mutant were streaked as a broad band on HIA plates. A 3-ml drop of 50 mM MK-4 in ethanol was placed on the border of the streaks. Cell growth at 37°C was recorded after 2 days. For growth in HIB, overnight cultures were used to inoculate fresh cultures in HIB supplemented with 35 μg ml^{-1} of kanamycin with starting OD_{600} of 0.1. OD_{600} was taken every hour, and the OD values were presented as averages of three independent experiments performed in duplicate. Calculation of generation time was performed using the formulas $k = \frac{logN\text{t-}logN0}{0.301t}$ and $g = \frac{1}{k}$, where N_0 and N_t is OD_{600} values at times 0 and t, respectively, where *t* is the time elapsed between N_t and N_0 recordings. *K* corresponds to growth rate and *g* corresponds to generation time expressed in hours [97]. Generation times were determined from at least two independent experiments performed in triplicate. Note, the MG1, Δ*nuoA*, and Δ*ubiE* strains contain an empty vector conferring kanamycin resistance.

2.10. Determination of the MdbA redox status by alkylation with Mal-PEG

Mid-logarithmic cultures of *A. oris* were harvested and suspended in SMM buffer (0.5M sucrose, 10mM MgCl2, 10mM maleate, pH 6.8). Bacterial cell suspensions were treated with mutanolysin at 37°C for 2 hours. Protoplasts were

collected by centrifugation at 1,500 x g for 10 min, suspended in alkylation buffer (100mM Tris-HCl pH 6.8, 1% SDS, 1X protease inhibitor) plus 10% TCA, and lysed by mechanical disruption using a micro-tube homogenizer (BeadBug) with 0.1 mm glass beads (MP Biomedical). The resulting cell lysates were incubated in ice for 30 minutes prior to acetone-wash and air-drying. For alkylation, obtained protein samples were suspended in alkylation buffer containing 10 mM Mal-PEG and incubated at 37°C for 1 h, followed by TCA precipitation and acetone-wash. All protein samples were suspended SDS-sample buffer, separated by SDS-PAGE, and immunoblotted with α-MdbA (1:2,000 dilution).

2.11. Whole cell ELISA

This experiment was performed according to a published protocol with some modifications [98]. Overnight cultures of *A. oris* strains were harvested and suspended in carbonate-bicarbonate buffer (15mM sodium carbonate, 35mM sodium bicarbonate, pH 9.6). Bacterial cells of different strains in equal numbers were used to coat high binding 96-well polystyrene plates, which were incubated for 1 h at 37^0C. Plates were washed with PBS containing 0.05% Tween 20 (PBS-T), and blocked with 2% BSA in PBS-T for 1 h at 25^0C. After removing blocking solution, plates were incubated for 2 hours at 25^0C, with α-CafA (1:5,000) diluted in 1% BSA in PBS-T. Next, plates were washed with PBS-T, and incubated for 1 h at 25^0C with secondary antibody conjugated to HRP (1:20,000) diluted in 1% BSA in PBS-T, followed by the 3,3',5,5' tetramethylbenzidine (TMB). The reaction was quenched by addition of 1M H_2SO_4, and the absorbance at 450 nm was measured using a plate reader (Tecan Infinite M1000).

2.12. Site-directed mutagenesis of pMCSG7-TsdA-C129S

To generate the C-to-S mutation at position 129 of TsdA, inverse PCR was utilized using the pMCGS7-TsdA plasmid as template (Table 2.1). Adjacent divergent primers (Table 2.2) with mutation sites designed into the 5′-end were 5' phosphorylated and used for PCR amplification of the plasmid template with Phusion DNA polymerase (NEB). The resulting linear plasmid was purified, ligated and transformed into *E. coli* DH5α. The C-to-S mutation was confirmed by DNA sequencing. Plasmids with the desired mutation were transformed into *E. coli* BL21 (DE3).

2.13. 5' Rapid Amplification of cDNA Ends (RACE) PCR

Identification of the *tsdA* transcriptional start site was performed using the Invitrogen 5' RACE system for rapid amplification of cDNA ends. Briefly, first strand cDNA was PCR amplified using total wild-type and Δ*mdbA*-S1 mRNA, primer GSP1-tsdA (Table 2.2) that anneals at the 3' end of *tsdA* mRNA, and SuperScript™ II RT. Generated cDNA was purified with an S.N.A.P. column provided by the manufacturer. Subsequently, a homopolymeric tail was added to the cDNA 3' end using dCTP and Terminal deoxynucleotidyl transferase (TdT). dC-tailed cDNA was PCR amplified using *Taq* DNA polymerase (Fisher Scientific), GSP2-tsdA primer and abridged anchor primer (AAP) provided by the manufacturer. This PCR product was diluted (0.1%) and used in a nested PCR reaction using GSP3-tsdA primer and Abridged Universal Amplification Primer (AUAP) provided by the manufacturer, to enrich for specific PCR products. The obtained 5' RACE PCR products were characterized by Sanger sequencing to identify the specific *tsdA* transcriptional start site.

2.14. Quantitative real-time PCR (qRT PCR)

Log-phase cultures of *C. diphtheriae* were normalized to an OD_{600} of 1.0, two volumes of RNA Protect® Bacteria Reagent (Qiagen) were added and cells were incubated at room temperature for five minutes. Then cells were collected by centrifugation, washed once with PBS, re-suspended in RLT buffer (RNeasy Mini Kit, Qiagen) containing β-marcaptoethanol (BME) and lysed by mechanical disruption with 0.1-mm silica spheres (MP Bio) in a ribolyser (Hybaid). Total RNA from cell lysates was extracted using the RNAeasy Mini Kit (Qiagen). Purified total RNA was treated with DNAse I to digest remaining DNA. After the enzymatic reaction, RNA was cleaned using the RNeasy MinElute Cleanup Kit (Qiagen). cDNA was synthesized with SuperScript™ II RT First-Strand Synthesis System (Invitrogen). For qRT-PCRs cDNA was mixed with iTAQ SYBR green supermix (Bio-Rad), along with appropriate primer sets (Table 2.2). Cycle threshold ($\mathbf{C_T}$) values were determined, and the 16S rRNA gene was used as a control to calculate relative mRNA expression level by the $2^{-\Delta\Delta}\mathbf{CT}$ method [99].

2.15. Cell fractionation and western blotting

Cells were grown to mid-log phase, normalized to an OD_{600} of 1.0, and separated into medium (M) and cell fractions by centrifugation. The cell fraction was washed and re-suspended in hydrolase buffer (0.5M sucrose, 10mM $MgCl_2$, phosphate buffered saline (PBS) pH 7.4), and then incubated with cell wall hydrolase enzymes at 37°C for 3 hours. After treatment, the soluble cell wall fraction (W) was separated from the protoplasts by centrifugation. The M and W fractions were TCA precipitated and acetone washed. Protein samples were re-suspended in SDS-

loading buffer and separated on Tris-glycine gels. Proteins were detected with rabbit antisera diluted in 5% milk (1.5:1,000 α-Pbp1A, 1.5:1,000 α-Pbp1B, 1:1,000 α-DT, 1:5,000 α-TsdA) followed by horseradish peroxidase (HRP) (1:10,000) conjugated goat anti-rabbit IgG for detection by chemiluminescence.

2.16. Protein Purification

E. coli cells harboring plasmid for *C. diphtheriae* C129S mutant TsdA protein expression were cultured in LB medium supplemented with ampicillin (100 μg mL^{-1}) at 37°C. When the optical density at 600 nm reached 0.8, cultures were transferred to 4°C for 1 hour. Isopropyl β-D-1-thiogalactopyranoside (IPTG) was added to a final concentration of 0.5 mM for overnight induction at 18°C. Cells were harvested by centrifugation, disrupted by sonication, and the insoluble cellular material was removed by centrifugation. TsdA C129S protein was purified from other contaminating proteins using Ni-NTA (Qiagen) affinity chromatography with the addition of 5 mM β-mercaptoethanol in all buffers. The protein was digested with 0.15 mg TEV protease per 20 mg of purified protein for 16 h at 4°C, and then passed through a Ni-NTA column to remove both the TEV protease and cleaved N-terminal tags. The final step of purification was gel-filtration on HiLoad 16/60 Superdex 200pg column (GE Healthcare) in 10 mM HEPES buffer pH 7.5, 200 mM NaCl and 1 mM DTT. The protein was concentrated on Amicon Ultracel 10K centrifugal filters (Millipore) up to 60 mg/ml concentration.

2.17. Protein crystallization

The initial crystallization condition was determined with a sparse crystallization matrix at 4°C and 16°C temperatures using the sitting-drop vapor-diffusion technique

using MCSG crystallization suite (Microlytic), Pi-minimal and Pi-PEG screen [100] (Jena Bioscience). The first crystals grew in numerous conditions after two days. The best crystals were obtained from F2 conditions of Pi-PEG screen (6.4% PEG 200, 21.4% PEG 2000, 50 mM acetate buffer pH 5.2) at 4°C temperature. Crystals selected for data collection were briefly soaked in crystallization buffer with addition of 20% ethylene glycol as cryo-protectant and then flash-cooled in liquid nitrogen.

2.18. X-ray crystallography data collection, structure determination and refinement

Single-wavelength X-ray diffraction data were collected at a temperature of 100°K using the 19-ID beamline of the Structural Biology Center [101] at the Advanced Photon Source at Argonne National Laboratory employing the program SBCcollect. The intensities were integrated and scaled with the HKL3000 suite [102]. The TsdA C129S protein structure was determined by molecular replacement using HKL3000 suite [102] incorporating MOLREP program [103]. The structure of selenomethionine derivative of the wild-type protein (unpublished results) was used as the starting model. Several rounds of manual adjustments of structure models using COOT [104] and refinements with Refmac program [105] from CCP4 suite [106] were performed. The stereochemistry of the structure was validated with PHENIX suite [107] incorporating MOLPROBITY [108] tools. The secondary structure assignment was generated by DSSP program[109] incorporated in ESPRIPT [110] server.

2.19. Fluorescence quantification

Overnight cultures of *C. diphtheriae* were diluted and grown at 37°C until reaching mid-log phase, at this point a subset of bacterial cultures were shifted to 40°C for 30 minutes. Cells were collected by centrifugation, washed with PBS and normalized to OD_{600}: 0.5 in PBS. Cell suspension aliquots were dispensed into 96-well, high-binding, clear F-Bottom (Chimney well), black microplates (Greiner bio-one). Fluorescence was measured using excitation/emission wavelengths 485nm/507nm with a Tecan M1000 plate reader. Purified GFP was used as gain reference and the fluorescence of the wild-type strain carrying no plasmid was used as background fluorescent signal.

2.20. Fluorescence microscopy

Overnight cultures of *C. diphtheriae* were diluted and grown at 37°C until reaching mid-log phase, at this point a subset of bacterial cultures were shifted to 40°C for 30 minutes. Cells were then placed on a 2μL agarose (1.5%) pad on 15-well multitest slides (MP Biomedicals, LLC). DIC and fluorescence images at excitation/emission wavelengths 504nm/510nm were obtained on an Olympus IX81-ZDC inverted microscope using Slidebook imaging software. Image analysis was completed using ImageJ.

2.21. Statistical analysis

Statistical analysis in this study was performed using GraphPad Prism 5 (La Jolla, CA), with significant differences determined by One-way ANOVA (biofilm assays), unpaired *t* test with Welch's correction, or the pair, two-tailed *t* test (growth curves, generation time, ELISA, qRT-PCR and fluorescence quantification). The

results are presented as the average values from at least two independent experiments performed in triplicate ± standard deviations (SD).

Table 2.1. Strains and Plasmids used in this study

Strains & Plasmids	Description	Reference
A. oris strains		
MG1	Parental strain	[96]
CW1	*ΔgalK*; an isogenic derivative of MG1	[96]
AR4	*ΔfimA*; an isogenic derivative of CW1	[96]
AR5	*ΔcafA*; an isogenic derivative of CW1	[111]
JCYC1	*ΔnuoA*; an isogenic derivative of CW1	[112]
JCYC2	*ΔnuoB*; an isogenic derivative of CW1	[112]
BCS3	*ΔnuoG*; an isogenic derivative of CW1	[112]
JCYC3	*ΔnuoJ*; an isogenic derivative of CW1	[112]
JCYC5	*ΔnuoAG*; an isogenic derivative of CW1	[112]
JCYC6	*ΔnuoAJ*; an isogenic derivative of CW1	[112]
BCS2	*ΔnuoBJ*; an isogenic derivative of CW1	[112]
BCS10	*ΔubiE*; an isogenic derivative of CW1	[112]
BCS4	JCYC1 containing pNuoA	[112]
BCS13	JCYC1 containing pMdbA	[112]

BCS11	BCS10 containing pUbiE	[112]
BCS14	BCS10 containing pMdbA	[112]
S. oralis strains		
S. oralis So34	RPS-positive	[113]
C. diphtheriae strains		
NCTC13129	Parental Strain (wild-type)	[19]
NJ2	*ΔmdbA*; an isogenic derivative of NCTC13129	[56]
NJ6	NJ2 containing pMdbA	[56]
NJ7	NJ2 containing pMdbA-C94A	[56]
MR119	NJ1 suppressor 1 (S1)	[114]
MR122	*ΔtsdA*; an isogenic derivative of NCTC13129	[114]
AHG146	Δ*dtxR;* an isogenic derivative of NCTC13129	[115]
BCS15	Δ*sigH;* an isogenic derivative of NCTC13129	This study
BCS16	BCS1 containing pSigH	This study
BCS17	MR122 containing pP^{tsdA}-GFP	This study
BCS18	MR122 containing p$P^{tsdA\text{-}T2G}$-GFP	This study
BCS19	Δ*pbp1A;* an isogenic derivative of NCTC13129	This study
BCS20	Δ*pbp1B;* an isogenic derivative of NCTC13129	This study

BCS21	NJ2 containing pPbp1A	This study
BCS22	NJ2 containing pPbp1B	This study
BCS23	NJ2 containing pPbp1A-1B	This study
BCS24	NJ2 containing pPbp1A-1B-2A	This study
E. coli strains		
BCS25	BL21 containing pMCSG7-TsdA-C129S	This study
BCS26	BL21 containing pMCSG7-Pbp1A	This study
BCS27	BL21 containing pMCSG7-Pbp1B	This study
Plasmids		
pCWU2	Integrative plasmid expressing the galactokinase *galK* gene under the control of the *rpsJ* promoter	[96]
pCWU2-NuoA	pCWU2 allelic replacement of *nuoA*	[112]
pCWU2-NuoB	pCWU2 allelic replacement of *nuoB*	[112]
pCWU2-NuoG	pCWU2 allelic replacement of *nuoG*	[112]
pCWU2-NuoJ	pCWU2 allelic replacement of *nuoJ*	[112]
pCWU2-UbiE	pCWU2 allelic replacement of *ubiE*	[112]
pCWU10	*E. coli*/*A. oris* shuttle vector; kanamycin resistant	[87]
pNuoA	pCWU10 expressing *A. oris* wild-type *nuoA*	[112]

pUbiE	pCWU10 expressing *A. oris* wild-type *ubiE*	[112]
pJRD215	*E. coli*/*Actinomyces* shuttle vector; kanamycin and streptomycin resistant	[116]
pMdbA	pJRD215 expressing *A. oris* wild-type *mdbA*	[55]
pCGL0243	*Corynebacterium/E. coli* shuttle vector; kanamycin resistant	[89]
pK19MobsacB	*Corynebacterium* integration plasmid; kanamycin resistant	[93]
pMCSG7	Ligation-independent cloning for protein expression; ampicillin resistant	[90]
pMCSG7-TsdA	For expression of recombinant *C. diphtheriae* TsdA	[114]
pMCSG7-TsdA-C129S	For expression of recombinant *C. diphtheriae* TsdA harboring C129S mutation	This study
pK19mobsacB-SigH	pK19mobsacB allelic replacement of *sigH*	This study
pBsk-GFP	GFP expressing plasmid (Addgene plasmid #29459)	[88]
pP^{tsdA}-GFP	pCGL0243 expressing GFP from *C. diphtheriae* wild-type *tsdA* promoter	This study
p$P^{tsdA\text{-}T2G}$-GFP	pCGL0243 expressing GFP from T2G *tsdA* mutant promoter	This study
pSigH	pCGL0243 expressing *C. diphtheriae* wild-type *sigmaH*	This study
pMCSG7-Pbp1A	For expression of recombinant *C. diphtheriae* Pbp1A	This study
pMCSG7-Pbp1B	For expression of recombinant *C. diphtheriae* Pbp1B	This study
pPbp1A	pCGL0243 expressing *C. diphtheriae* wild-type *pbp1A*	This study
pPbp1B	pCGL0243 expressing *C. diphtheriae* wild-type *pbp1B*	This study
pPbp1A-1B	pCGL0243 expressing *C. diphtheriae* wild-type *pbp1A* and *pbp1B*	This study

pPbp1A-1B-2A	pCGL0243 expressing *C. diphtheriae* wild-type *pbp1A, pbp1B and pbp12A*	This study

Table 2.2. Primers used in this study

Primer	Sequence[(a)]	Application
Ana1624-A-KpnI	AAAAAGGTACCGTTGAGGAGCATCTCGGGGC	*nuoA* deletion
Ana1624-B	CCCATCCACTAAACTTAAACAGACTGAAGCCGCTCTGACCG	*nuoA* deletion
Ana1624-C	TGTTTAAGTTTAGTGGATGGGGGGGTTCATGCTTCCGGCAC	*nuoA* deletion
Ana1624-D-HindIII	AAAAAAGCTTCCCAGGCCACCGCCATCGAC	*nuoA* deletion
Ana1623-A- KpnI	AAAAAGGTACCCGTGGGTCAGGCTCATGAGCTGG	*nuoB* deletion
Ana1623-B	CCCATCCACTAAACTTAAACAGTCGAGGCCGCCGCGCTGTC	*nuoB* deletion
Ana1623-C	TGTTTAAGTTTAGTGGATGGGGGCGTTGTGCTTCTTCATGCTCTTCAC	*nuoB* deletion
Ana1623-D-HindIII	AAAAAAGCTTGCGCAAGCGCCTCATGAAGC	*nuoB* deletion
Ana1615-A-KpnI	AAAAAGGTACCGTTCCTCGGCGGGCAGGCCC	*nuoJ* deletion
Ana1615-B	CCCATCCACTAAACTTAAACAGTCTCCCCATCACCGTCTACCTC	*nuoJ* deletion
Ana1615-C	TGTTTAAGTTTAGTGGATGGGCAGCAGGGTGCTCATCGCAG	*nuoJ* deletion
Ana1615-D-HindIII	AAAAAAGCTTTGATGCCCCGCTACCATGGTC	*nuoJ* deletion
Ana1618-A-KpnI	AAAAAGGTACCAGTGCGTGGACCAGCCGCCCAGG	*nuoG* deletion
Ana1618-B	CCCATCCACTAAACTTAAACACTCCCAGGTCACCGTGACCCATGCAGCGG	*nuoG* deletion
Ana1618-C	TGTTTAAGTTTAGTGGATGGGCCGCGGGTGCGGAGCTCTTGGTGG	*nuoG* deletion

Ana1618-D-HindIII	AAAAAAGCTTCGGCGGCATCCGTCCCGGCC	*nuoG* deletion
Ana1626- A-HindIII	CGCAAGCTTCGGGCCGAGACACCTCCG	*ubiE* deletion
Ana1626-B	GGGCACGGGCCGCGTGGCAATCCCGGCCGCGGTCAC	*ubiE* deletion
Ana1626-C	GTGACCGCGGCCGGGATTGCCACGCGGCCCGTGCCC	*ubiE* deletion
Ana1626-D-HindIII	CGCAAGCTTCGTACCGGCCAGCACCC	*ubiE* deletion
pUbiE-F-HindIII	CGCAAGCTTGCCAGCCGGTGGTGTCCA	*ubiE* complementation
pUbiE-R-EcoRI	CGCGAATTCAGGTGATCGCGCCCAGCG	*ubiE* complementation
Pnuo-F-KpnI	AAAAAGGTACCTAGGACACAGGTCCCGTCCGAC	*nuoA* complementation
PnuoA-R	CCATCCTTGTCAGGAGCTGGTCGGGCTTCCCTCCTCGG	*nuoA* complementation
nuoA-F	CCAGCTCCTGACAAGGATGGTGC	*nuoA* complementation
nuoA-R-HindIII	AAAAAAAGCTTGGCTTCAGTCCCAGTCCAGTCCG	*nuoA* complementation
Tn5-1	CGAACTGTTCGCCAGGCTCAAG	TAIL-PCR
Tn5-2	CTGACCGCTTCCTCGTGCTTTA	TAIL-PCR
Tn5-3	GCCTTCTTGACGAGTTCTTCTGAGCG	Sequencing
AD-1	SWGAXAWGAA[b]	TAIL-PCR
GSP1-tsdA	GTTAGACCAGCGGGCACAGAA	5’ RACE
GSP2-tsdA	GGGGCACTCGAAGTCAGAGAA	5’ RACE
GSP3-tsdA	TTCCGTAATCACCAGCGGTGC	5’ RACE

RTPCR-*tsdA*-F	TAGCGGTAAGGCGGGTTCG	RT-PCR
RTPCR-*tsdA*-R	GATCTTTCGCGTTACGACGGTG	RT-PCR
TsdA-C129S-F	AGCGCCCGCTGGTCTAACCAGACCGAG	Site-directed mutagenesis
TsdA-C129S-R	GAAGGGGCACTCGAAGTCAGAGAATTC	Site-directed mutagenesis
PtsdA-HindIII-F	AAAAAAAGCTTCGTAGAAAACTCGGTAAGTAAGCC	pP^{tsdA}-GFP reporter
PtsdA-GFP-R	CGCTGACTTCTGCATGAAGTACATATGTCTAAAGGTGAAGAACTGTTC	pP^{tsdA}-GFP reporter
GFP-F	ATGTCTAAAGGTGAAGAACTGTTC	pP^{tsdA}-GFP reporter
GFP-BamHI-R	AAAAAGGATCCCTATTTGTAGAGCTCATCCATGCC	pP^{tsdA}-GFP reporter
sigH-A-HindIII	AAAAAAAGCTTGAGCCAGCACGTTGGGGA	*sigH* deletion
sigH-B-R	GTCGCTTGTTTTCGTAGCCAC	*sigH* deletion
sigH-C-F	GTCGCTTGTTTTCGTAGCCACCCGGCTACATTGCGGGAAAA	*sigH* deletion
sigH-D-BamHI	AAAAAGGATCCCCGTTTGTCGCGATGAAGATC	*sigH* deletion
PsigH-HindIII-F	AAAAAAAGCTTCGCCGCCTTTTTTAGGCT	*sigH* complementation
PsigH-BamHI-R	AAAAAGGATCCGGAAAAGATCCCTTAAGCCAC	*sigH* complementation
LIC-Pbp1A-F	TACTTCCAATCCAATGCAGGCGTGGCCGTCGACCGT	Recombinant Pbp1A
LIC-Pbp1A-R	TTATCCACTTCCAATGttaTCCATTGGGTAGTCCCTGTGG	Recombinant Pbp1A
LIC-Pbp1B-F	TACTTCCAATCCAATGCACCTAGCGAGCTGGTGACCAAA	Recombinant Pbp1B

LIC-Pbp1B-R	TTATCCACTTCCAATGttaGTGATACCGC CACGAAGTTGG	Recombinant Pbp1B
pbp1A-A-HindIII-F	aaaaaAAGCTTCGCCTGCTCAGCGGTAA C	*pbp1A* deletion
pbp1A-B-R	GCTAAGGACTGCCCGTGG	*pbp1A* deletion
pbp1A-C-F	CCACGGGCAGTCCTTAGCGCACGAACA GCCGTGGAT	*pbp1A* deletion
Pbp1A-D-EcoRI-F	aaaaaGAATTCCGACTGGGGGTGCGTTT T	*pbp1A* deletion
pbp1B-A-HindIII-F	aaaaaAAGCTTTCAGGCAATGTGGCGAA C	*pbp1B* deletion
pbp1B-B-R	GCTTCCTTGATCTGCGGT	*pbp1B* deletion
pbp1B-C-F	ACCGCAGATCAAGGAAGCCCTGATTCT TACAGGGGGCAC	*pbp1B* deletion
Pbp1B-D-EcoRI-R	aaaaaGAATTCGCGGCCACAACTTAAAC G	*pbp1B* deletion
Ppbp1A-MluI-R	aaaaaACGCGTCTCCCCCTGCTGAGTAT	*pbp1A* complementation
Ppbp1B-1A-overlap-R	TATCCACGGCTGTTCGTG	*pbp1A-1B* complementation
Ppbp1A-MluI-R	aaaaaACGCGTTATCCACGGCTGTTCGT G	*pbp1A* complementation
Ppbp1A-1B-overlap-F	CACGAACAGCCGTGGATAACCTGCTGA ATTCGGTGA	*pbp1A-1B* complementation
Ppbp1B-MluI-F	aaaaaACGCGTACCTGCTGAATTCGGTG A	*pbp1B* complementation
Ppbp1B-MluI-R	aaaaaACGCGTGCCCCCTGTAAGAATCA G	*pbp1B* complementation
pbp2A-1A-1B-overlap-F	GCCCCCTGTAAGAATCAGATCGAAGAA GCCGTTCGA	*pbp1A-1B-2A* complementation
Ppbp2a-MluI-R	aaaaaACGCGTGGTGGGATGTCCAGGTT T	*pbp1A-1B-2A* complementation

RTPCR-Pbp1A-F	ACCCCGACGCGGTGATGG	RT-PCR
RTPCR-Pbp1A-R	GCTGGTCGGTGCTCAAGCCTT	RT-PCR
RTPCR-Pbp1B-F	GCTATCTTGGGCCAGCTCACC	RT-PCR
RTPCR-Pbp1B-R	CCGTAGGCATTGCGGCCG	RT-PCR

[a]Underlined are restriction site sequences.

[b]X(A/G/C/T), S(G/C), and W(A/T).

CHAPTER 3. Electron Transport Chain Is Biochemically Linked to Pilus Assembly Required for Polymicrobial Interactions and Biofilm Formation in the Gram- Positive Actinobacterium *Actinomyces oris*

This chapter is based upon work published in the journal mBio entitled "Electron Transport Chain Is Biochemically Linked to Pilus Assembly Required for Polymicrobial Interactions and Biofilm Formation in the Gram- Positive Actinobacterium Actinomyces oris". mBio. ***2017****: 8: e00399-17. Belkys C. Sánchez is co-first author of this publication (****Belkys C. Sanchez****, Chungyu Chang, Chenggang Wu, Bryan Tran, Hung Ton-That) and was responsible for preparing the original manuscript and conducted the majority of experiments described. Copyright of all material published in mBio remains with the authors.*

For additional information about ASM's permission policies associated with commercial reuse of mBio content, see http://mbio.asm.org/site/misc/reprints.xhtml

3.1. INTRODUCTION

Found only in Gram-positive bacteria, such as *Actinomyces* spp., *Corynebacterium diphtheriae*, *Bacillus cereus*, streptococci and enterococci, covalently-linked pili, also termed fimbriae, are important virulence determinants [20, 117]. These adhesive pilus structures are assembled and linked to bacterial peptidoglycan by conserved transpeptidase enzymes collectively named sortase [118]. Initially reported in *C. diphtheriae* [19, 20], sortase enzymes that polymerize pilin subunits into covalently-linked pilus polymers are often called pilus-specific sortases, or class C sortases [118, 119]. Generally, the housekeeping sortase and non-polymerizing sortase enzymes anchor pilus polymers to the bacterial cell wall [120-124] via a process similar to cell wall anchoring of surface proteins by the archetype SrtA of *Staphylococcus aureus* [125, 126].

Pili were discovered in many species of *Actinomyces* in the 1970s [127, 128], and early pilus characterizations focused on the fimbriae of *Actinomyces naeslundii* genospecies 2 [129], which was later renamed *Actinomyces oris* [130]. In the biofilm-forming actinobacterium *A*. *oris*, two types of fimbriae have been identified. Type 1 fimbriae – consisting of the pilus shaft FimP and the tip pilin FimQ [116] – mediate bacterial binding to salivary proline-rich proteins on the tooth surface [9]. SrtC1, the pilus-specific sortase encoded by the type 1 fimbrial gene locus, specifically catalyzes pilus polymerization of FimP and FimQ [113, 116]. Type 2 fimbriae, with SrtC2 as their pilus-specific sortase [96, 113], are made of the pilus shaft FimA and the canonical tip pilin FimB [96].

Biofilm formation and *Actinomyces* interactions with oral streptococci in biofilm, termed coaggregation [129], are well-documented phenotypes associated with the type 2 fimbriae since a *fimA* mutant fails to mediate biofilm formation and bacterial coaggregation [12, 96]. Nonetheless, it has recently been discovered that a coaggregation factor named CafA hijacks the sortase SrtC2 machine, forming a distinct pilus tip with the pilus shaft FimA independent of FimB [111]. It is now clear that CafA is the major coaggregation factor of *A. oris* as deletion of *cafA* results in the same coaggregation defect as *fimA* deletion; additionally, a specific antibody against recombinant CafA or addition of this protein blocks bacterial coaggregation [111]. Thus, the coaggregation defect of the *fimA* mutant can be attributed to the loss of CafA pilus assembly on the bacterial cell wall, while the role of FimB in oral colonization and biofilm formation remains unknown.

Consistent with the above, in a previous small-scale Tn5 transposon screen intended to identify *A. oris* mutants that fail to aggregate with *Streptococcus oralis*, we found 3 mutants with Tn5 insertions in *fimA* and *srtC2*; the fourth mutant was mapped to *vkor*, which encodes a bacterial vitamin K epoxide reductase (VKOR) [55]. Importantly, an in-frame, nonpolar *vkor* deletion mutant was shown to be severely defective in pilus assembly. Further characterizations established that VKOR is required for reoxidation of the thiol-disulfide oxidoreductase MdbA [55]. It is noteworthy that a *Mycobacterium tuberculosis* homolog of *A. oris* VKOR was initially shown to replace DsbB in reoxidation of the disulfide bond forming oxidoreductase DsbA when expressed in *Escherichia coli* [131]. Unlike *E. coli dsbA*, *mdbA* is an

essential gene and a conditional *mdbA* deletion mutant failed to assemble adhesive pili [55].

It was shown that MdbA and VKOR together form the thiol-disulfide oxidoreductase pair that catalyzes oxidative protein folding in *A. oris* [132]. Thus, based on available evidence centered on the type 2 fimbriae, a model of pilus assembly in *A. oris* has been proposed [55, 111] (Figure 3.1). Synthesized in the cytoplasm, pilin precursors, such as FimA, FimB, and CafA, are transported across the cytoplasmic membrane by the Sec translocon in an unfolded state. The thiol-disulfide oxidoreductase MdbA catalyzes oxidative folding of nascent pilin precursors before they are embedded into the membrane. Membrane-bound pilin precursors are polymerized by the pilus-specific sortase SrtC2, resulting in formation of type 2 fimbriae with two distinct tip pilins, FimB and CafA. The resulting polymers are presumably anchored by the housekeeping sortase SrtA. While it is clear in this model that the sortase and oxidative folding machines are central elements of pilus assembly in *A. oris*, it is unknown if there are additional factors directly or indirectly involved in the pilus assembly process.

Because *A. oris* coaggregation and pilus assembly are tightly associated, we exploited this property in a high-throughput assay to screen more than 6,200 Tn5 transposon mutants for clones that are variably defective in coaggregation with *S. oralis* So34, an indicator strain expressing pilus receptor cell-surface polysaccharides (RPS) [12, 96, 133]. Using a modified-visual coaggregation scoring system, we were able to identify auxiliary factors contributing to pilus assembly that might have been missed in the previously reported small-scale screen, which was solely based on

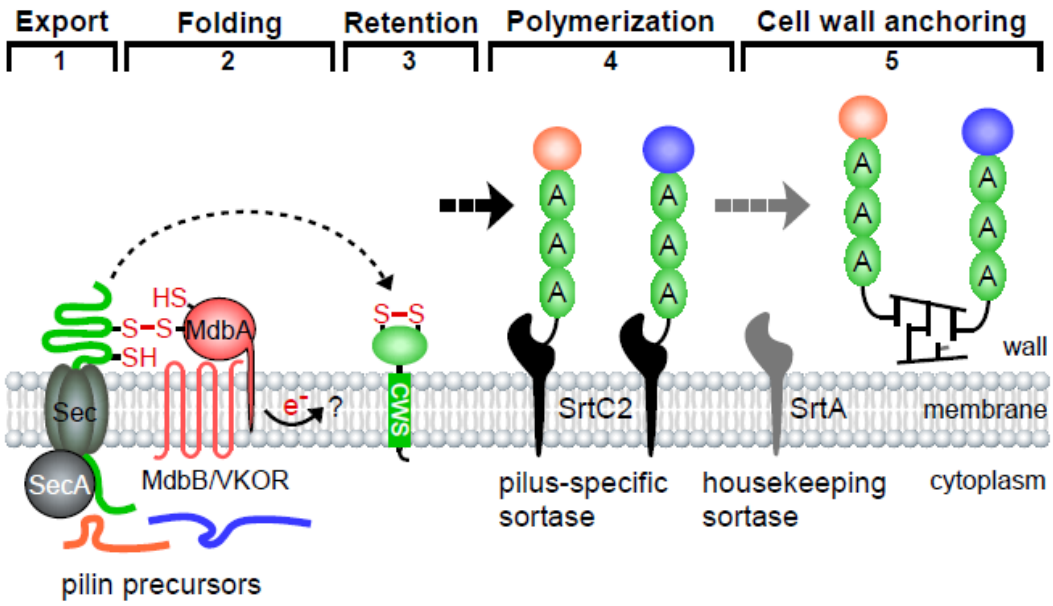

Figure 3.1. A model of pilus assembly in *A. oris*. Presented is a simplified model of pilus assembly in *A. oris* that is centered on the type 2 fimbriae (see text for details); FimA, FimB, and CafA are colored in green, orange, and blue, respectively. The thiol-disulfide oxidoreductase MdbA catalyzes oxidative folding of nascent protein precursors as they are translocated into the exoplasm by the Sec machinery. Reoxidation of MdbA requires the membrane-bound oxidoreductase VKOR. Folded pilin precursors are polymerized and anchored to the cell wall by the tandem sortase enzymes. It is not known how electrons generated from reoxidation of MdbA/VKOR are transferred to (question mark). Dashed arrows denote potential multiple steps; adapted after [55, 111].

positive or negative-coaggregation phenotype scoring [55]. By characterizing a subset of these coaggregation-defective mutants, we demonstrate here that the NADH dehydrogenase and menaquinone, components of the electron transport chain (ETC), are involved in reoxidation of the major disulfide bond-forming machine MdbA/VKOR in *A. oris*.

3.2. RESULTS

3.2.1. A Tn5 transposon screen revealed *A. oris* mutants defective in polymicrobial interactions

Since pilus assembly and bacterial coaggregation in *A. oris* are coupled [96, 111], we sought to identify *trans*-acting factors involved in pilus assembly by screening a large number of *A. oris* Tn5 mutants using a previously reported coaggregation assay in a 96-well plate format [55]. Following a published protocol [55, 92], a Tn5 transposon library of roughly 6,240 *A. oris* mutants (> 3-fold genome coverage) was constructed and screened. Coaggregation efficiency of the Tn5 mutants was scored largely based on the visual scoring system reported by Cisar et al. [94], whereby the coaggregation-positive phenotype of the parental strain MG1 was designated as 4 and the coaggregation-negative phenotype of type-2 fimbria-less mutants, i.e. Δ*fimA*, Δ*cafA*, and Δ*srtC2*, was set as 1; tiny clumps of aggregates were scored as 2, whereas the larger clumps were considered as 3. We obtained 13 mutants with the coaggregation score (CS) of 1, 7 mutants with the CS of 2 or CS-2, and 13 mutants with CS-3; of note, the Tn34 mutant exhibiting a coaggregation phenotype similar to that of MG1 was included for comparison (Figure 3.2). These coaggregation-defective Tn5 mutants were then subjected to mapping by thermal

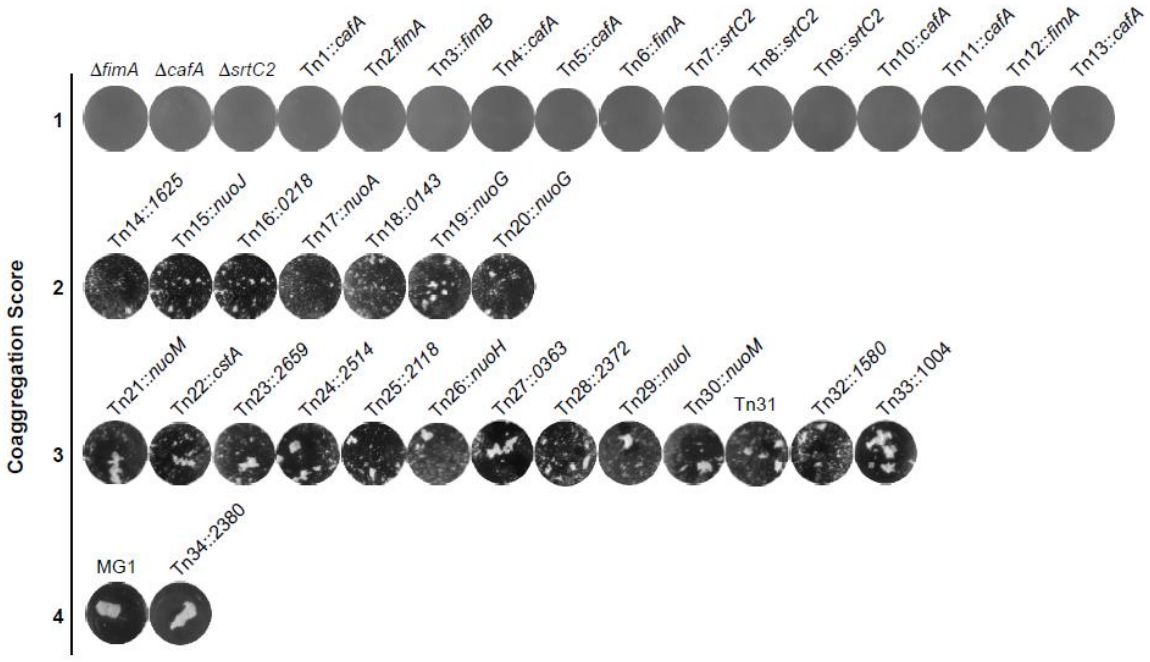

Figure 3.2. Identification of *A. oris* coaggregation-defective mutants by Tn5 transposon mutagenesis. Thirty-three *A. oris* coaggregation-defective Tn5 mutants identified by a cell-based screen were confirmed by a standard coaggregation assay [87]. Equal cell numbers of *A. oris* mutants and *S. oralis* So34 were mixed together, and coaggregation was imaged using an AlphaImager. Coaggregation scores indicate the degrees of coaggregation, with the phenotype of the parental MG1 strain considered as 4 and that of the *fimA*, *cafA*, and *srtC2* deletion mutants considered as 1; 2 and 3 represent small and larger clumps of bacterial aggregates. Tn5 target genes were mapped by TAIL-PCR. *Chungyu Chang, PhD and Bryan Tran performed the Tn5 transposon mutagenesis and coaggregation screen.*

asymmetric interlaced PCR (TAIL-PCR) and DNA sequencing as previously described [55].

As expected, 13 coaggregation-negative mutants, i.e. with the CS of 1, were mapped to genes encoding CafA, FimA and SrtC2, which are known fimbrial factors essential for *A. oris* coaggregation with oral streptococci [12, 96, 111]. Intriguingly, 4 out of 7 CS-2 mutants contained Tn5 insertions in *nuoA*, *nuoJ*, and *nuoG* genes; the remainder were mapped to genes, i.e. ANA_1625, ANA_0218, and ANA_0143, which code for geranylgeranyl reductase (GGR), a putative metal-binding protein, and β-glucosidase, respectively. Finally, the CS-3 mutants were mapped to genes encoding many hypothetical proteins, a carbon starvation protein A (CstA), a two-component system sensor kinase, an ABC-2 type transporter, and the H, I, M subunits of NADH dehydrogenase (i.e. NuoH, NuoI, and NuoM) (Figure 3.2 and Table 3.1). Since a large number of the *nuo* genes was repeatedly targeted by the Tn5 transposon, they were further characterized and reported in this study; the remaining candidates will be investigated in future studies.

3.2.2. Genetic disruption of the *A. oris* NADH dehydrogenase (complex I) subunits caused significant defects in CafA-mediated coaggregation and CafA pilus assembly

The *ggr*, *nuoA*, *nuoG*, *nuoH*, *nuoJ*, and *nuoM* genes revealed from the Tn5 screen above are part of the *nuo* gene locus in *A. oris* MG1, (see http://genome.brop.org/), which are predicted to encode the NADH dehydrogenase enzyme – often referred to as the NADH:ubiquinone oxidoreductase or respiratory complex I of the ETC [134] (Figure 3.3A). To confirm that the coaggregation defects

Table 3.1. Mapping of *A. oris* coaggregation-defective Tn5 mutants

Tn5 mutants	Genomic Tn5 Position[a]	Target Gene	Predicted Function
1	2,422,225	*cafA*	Coaggregation factor A
2	38,189	*fimA*	Type 2 fimbrial shaft pilin
3	36,541	*fimB*	Type 2 fimbrial tip pilin
4	2,420,317	*cafA*	Coaggregation factor A
5	2,421,799	*cafA*	Coaggregation factor A
6	38,174	*fimA*	Type 2 fimbrial shaft pilin
7	39,115	*srtC2*	Type 2 pilus-specific sortase
8	39,481	*srtC2*	Type 2 pilus-specific sortase
9	39,749	*srtC2*	Type 2 pilus-specific sortase
10	2,421,087	*cafA*	Coaggregation factor A
11	2,421,136	*cafA*	Coaggregation factor A
12	38,721	*fimA*	Type 2 fimbrial tip pilin
13	2,420,135	*cafA*	Coaggregation factor A
14	1,755,107	*ana_1625*	Geranylgeranyl reductase
15	1,744,569	*nuoJ*	NADH dehydrogenase I, subunit J

16	230,679	*ana_0218*	Zn^{2+}/Mn^{2+} transport system substrate-binding protein
17	1,754,944	*nuoA*	NADH dehydrogenase I, subunit A
18	162,115	*ana_0143*	β-D-glucoside glucohydrolase
19	1,747,764	*nuoG*	NADH dehydrogenase I, subunit G
20	1,748,226	*nuoG*	NADH dehydrogenase I, subunit G
21	1,741,097	*nuoM*	NADH dehydrogenase , subunit M
22	2,348,384	*cstA*	Carbon starvation protein A
23	2,863,369	*ana_2659*	Ni/Fe-hydrogenase III large subunit
24	2,711,713	*ana_2514*	Histidine kinase (two-component system)
25	2,295,587	*ana_2118*	Permease component of ABC-type multidrug transport system
26	1,746,526	*nuoH*	NADH dehydrogenase I, subunit H
27	382,186	*ana_0363*	Conserved hypothetical protein
28	2,566,963	*ana_2372*	Hypothetical protein with Ser/Arg repeats
29	1,745,086	*nuoI*	NADH dehydrogenase I, subunit I
30	1,739,922	*nuoM*	NADH dehydrogenase I, subunit M
31	2,513,949	*ana_2325*/ *ana_2326*[b]	Ana_2325 (Cys/His-dependent amidohydrolase/peptidase); Ana_2326 (hypothetical protein)
32	1,712,411	*ana_1580*	Conserved hypothetical protein

33	1,080,892	*ana_1004*	Hypothetical protein
34	2,576,712	*ana_2380*	Conserved hypothetical protein

[a]Shown is the nucleotide position of the Tn5 transposon mapped in the genome.

[b]Tn5 insertion was found within the intergenic region of *ana_2325* and *ana_2326*.

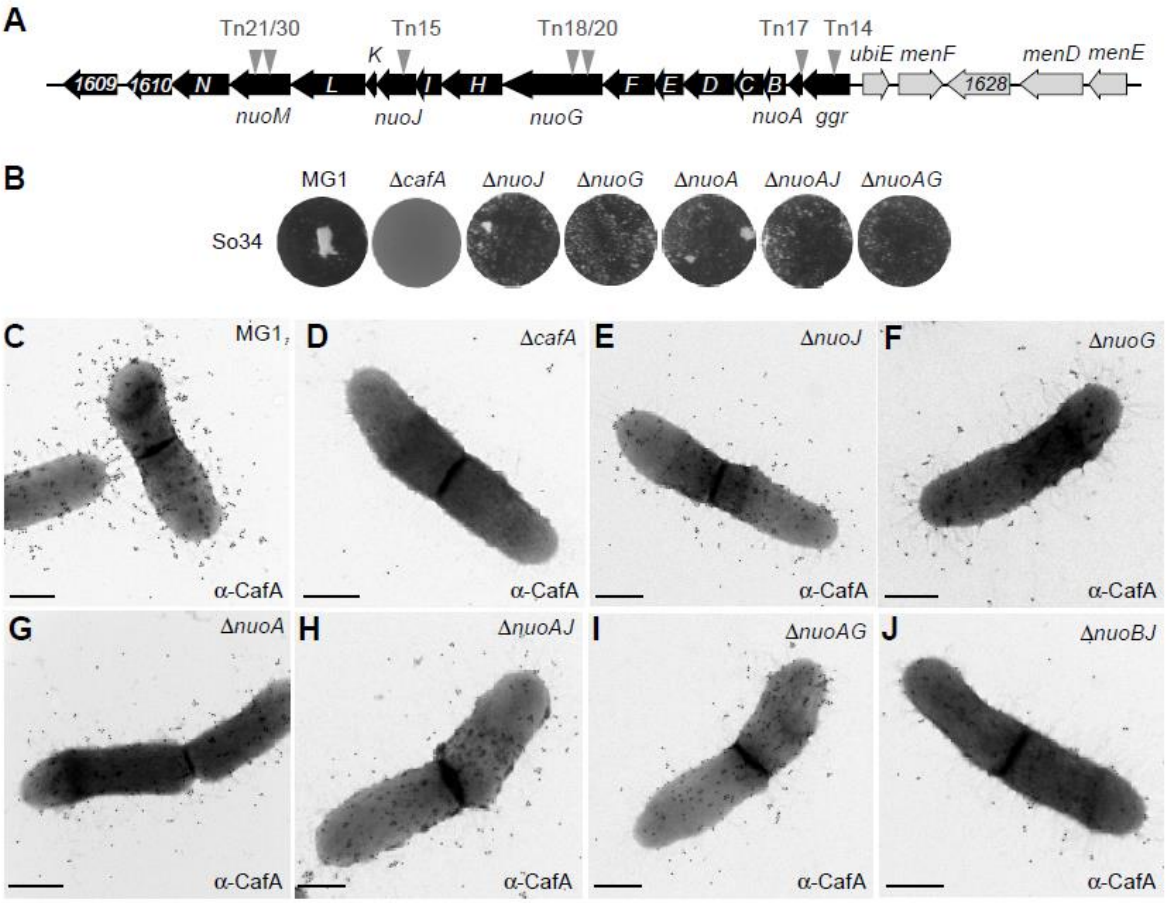

Figure 3.3. Involvement of *nuo* genes in CafA-mediated coaggregation and pilus assembly. (A) The *nuo* operon and adjacent genes are shown in black and genes involved in ubiquinone/menaquinone biosynthesis are shown in grey. Arrowheads indicate the locations of Tn5 transposon. (B) Coaggregation of *A. oris* strains and *S. oralis* So34 was performed as described in Figure 2C-J, *A. oris* cells were immobilized in nickel-carbon grids and labeled with α-CafA antibodies, followed by labeling with anti-rabbit IgG antibodies conjugated to 18-nm gold particles. Samples were stained with 1% uranyl acetate and viewed by a transmission electron microscope. Scale bars indicate 0.5 µm. *Chungyu Chang, PhD contributed to the generation of A. oris deletion mutants.*

of the Tn5::*nuo* mutants are not due to polar effects, we generated individual and combinations of in-frame, nonpolar deletion mutants of *nuoJ*, *nuoG*, *nuoA*. The generated mutants were confirmed for their inability to aggregate with *S. oralis* via CafA-mediated coaggregation using a standard coaggregation assay [111], whereby *A. oris* cells were mixed in equal volume with *S. oralis* So34, and coaggregation was determined after a few minutes of mixing. As shown in Figure 3.3B, deletion of *nuoJ*, *nuoG*, *nuoA*, or combination of *nuoA* and *nuoJ* or *nuoA* and *nuoG* caused significant coaggregation defects as compared to the wild-type level.

Since CafA pilus assembly is essential for *A. oris* coaggregation [111], we next examined whether the observed coaggregation defects are due to pilus assembly defects of CafA by immunoelectron microscopy (IEM). In this assay, *A. oris* cells were stained with antibodies against CafA (α-CafA), followed by staining with gold particles conjugated with IgG, and the samples were viewed by a transmission electron microscope (TEM) after staining with 1% uranyl acetate. In the parental strain MG1, CafA signal was found abundantly on the bacterial surface and at the distal end of pili; as expected, the CafA signal was absent in the *cafA* deletion mutant [111]. Importantly, CafA labeling was significantly reduced in the *nuoJ*, *nuoG*, *nuoA*, *nuoAJ*, *nuoAG*, and *nuoBJ* mutants (Figure 3.3C-J). Since the CafA assembly defects among these mutants were apparently equal, we chose to focus on the *nuoA* mutant for further characterizations (see below) as *nuoA* is typically the first gene in bacterial *nuo* operons [135]. To support that the generated *nuoA* mutant is non-polar, we introduced in this mutant a plasmid constitutively expressing *nuoA*; as shown in Figure 3.4, ectopic expression of *nuoA* rescued the assembly defects of both type 1

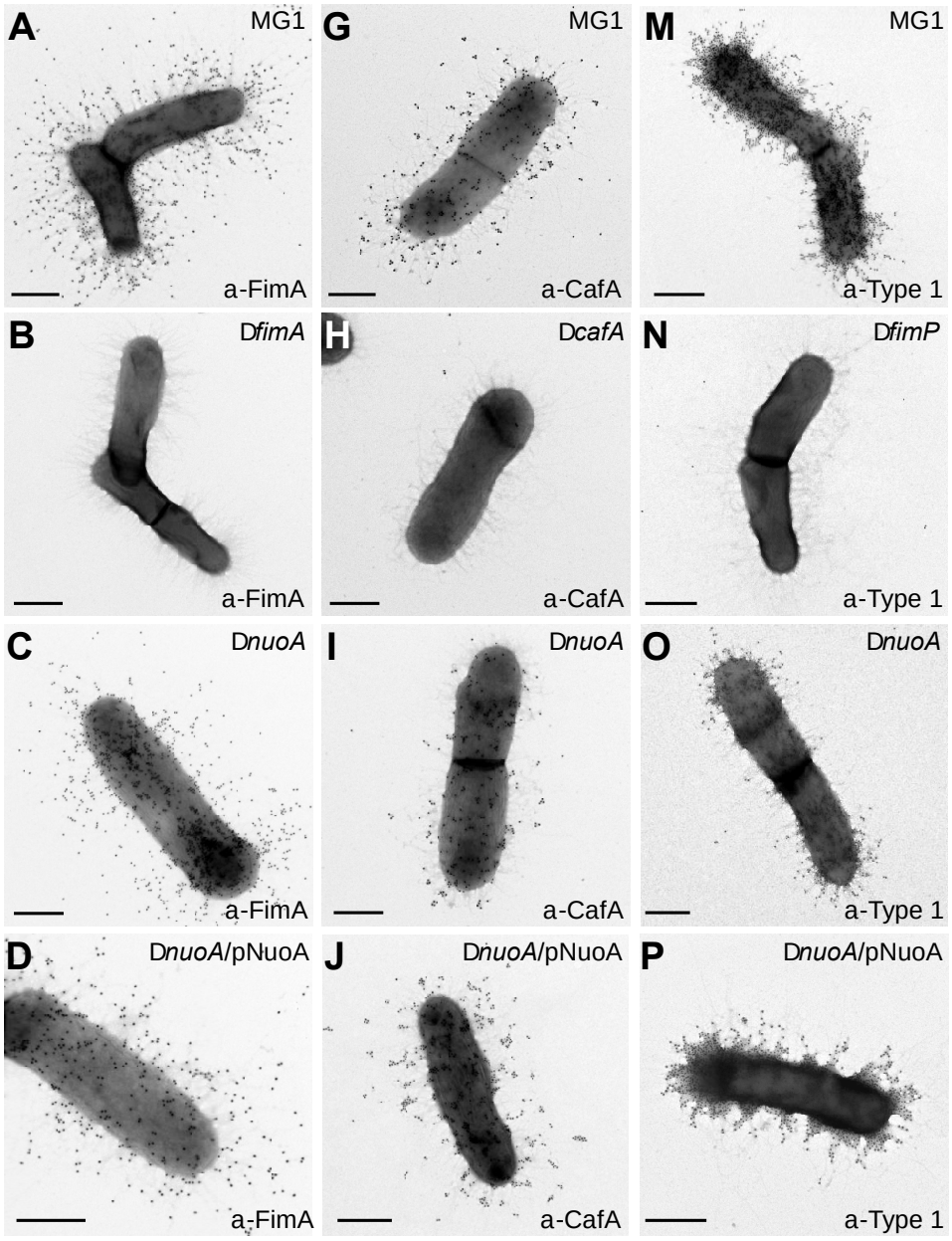

Figure 3.4. Requirement of *nuoA* for pilus assembly. *A. oris* cells of indicated strains were immobilized on carbon-coated n nickel grids and stained with α-FimA (**A**-**D**), α-CafA (**G-J**), or α-Type1 antibodies (**M-P**), followed by staining with IgG conjugated to 18-nm gold particles. Samples were stained with 1% uranyl acetate prior to be analyzed by electron microscopy. Scale bars indicate 0.5 µm.

and type 2 pili of the *nuoA* mutant. Of note, the defects in pilus assembly and coaggregation might not be due to the cell growth defect as the growth rate of the *nuoA* mutant was not significantly different from that of the parental strain (Figure 3.5). Together, the results confirm the requirement of the NADH dehydrogenase for optimal bacterial coaggregation and CafA pilus assembly.

3.2.3. The menaquinone C-methyltransferase UbiE is involved in *A. oris* coaggregation, biofilm formation, and pilus assembly

In *E. coli*, the NADH dehydrogenase, encoded by 14 *nuo* genes (A to N), generates energy by coupling the transfer of electrons from NADH to ubiquinone with proton translocation across the membrane [134]. We observed that upstream of the *A. oris nuo* locus in the MG1 genome are genes encoding part of the ubiquinone/menaquinone biosynthesis pathway, with the C-methyltransferase encoding-gene *ubiE* adjacent to *ggr* (Figure 3.3A). In *E. coli* UbiE catalyzes the carbon methylation reaction in the biosynthesis of ubiquinone/menaquinone, which are essential components of the ETC [136]. This information prompted us to examine whether the ubiquinone/menaquinone biosynthesis pathway is also linked to *A. oris* coaggregation and pilus assembly. Since *ubiE* is not an essential gene in *E. coli* [136], we decided to generate an in-frame, nonpolar deletion mutant of *A. oris ubiE*. The generated mutant was examined for its ability to aggregate with *S. oralis*, to mediate biofilm formation, and to produce pili using published assays [111].

In the coaggregation assay, the *ubiE* mutant exhibited a severe defect in bacterial coaggregation with *S. oralis* when compared to the parental strain MG1, and this defect was rescued by ectopic expression of UbiE (Figure 3.6A). The same set

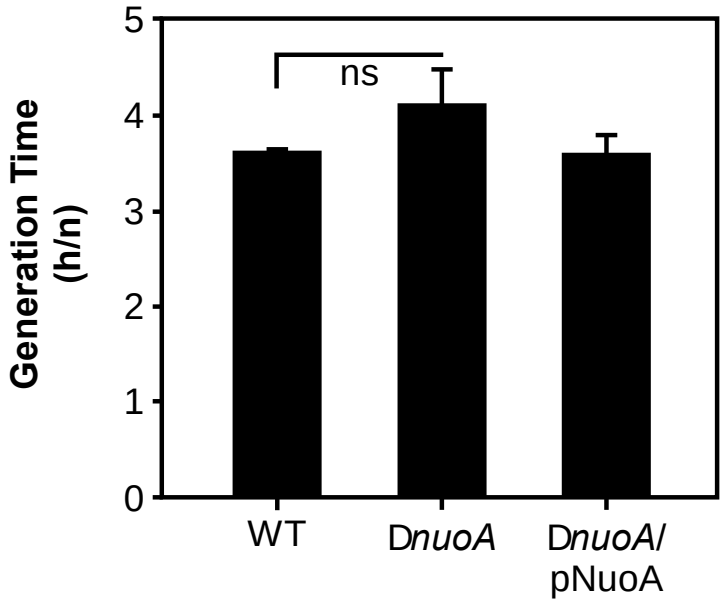

Figure 3.5. Generation times of the *A. oris* MG1 and Δ*nuoA* mutant strains. (A) Growth of the wild-type MG1, Δ*nuoA* and Δ*nuoA*/pNuoA strains was measured by optical density (OD_{600}). Generation times were calculated as described in materials and methods. The results are representative of three independent experiments performed in triplicate. Error bars represent standard deviations, with ns for not significant.

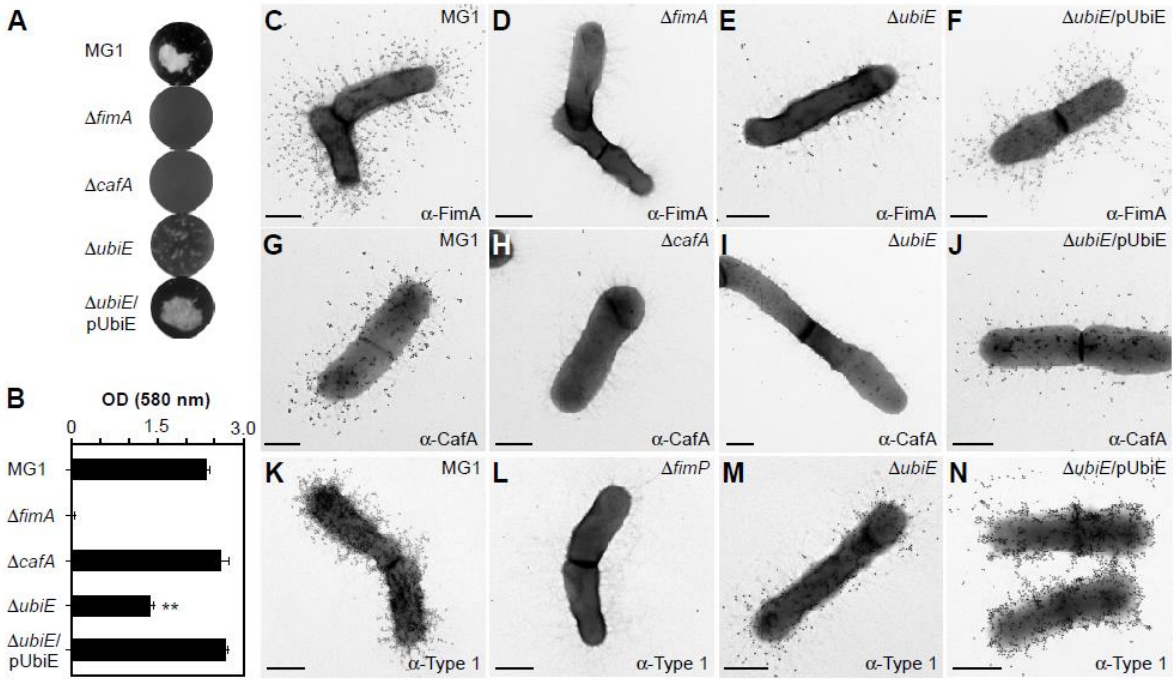

Figure 3.6. Requirement of ubiE for bacterial coaggregation, biofilm formation, and pilus assembly. (A) Coaggregation of *A. oris* strains and *S. oralis* So34 was determined as described in Figure 3.2. (B) Biofilms were obtained by growing the indicated strains in HIB containing 1% sucrose for 48 h. Harvested biofilms were subjected to crystal violet staining and optical density measurement at 580 nm using a microplate reader. The results are shown as representatives of 3 independent experiments performed in triplicate; ** denotes $P < 0.0025$, calculated using a One-way ANOVA (Duncan's method, non-parametric) with GraphPad Prism. (C-N) *A. oris* cells were immobilized in nickel grids and stained with α-FimA (C-F), α-CafA (G-J), or α-Type1 antibodies (K-N), followed by staining with IgG conjugated to 18-nm gold particles. Samples were stained with 1% uranyl acetate prior to be analyzed by electron microscopy. Scale bars indicate 0.5 µm.

of strains was then examined in biofilm formation assays, in which *A. oris* biofilms were cultivated in Heart Infusion broth (HIB) supplemented with 1% sucrose, followed by biofilm staining with 1% crystal violet and quantification by OD_{580}. Consistent with the results above, deletion of *ubiE* significantly reduced biofilm formation as compared to the wild-type level, and expression of *ubiE* in *trans* restored biofilm formation to the wild-type (Figure 3.6B).

To examine if the coaggregation and biofilm defects are associated with pilus assembly, we employed IEM using α-CafA and antibodies against the type 2 fimbrial shaft FimA (α-FimA). Compared to the MG1 strain, which produced abundant signals of FimA and CafA, FimA and CafA detection was drastically reduced in the *ubiE* mutant; these defects were rescued in the *ubiE* mutant expressing UbiE from a plasmid (Figure 3.6C-J and Figure 3.7). Finally, to determine if the role of UbiE also extends to the type 1 fimbriae, we used antibodies against type 1 fimbriae [137] (α-Type 1) in IEM experiments. Consistently, the type 1 fimbrial signal was significantly reduced in the *ubiE* mutant as compared to the parental MG1 and UbiE complementing strains (Figure 3.6K-N). Altogether, these results suggest that the defects of *ubiE* deletion in bacterial coaggregation and biofilm formation are directly linked to assembly deficiencies of adhesive fimbriae, which are the major factors required for the aforementioned processes in *A. oris* [96, 111].

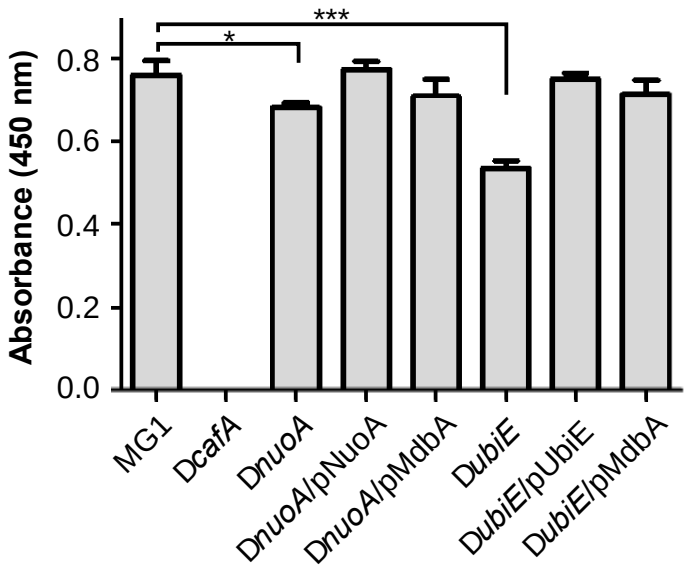

Figure 3.7. Requirement of *nuoA* and *ubiE* for surface expression of CafA. (A) The expression of CafA on the cell surface was determined by whole cell ELISA using polyclonal α-CafA antibodies. The absorbance measurments at 450nm, as compared to *cafA* mutant as background, were determined from three independent experiments performed in triplicate. Error bars represent standard deviations. *, *** indicate P<0.05, P<0.001, respectively, which were determined using the unpaired, two-tailed *t*-test with GraphPad Prism.

3.2.4. Requirement of the menaquinone C-methyltransferase UbiE and NADH dehydrogenase subunit NuoA in reoxidation of the major thiol-disulfide oxidoreductase MdbA

As mentioned above, disulfide bond formation is required for correct folding of pilin precursors, and this process is catalyzed by the major thiol-disulfide oxidoreductase MdbA in *A. oris* [55]. Given UbiE and several subunits of the NADH dehydrogenase are associated with pilus assembly as presented above, we hypothesized that the pilus assembly defects in the *ubiE* and *nuo* mutants might be due to aberrant oxidative folding of pilus proteins. Reactivation of MdbA normally requires the membrane-bound oxidoreductase VKOR, but overexpression of MdbA in a *vkor* mutant can compensate the loss of VKOR [55]. Here, we examined if ectopic expression of MdbA in the absence of UbiE or Nuo subunits would rescue the pilus assembly defects by introducing a recombinant plasmid that constitutively expresses MdbA into the *ubiE* and *nuoA* mutants. The resulting strains, along with the mutants, were examined for their ability to assemble pili by IEM with α -FimA. Compared to the parental MG1 strain, the *ubiE* mutant produced significantly less FimA (compare Figure 3.6C and Figure 3.8A), whereas overexpression of MdbA in this mutant resulted in abundant production of FimA pili (Figure 3.8B). While the assembly defect of FimA in the *nuoA* mutant was not as severe as that of the *ubiE* mutant, MdbA overexpression in this *nuoA* mutant also increased pilus production (Figure 3.8C & D and Figure 3.7). These results suggest that MdbA was not sufficiently reoxidized by VKOR in the absence of UbiE or NuoA.

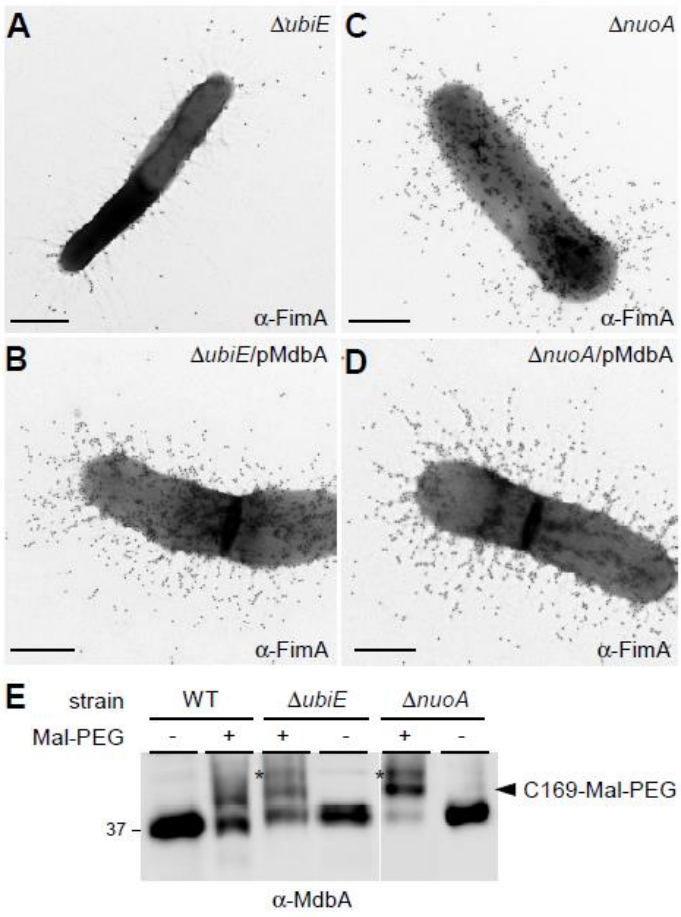

Figure 3.8. Requirement of NuoA and UbiE in oxidation of the thiol-disulfide oxidoreductase MdbA. (A-D) Cells of indicated *A. oris* strains were subjected to immunogold-labeling with α-FimA as described in Figure 3.6; scale bars of 0.5 µm. (E) Whole cell lysates of *A. oris* strains were prepared by mechanical disruption and treated (+) or not treated (-) with Mal-PEG. Protein samples were immunoblotted with antibodies against the thiol-disulfide oxidoreductase MdbA (α-MdbA). A reduced form of MdbA is shown by an asterisk, whereas the MdbA species labeled by Mal-PEG at C169 are indicated by a black arrowhead.

To confirm this, we examined the oxidation status of MdbA by alkylation with methoxypolyethylene glycol-maleimide (Mal-PEG) as previously reported [55, 56]. In this assay, protein samples acid-trapped by TCA precipitation from cell lysates of the MG1, Δ*ubiE*, and Δ*nuoA* strains were treated with 10 mM Mal-PEG or mock-treated prior to immunoblotting with antibodies against MdbA (α-MdbA). As the wild-type MG1 strain contains MdbA with the catalytic CXXC motif, C139/142, and a non-catalytic cysteine residue C169 [55], Mal-PEG treatment caused an up-shift in MdbA mobility that was due to Mal-PEG modification of the free sulfhydryl group of C169 as previously reported [55] (Figure 3.8E; lanes WT, black arrow). Significantly, Mal-PEG treatment of the Δ*ubiE*, and Δ*nuoA* mutants resulted in a higher up-shift as compared to the MG1 strain in the same condition, consistent with Mal-PEG modification of additional reduced sulfhydryl groups at the active site of MdbA (Figure 3.8E; the last 4 lanes, asterisks). These results support the conclusion that the catalytic cysteine residues C139/142 in the CXXC motif are in a reduced form when *ubiE* and *nuoA* are genetically disrupted, very much like the phenotype of MdbA when VKOR is absent [55].

3.2.5. Exogenous menaquinone rescues the pilus assembly and cell growth defects of the *ubiE* mutant

In the majority of Gram-positive bacteria, menaquinone plays a central role in the ETC, functioning as a conduit to receive electrons from electron donors, e.g. NADH dehydrogenase, and transfer them to an electron acceptor, e.g. cytochrome c reductase [138, 139]. As UbiE catalyzes the conversion of dimethyl-menaquinone to menaquinone [136, 140], the lack of *ubiE* potentially reduces the quinone pool in the

mutant cells, leading to the pleiotropic effects discussed above. To examine this, we monitored the growth rates of *A. oris* strains grown in HIB by optical density (OD_{600}) over time. Indeed, the *ubiE* mutant displayed a growth defect as compared to the parental strain, and complementing this strain with the pUbiE plasmid rescued this growth defect (Figure 3.9A). Importantly, addition of 0.1 mM menaquinone-4 (MK-4) to the culture medium increased the growth rate to a level comparable to the complementing strain after 16 h of growth (Fig 3.9A; black and grey triangles).

To further confirm this phenotype, we adapted a streaking assay with menaquinone [141], whereby the parent MG1 strain and its *ubiE* isogenic mutant were streaked as a broad band on heart infusion agar plate, and a 3-µl drop of 50 mM MK-4 was placed on the border of the streak. Cell growth at 37^{o}C was recorded after 48 h. As shown in Figure 3.9B, the MG1 strain exhibited abundant growth inside and outside of the MK-4 diffusing zone (dashed lines), whereas the *ubiE* mutant cells inside the MK-4 diffusing zone grew significantly better than those found outside.

Finally, to determine whether menaquinone can also rescue pilus assembly defects, we collected the *ubiE* mutant cells grown in the presence or absence of MK-4 for IEM using α-CafA. Indeed, the mutant cells grown in the presence of MK-4 produced abundant CafA signal at the level comparable to the MG1 and the complementing strains (Figure 3.9C-6F). Altogether, the results support that the defects of the Δ*ubiE* mutant in pilus assembly, cell growth, and MdbA reoxidation are mainly due to the reduced level of endogenous menaquinone.

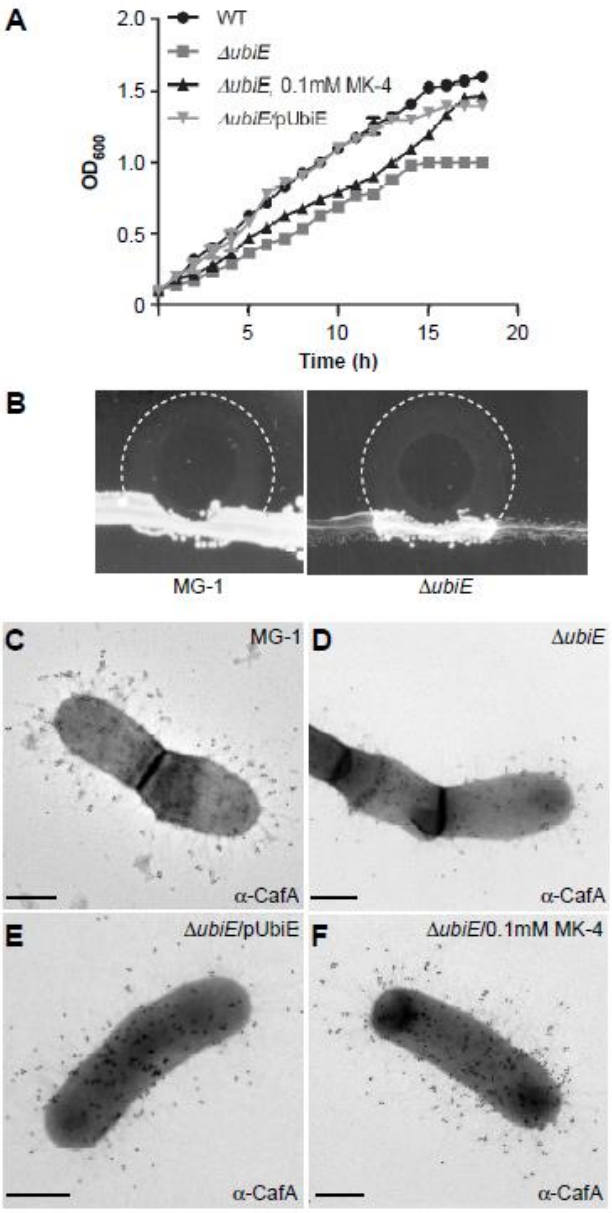

Figure 3.9. Exogenous menaquinone rescues the growth and pilus assembly defects of the Δ*ubiE* mutant. (A) Growth of the wild-type strain (black circle), Δ*ubiE* (grey square), Δ*ubiE*/pUbiE (grey inverted triangle), and Δ*ubiE* in the presence of 0.1mM of MK-4 (triangle) was measured by optical density (OD_{600}). The results are representative of three independent experiments performed in duplicate. ***

represents P ≤ 0.0001 determined by the paired, two-tailed *t* test with GraphPad Prism. (B) *A*. *oris* strains were streaked as a broad band on HIA plates. A 3-µl drop of 50 mM menaquinone-4 (MK-4) was placed on the border of the streaks and growth the strains at 37ºC was recorded after 48 h. Areas of MK-4 diffusion are marked with dashed lines. (C-F) *A. oris* cells of WT, Δ*ubiE*, Δ*ubiE*/pUbiE, and Δ*ubiE* grown in the presence of 0.1 mM MK-4 were subjected to immunogold-labeling with α-CafA as described in Figure 3.6. Scale bars indicate 0.5 µm.

3.3. DISCUSSION

Because pilus assembly and bacterial coaggregation are mutually inclusive in *A. oris*, this inherent property was used in our Tn5 transposon screen intended to identify factors involved in pilus assembly. This screen revealed numerous mutants that display varying defects in *Actinomyces* coaggregation with *S. oralis*. As expected, roughly one-third of the coaggregation-defective mutants were mapped to genes encoding the major pilus shaft FimA, the coaggregation factor CafA, and the pilus sortase machine SrtC2 (Figure 3.2). Mapping of the remainder surprisingly uncovered the association of coaggregation with the NADH dehydrogenase (complex I) (Table 3.1), whose genes are adjacent to the ubiquinone/menaquinone biosynthesis gene locus. By genetically and biochemically characterizing two representative in-frame, nonpolar mutants Δ*nuoA* and Δ*ubiE*, we have established that the two ETC components, the NADH dehydrogenase and menaquinone, are linked to pilus assembly via reoxidation of the major disulfide bond-forming machine MdbA, which is essential for oxidative folding of pilus proteins in *A. oris* [55, 132].

By electron microscopy, both Δ*nuoA* and Δ*ubiE* are shown to be defective in pilus assembly, although the latter displays the most striking defects (Figures 3.3 and 3.6). Since overexpression of MdbA in the Δ*ubiE* mutant rescues its pilus defects (Figure 3.8), we argued that in the absence of UbiE the disulfide bond-forming machine MdbA is not fully reoxidized, given that reoxidation of MdbA is required for its activity and oxidative folding of *A. oris* pilus proteins [55]. Indeed, by alkylation with Mal-PEG we detected a reduced form of MdbA, although oxidized MdbA was also observed (Figure 3.8E). The latter might be due to inefficient alkylation by Mal-PEG

and/or spontaneous oxidation of MdbA during the sampling process. Since menaquinone, 2-methyl-3-polyprenyl-1,4-naphthoquinone, is the main quinone utilized in the ETC of Gram-positive actinobacteria [142], the lack of UbiE certainly reduces the menaquinone pool in the cells as previously demonstrated in the *E. coli ubiE* mutant [136]. In fact, by adding MK-4, a menaquinone with 4 isoprene units, to the Δ*ubiE* cell cultures, we were able to rescue not only the cell growth deficiency but also the pilus assembly defect of the Δ*ubiE* mutant (Figure 3.9). The results strongly support that menaquinone is the major quinone source capable of reoxidizing the disulfide bond machine MdbA/VKOR in *A. oris*.

In *E. coli*, DsbA is the primary disulfide bond-forming catalyst, which catalyzes disulfide bond formation of nascent polypeptides transported to the periplasm by the Sec apparatus [34, 36, 143]. DsbA becomes reduced after catalysis, and reoxidation of DsbA requires DsbB [32, 39]. Our results presented here are in line with previous studies in *E. coli* that demonstrate the participation of the respiratory ETC in reoxidation of the DsbA/DsbB system [40, 43]. Kobayashi and colleagues showed that *E. coli* mutants lacking *hemA* – coding for glutamyl-tRNA reductase involved in protoheme and siroheme biosynthesis – or *ubiA-menA*, which encode products involved in menaquinone biosynthesis, are defective in reoxidation of DsbA when cells are grown in conditions deficient in protoheme or ubiquinone/menaquinone, respectively [43]. By reconstituting the *E. coli* disulfide bond-forming machine DsbA/DsbB with purified components, Bader and colleagues demonstrated that under anaerobic conditions menaquinone serves as an electron acceptor during DsbA/DsbB reoxidation; under aerobic growth ubiquinone acts as electron acceptor

that reoxidizes DsbB, which in turn reoxidizes DsbA [40]. It is interesting to note that structural studies of a VKOR homolog of *Synechococcus* sp. reveal the protein is complexed with ubiquinone [144]. Thus, it is plausible that a similar mechanism of MdbA/VKOR reoxidation occurs in *A. oris*, with menaquinone presumably acting as an electron acceptor for VKOR during this process; how menaquinone mechanistically reoxidizes MdbA/VKOR remains to be investigated in future studies.

Of note, the effect of the NADH dehydrogenase in MdbA/VKOR reoxidation, which has not been reported before with regard to DsbA/DsbB reoxidation, is somewhat puzzling. In many eukaryotic and prokaryotic systems, Complex I (NADH quinone:dehydrogenase) serves as an entry point for electrons to enter the respiratory chain, transferring 2 electrons from NADH to ubiquinone [145]. In *E. coli*, the NuoB, NuoD, NuoH, and NuoM subunits form a ubiquinone binding pocket [146]. Thus, it is possible that genetic disruption of the Nuo subunits in *A. oris* might disturb electron transfer and/or the quinone pool in the cells. However, the effects seen in the *nuo* deletion mutants in pilus assembly are not striking as those observed in the *ubiE* mutant, although their defects in coaggregation are obvious (Figure 3.3). Thus, it is possible that genetic disruption of the Nuo subunits potentially causes pleotropic effects. It is likely that many other dehydrogenases, such as the malate and succinate [147], may compensate the loss of the NADH dehydrogenase.

While the association of the NADH dehydrogenase and menaquinone in pilus assembly is clear, the role of other factors identified from the aforementioned coaggregation-defective screen with Tn5 mutagenesis is not obvious as many of these factors are hypothetical proteins (Table 3.1). Except for ANA_0218 and

ANA_0143, which are predicted to be a Zn2+/Mn2+ transport system substrate-binding protein and β-D-glucoside glucohydrolase, respectively, the coaggregation defects of the remainder is not glaring. Given the nature of the two proteins mentioned above, it is more likely they may participate in receptor-related binding rather in pilus assembly. Finally, it is noteworthy that the Tn5 screen in this study is not saturated, which may explain why an *ubiE* mutant was not detected in this screen. Future Tn5 screens with multi-fold coverage designed to directly target pilus assembly will be necessary to reveal any additional novel pilus factors.

CHAPTER 4. Regulation of an Alternate Thiol-Disulfide Oxidoreductase in *Corynebacterium diphtheriae*

Note: This chapter is derived from work performed by Belkys Sánchez. The X-ray crystallography study and discussion of TsdA C129S is the work of Jerzy Osipiuk and Andrzej Joachimiak and was used with permission. The bacterial clone expressing recombinant TsdA C129S protein was created and supplied by Belkys Sánchez.

4.1. INTRODUCTION

Bacteria often express proteins that are structurally and functionally similar but play different roles. For instance, bacteria and archaea encode variations of thiol-disulfide oxidoreductase enzymes that catalyze disulfide bond formation and isomerization in broad or specific substrates that are important for survival in specific environmental niches [68]. Interestingly, even though these enzymes have distinct dedicated functions, they can sometimes replace each other in catalyzing folding of particular substrates [68, 148].

Bacterial pathogens like *Corynebacterium diphtheriae* are exposed to many environmental stresses, including those mediated by host immune defense mechanisms during infection. Iron is an essential nutrient for *C. diphtheriae* growth [149], but nutritional immunity exerted by mammalian hosts limits the availability of iron to pathogens [77]. Consequently, iron regulates gene expression and virulence in *C. diphtheriae* [149]. Interestingly, thiol-disulfide oxidoreductase enzymes expression can also be regulated by iron availability and induced under nutrient starvation conditions, which are commonly encountered within the host [75, 76].

Another immune defense mechanism is the production of oxygen-derived toxic compounds like hydrogen peroxide (H_2O_2) by phagocytic cells to kill engulfed pathogens [150]. *C. diphtheriae* has been reported to survive in the acidic and oxidizing harsh environment inside macrophages [151, 152]. This type of environmental condition disrupts proper protein folding. Interestingly, some oxidoreductase enzymes have a role in resistance to oxidative stress exerted by copper and are important for intramacrophage survival [64, 76, 153]

Important bacterial pathogens encode multiple homologs of disulfide bond forming enzymes which contribute to their pathogenicity [28, 154-156]. In *C. diphtheriae*, the main thiol-disulfide oxidoreductase MdbA is required for proper cell division and virulence in a model of diphtheritic toxemia [56]. Additionally, an alternate disulfide bond forming enzyme was identified in a Δ*mdbA* suppressor mutant screen that selected for three clones (S1, S2, S3) that grew at the non-permissive temperature similar to the wild-type strain [114].

The *C. diphtheriae* Δ*mdbA* suppressor mutants harbor a single T-to-G nucleotide substitution within the predicted -10 box of the promoter of a putative thiol-disulfide oxidoreductase, named TsdA (Temperature-sensitive disulfide bond forming protein A). This mutation caused significant overexpression of TsdA that restored disulfide bond formation [114]. However, the mechanism by which this DNA change alters expression of *tsdA* has not been investigated.

TsdA harbors thiol-disulfide oxidoreductase conserved features, and has been reported to have isomerase/reductase activity *in vitro* [157]. Disulfide isomerase enzymes cannot introduce *de novo* disulfide bonds into proteins [158]. Overexpression of TsdA in the Δ*mdbA* strain restores disulfide bond formation in the shaft pilin subunit SpaA, which contains one disulfide bond [56, 159]. This argues against the isomerase activity that has been reported for TsdA.

Although overexpression of TsdA rescues the Δ*mdbA* phenotype, *tsdA* deletion does not cause an apparent defect in disulfide bond formation [114]. Since a mutant lacking *tsdA* does not present evident phenotypic changes under standard laboratory growth conditions, we hypothesize that TsdA has a role in resistance to

environmental stress. In this chapter we describe in detail the promoter region of *tsdA* and investigate the regulation and role of the alternate thiol-disulfide oxidoreductase TsdA under stress conditions.

4.2. RESULTS

4.2.1. The Δ*mdbA* compensatory mutation creates a sigma factor σ^A extended promoter

The T-to-G nucleotide substitution identified in all Δ*mdbA* compensatory mutants was predicted to be within the *tsdA* promoter region. To further characterize the effects of this change in the Δ*mdbA* compensatory mutants, we precisely identified the transcriptional start site (TSS) of *tsdA* by Rapid Amplification of cDNA Ends (5’ RACE). Whole-cell RNA samples from wild-type and Δ*mdbA* compensatory mutant S1 were used in reverse transcription reactions to amplify cDNA between a defined internal site within the *tsdA* mRNA and unknown sequences at the 5'-end. The resulting cDNA was used as template to generate RACE PCR products, which were subjected to Sanger sequencing to identify the *tsdA* transcriptional start site. Both wild-type and S1 strains showed the same *tsdA* transcriptional start site (Figure 4.1-A). Based on the identified *tsdA* transcriptional start site, the upstream DNA region was analyzed for conserved promoter motifs, and the promoter structure shown in Figure 4.1 is proposed. This configuration is consistent with a -10 core hexamer recognized by the housekeeping sigma factor σ^A, directing initiation of *tsdA* transcription at the adenine identified by the 5’ RACE experiment (Figure 4.1-A). Analysis of -10 and -35 promoter elements suggests low conservation to sigma factor

σ^A consensus motifs (Fig. 4.1-B), which explains low expression of *tsdA* in the wild-type strain [114]. The distance between the transcriptional start site and -10 motif was 6bp, and the distance between -35 and the -10 motifs was 16bp, while spacing for canonical σ^A-type promoters in *C. diphtheriae* is 6-9bp and 16-20bp respectively [115, 160, 161]. In agreement with the 5' RACE data and findings from Wittchen, et al. [115], promoter activity of this DNA region was confirmed by a transcriptional reporter experiment as will be discussed in section 4.2.4 (Figure 4.5).

The T-to-G substitution identified in the *tsdA* promoter region creates an extended sigma factor σ^A promoter (Figure 4.1-B), which is characterized by a TG dinucleotide at position -15, -14 that lowers the thermal energy required to form an open RNA polymerase initiation complex [115, 160, 162, 163]. This results in increased basal strength of the promoter and increased levels of transcription. In agreement, the *tsdA* T-to-G mutant promoter activity was significantly higher compared to the wild-type *tsdA* promoter as discussed in section 4.2.4 (Figure 4.5). Altogether, the data demonstrate that the T-to-G nucleotide substitution at position -14 of the *tsdA* promoter region creates an extended sigma factor σ^A promoter that results in increased promoter activity and overexpression of this gene.

4.2.2. Characterization of an alternate thiol-disulfide oxidoreductase in *C. diphtheriae* by X-ray crystallization

Overexpression of TsdA rescues the disulfide bond forming defect in *C. diphtheriae* cells lacking the main thiol-disulfide oxidoreductase MdbA; this suggested that TsdA has disulfide bond forming capabilities. To further characterize this putative

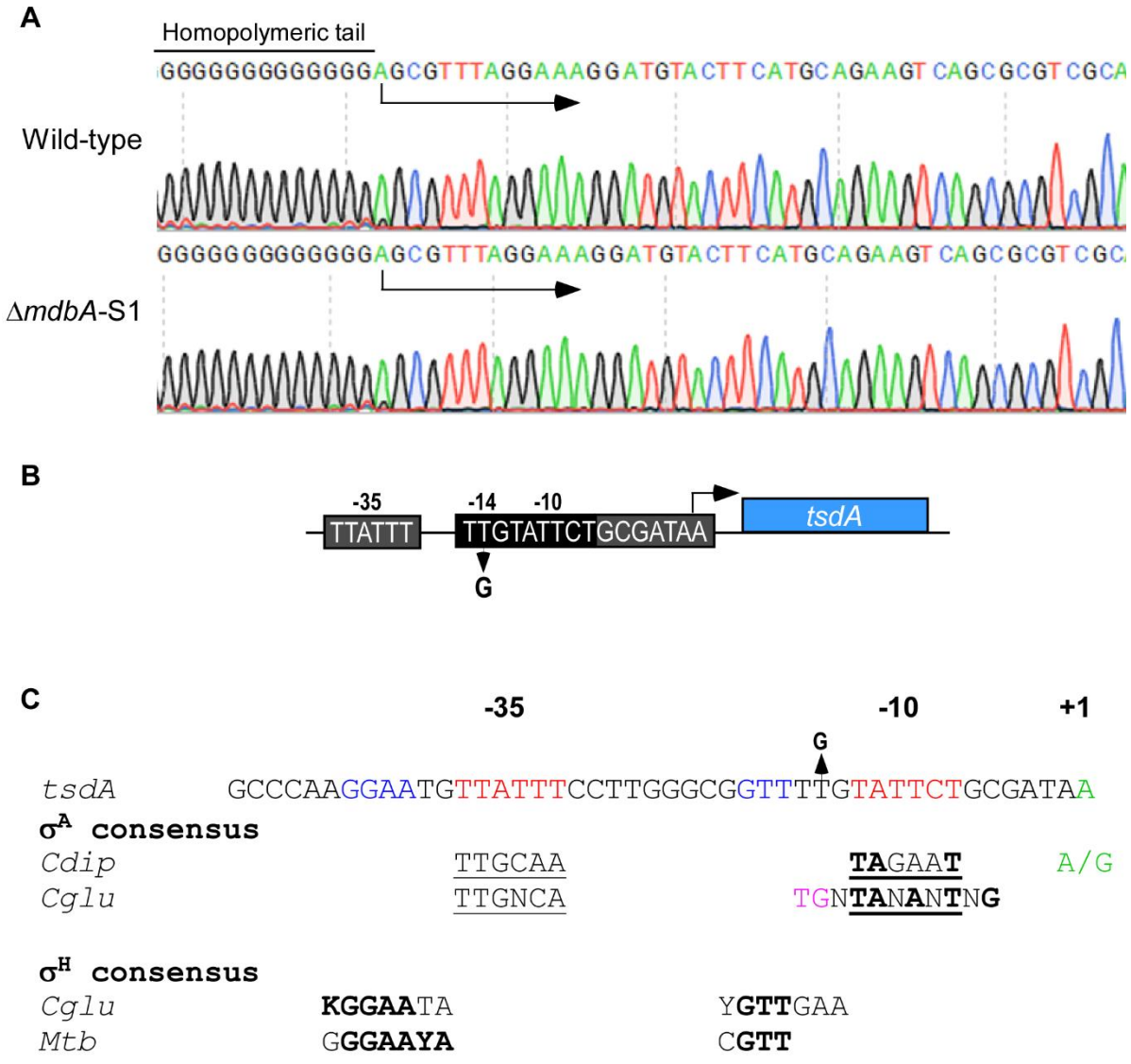

Figure 4.1. Δ*mdbA* suppressor mutation results in extended sigma factor σ^A promoter motif. (A) Determination of *tsdA* transcriptional start site by 5' RACE using Wild-type and Δ*mdbA*-S1 strains mRNA. DNA chromatograms from the sequencing reactions of 5' RACE PCR products are shown. The homopolymeric tail added to the 3' end of the cDNA used for the PCR reactions are shown. The nucleotides complementary to the 5' ends of mRNA are shown and the direction of the

transcription is indicated by arrows. **(B)** Genetic environment of *tsdA.* Transcriptional start site identified by 5' RACE (arrow) and upstream promoter motifs are depicted. The T-to-G substitution identified in *ΔmdbA* suppressor mutants is shown. **(B)** Alignment of *tsdA* and sigma factors σ^A and σ^H-dependent promoter consensus sequences from *C. diphtheriae* [115], *C. glutamicum* [160] and *M. tuberculosis* [164] are shown. Nucleotides conserved in consensus sequences are in bold, extended promoter nucleotides are in pink and transcriptional start site in green. Y = C or T; K=G or T. Core hexamers are underlined.

thiol-disulfide oxidoreductase, the *C. diphtheriae* C129S TsdA protein X-ray crystal structure was refined to 1.14 Å resolution with R-work and R-free factors equal to 11.4 and 13.3 %, respectively. The structure is a single continuous amino-acid chain covering 37-282 residues of the protein. Despite using the full-length 289-residue protein for crystallization, 36 N-terminal and 7 C-terminal residues are not visible in the structure, most likely due to flexibility of these fragments. The overall structure (Figure 4.2-A) represents a typical DsbA/MdbA protein family fold [57, 165] which incorporates a thioredoxin-like domain and an α-helical domain. The thioredoxin-like domain (residues 54-160 and 230-282) consists of a 5-strand β-sheet in an order of β1↑- β3↓- β2↓- β4↑- β5↓ and 6 flanking helices (one 3_{10}-helix, η1, and 5 α-helices, α2-4 and α9-10). The conserved catalytic CPFC motif, residues 126-129, forms the active site together with a conserved cis-Pro loop (residues T248 and P249) (Figure 4.2-B). The MdbA α-helical domain is comprised of 4 α-helices. The N-terminal end of the protein (residues 37-53 of the structure) is nearly unstructured with a short α1 helix. This fragment is visible due to stabilization by two neighbor protein molecules in crystals.

The C129S TsdA structure very closely resembles the wild-type protein structure obtained by our group (not shown) from the same crystallization conditions. Ser129 mimics exactly the catalytic Cys129 conformation in the wild-type structure (Figure 4.2-B). The rest of the protein is principally the same in both structures with RMSD (root-mean-square deviation of superimposed atoms in Å) equal to 0.181 Å for 237 aligned residues. Also, the wild-type TsdA structure deposited into PDB by Um *et al.* (PDB entry: 4PWO) does not differ remarkably from our structures [157].

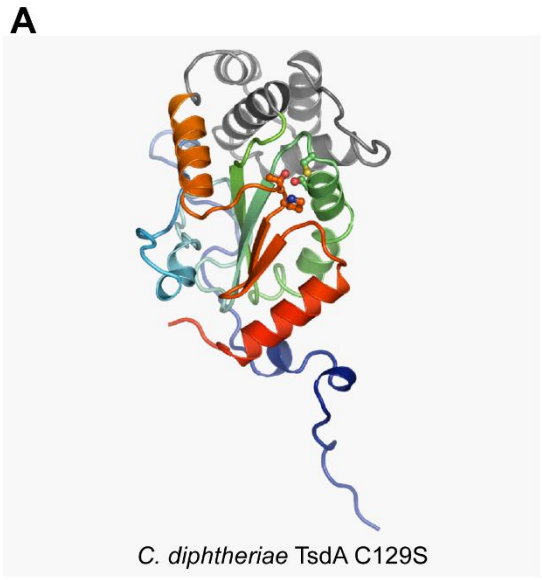
A
B
C
D
E
F
C. diphtheriae TsdA C129S
C. diphtheriae TsdA vs. C129S TsdA
B. subtilis BdbD vs. C129S TsdA
A. oris MdbA vs. C129S TsdA
C. diphtheriae MdbA vs. C129S TsdA

Figure 4.2. TsdA is an alternate disulfide bond-forming enzyme in *C. diphtheriae.* (A) Overall structure of the *C. diphtheriae* TsdA generated using Pymol. Rainbow colors from blue to red indicate the positions of N-terminal and C-terminal residues. Alpha-helical domains are shown in gray. **(B)** Structure superposition of active centers of *C. diphtheriae* TsdA structures of the C129S mutant (orange and green) and wild-type proteins (grey). The wild-type structure was shifted after superposition for better picture clarity. **(C-F)** Structure alignments of *C. diphtheriae* C129S TsdA (shown in green) with wild-type TsdA (**C**, PDB: 4PWO), *B. subtilis* BdbD (**D**, PBD: 3EU3), *A. oris* MdbA (**E**, PDB: 4Z7X) and *C. diphtheriae* MdbA (**F**, PDB: 5C00). *Crystallization and structural determination of TsdA C129S were performed by Jerzy Osipiuk and Andrzej Joachimiak and used with permission.*

The active site configuration is exactly the same as the one in our wild-type protein structure. The main difference between the structures is the N-terminus positioning of the TsdA C129S variant which is moved farther away from the wild type protein main body by 2-4 Å (Figure 4.2C). There are also slight changes in conformation of 66-77 and 245-247 loops. Those differences are unlikely to have any biological impact and probably result from slightly different crystallization conditions and crystal packing. RMSD for the C129S TsdA and the 4PWO.pdb structures is equal to 0.760 Å for 234 aligned residues.

The TsdA structure evidently has features characteristic of DsbA family protein (Figure 4.2). According to DALI server [166], the closest TsdA structural homolog is BdbD protein from *Bacillus subtilis*, described as an oxidoreductase containing a novel metal site [167] (PDB entry: 3EU3). The BdbD calcium binding site is not present in TsdA. The major difference between structures is the N-terminal part of the enzymes, which is significantly shorter in the case of BdbD (Figure 4.2-D). The alignment of those structures has Z score and RMSD equal to 20.8 and 2.0, respectively, for 186 equivalent residues. The next closest structural homologs are *Silicibacter pomeroyi* DSS-3 protein (3GYK PDB entry) and *Salmonella enterica* serovar Typhimurium ScsC protein [168] (4GXZ PDB entry) having Z scores equal to 19.2 and 18.3, and RMSD – 2.3 and 2.1, respectively.

4.2.3. Investigation of the regulation of *tsdA* expression

Even though TsdA is overexpressed in the Δ*mdbA* compensatory mutants, its expression in the wild-type strain under standard laboratory growth conditions is very

low [114]. In order to identify transcriptional regulators of *tsdA,* we utilized a bioinformatic approach to identify DNA motifs involved in regulation of *tsdA* expression. We scanned the region upstream of the *tsdA* transcriptional start site for motifs with homology to known transcriptional regulator binding sites. One motif with 32% identity to the consensus binding motif of the iron-dependent repressor DtxR (Diphtheria toxin repressor) [169] was identified (Figure 4.3-A). The DtxR binding site identified is localized upstream of the -10 core hexamer of the *tsdA* promoter. Interestingly, the T-to-G nucleotide change identified in the Δ*mdbA* compensatory mutants occurred in proximity to the predicted DtxR binding motif.

Acquisition of iron by bacterial pathogens is an important virulence trait due to the low iron availability within mammalian hosts [77]. DtxR controls iron uptake, diphtheria toxin production and virulence in *C. diphtheriae* [170-172]. To test regulation of *tsdA* by DtxR, we determined *tsdA* expression in a *dtxR* mutant strain by qRT-PCR and Western blotting using specific α-TsdA antibodies (Figure 4.3-B & C). We found no evidence of DtxR-dependent regulation of *tsdA* by these methods. As a complementary approach, we tested if *tsdA* expression is induced in low iron concentrations. To achieve this, *C. diphtheriae* cell cultures were depleted of iron by treatment for 2 hours with the iron chelator ethylenediamine-di-(o-hydroxyphenylacetic) acid (EDDA). Diphtheria toxin isolated from the culture medium by centrifugation was used as a positive control for iron-dependent protein expression. Bacterial cells and culture medium were subjected to Western blotting using α-TsdA and α-Diphtheria toxin, respectively. Depletion of iron did not affect TsdA protein expression, in contrast to the positive control diphtheria toxin that

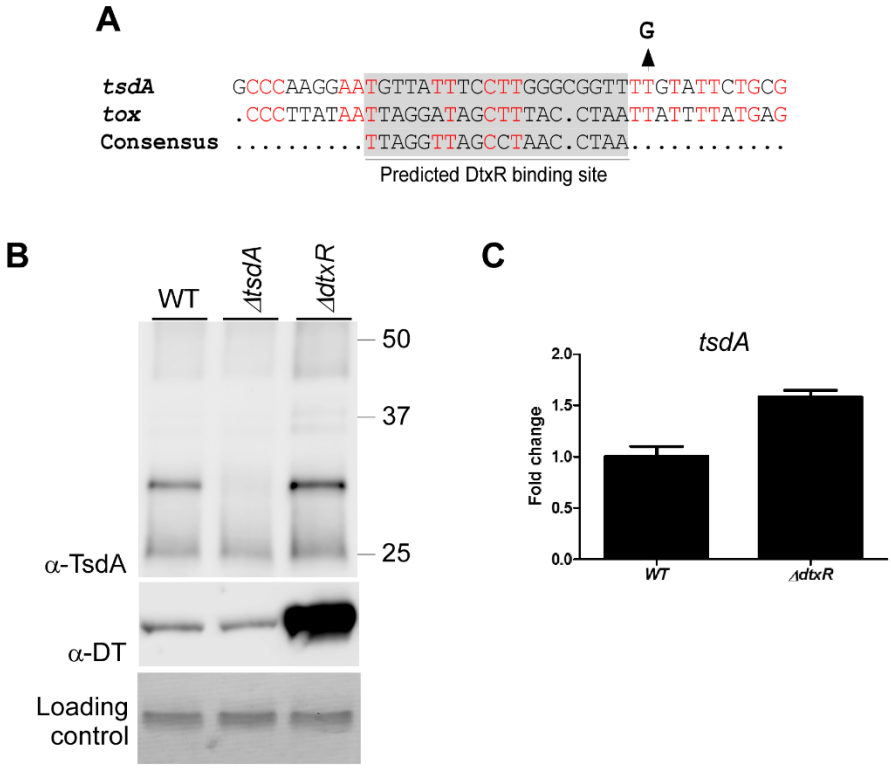

Figure 4.3. The iron-dependent regulator DtxR is not involved in *tsdA* transcriptional regulation. (A) Alignment of the predicted regulatory sequences of *tsdA* and *tox* (encoding Diphtheria toxin), and consensus DtxR binding sequence by Kunkle and Schmitt, 2003. Red represents conserved nucleotides. TheT-to-G substitution from a Δ*mdbA* suppressor mutant is shown. **(B)** Equal amounts of protein samples obtained from membrane fractions and culture medium of *C. diphtheriae* strains were subjected to immunoblotting with α-TsdA and α-Diphtheria toxin (DT). Coomassie blue staining of protein samples was used as loading control. **(C)** Expression of *tsdA* was determined by qRT-PCR. Average values of two experiments performed in triplicate are shown.

showed significantly higher levels of expression in cultures from cells lacking DtxR and containing low iron (Figure 4.3 & 4.4). Altogether, our data agree with the RNA sequencing studies by Wittchen, et al. [115] suggesting DtxR is not involved in *tsdA* transcriptional regulation.

4.2.4. Expression of *tsdA* is induced under heat stress

The physiological role of TsdA *in vivo* has not been elucidated. Because deletion of *tsdA* does not cause an apparent defect in disulfide bond formation under normal laboratory growth conditions [114], we hypothesized that TsdA has a role in resistance to stress conditions encountered within the host. To identify stress conditions that regulate expression of *tsdA*, we measured transcription of *tsdA* using a transcriptional reporter vector. Promoter-*gfp* transcriptional reporter vectors were generated by cloning *tsdA* wild-type promoter or T-to-G mutant promoter DNA immediately upstream of a promoter-less *gfp* reporter gene. To assay promoter activity, transcriptional fusion vectors were electroporated into *C. diphtheriae* Δ*tsdA*, and cells were exposed to various stress conditions. Promoter activity was determined by detecting GFP fluorescence using microscopy and microplate monitoring. As expected, strains expressing GFP from the T-to-G mutant *tsdA* promoter showed significantly increased levels of GFP fluorescence in contrast to strains expressing GFP from the wild-type *tsdA* promoter (Figure 4.5-A & B). No difference in GFP expression compared to untreated samples was observed when cells expressing GFP from the wild-type *tsdA* promoter were exposed to hemoglobin, hemin, manganese or H_2O_2. Additionally, a plate sensitivity assay did not show a

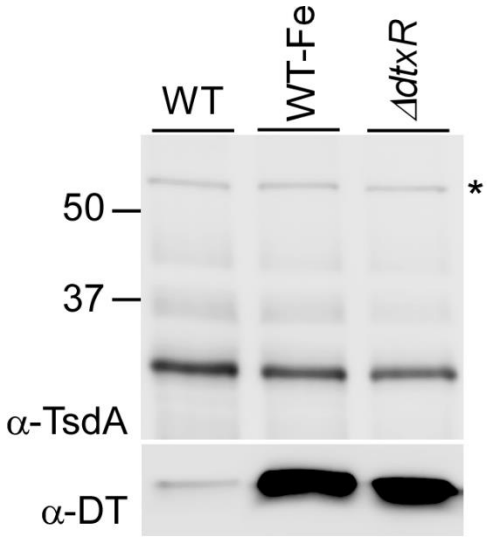

Figure 4.4. TsdA protein levels are not affected by iron depletion. (A) Equal amounts of protein samples obtained from membrane fractions and culture medium of *C. diphtheriae* strains were subjected to immunoblotting with α-TsdA and α-diphtheria toxin (DT). WT-Fe indicates protein samples from wild-type bacterial cultures depleted of iron by treatment for 2 hours with the iron chelator EDDA. A nonspecific band at approximately 50 kDa was used as a loading control (*).

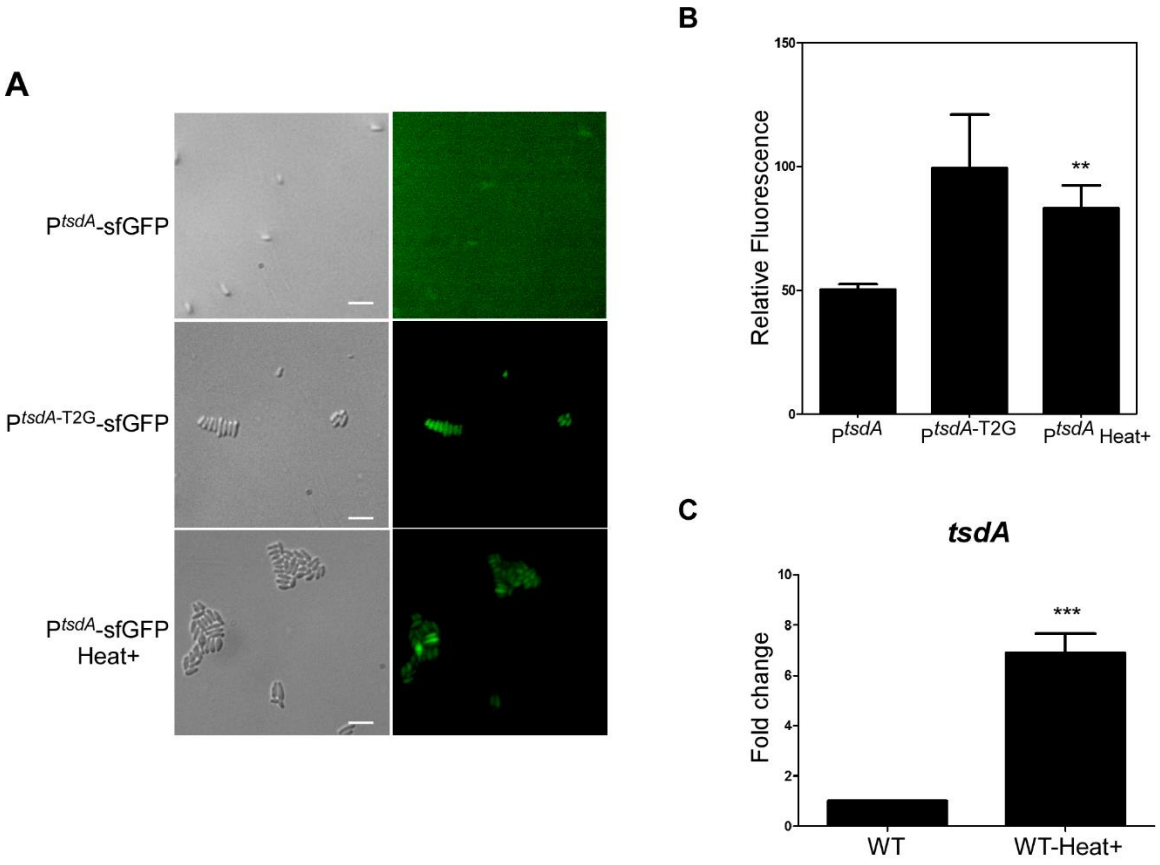

Figure 4.5. *tsdA* transcription is induced under heat stress. Activity of the *tsdA* promoter was determined using a P^{tsdA}-sfGFP transcriptional reporter by fluorescence microscopy **(A)** and measuring relative fluorescence using a microplate reader **(B)**. Error bars represent standard deviations from biological triplicates. **(C)** Expression of *tsdA* was determined by qRT-PCR. Average values of two experiments performed in triplicate are shown. Heat+ bacterial cultures were exposed to 40°C for 30 minutes. Scale bar indicates 5μm. **p<0.005 and ***p<0.0001 determined by unpaired two-tailed *t* test using GraphPad Prism.

difference in sensitivity to oxidative stress caused by iron, copper, manganese, DTT or H_2O_2 between Δ*tsdA* and the wild-type strain (data not shown).

Strikingly, increased *tsdA* promoter activity, indicated by significantly higher GFP fluorescence detected by microscopy and microplate monitoring (Figure 4.5-A & B), was observed when cells were exposed to heat stress (40°C) for 30 minutes. Consistent with these results, quantitative RT-PCR studies demonstrated that *tsdA* expression was induced nearly 8-fold after heat stress (Figure 4.5-C). These data strongly suggest that *tsdA* expression is regulated under heat stress, and that TsdA could be important for resistance of *C. diphtheriae* to heat shock.

4.2.5. The sigma factor σ^H is involved in *tsdA* transcriptional regulation

We next sought to identify transcription factors that mediate induction of *tsdA* under heat stress. Our bioinformatic analysis of the *tsdA* promoter region showed a putative alternative sigma factor σ^H binding sequence (Figure 4.1-B) [164].

Alternative sigma factors regulate gene expression, mainly when cells encounter extra or intracellular stress [173]. In particular, sigma factor σ^H is responsible for regulating expression of genes that are involved in survival when exposed to heat stress [160]. To characterize the potential role of sigma factor σ^H in *tsdA* expression, we created a non-polar in-frame deletion mutant of sigma factor σ^H in *C. diphtheriae.* Quantitative RT-PCR showed that cells lacking sigma factor σ^H had increased expression of *tsdA* compared to the wild-type strain. Interestingly, this phenotype was not rescued in a Δ*sigH* strain expressing sigma factor σ^H from a plasmid (Figure 4.6). Overexpression of *sigH* from a multicopy plasmid caused slow

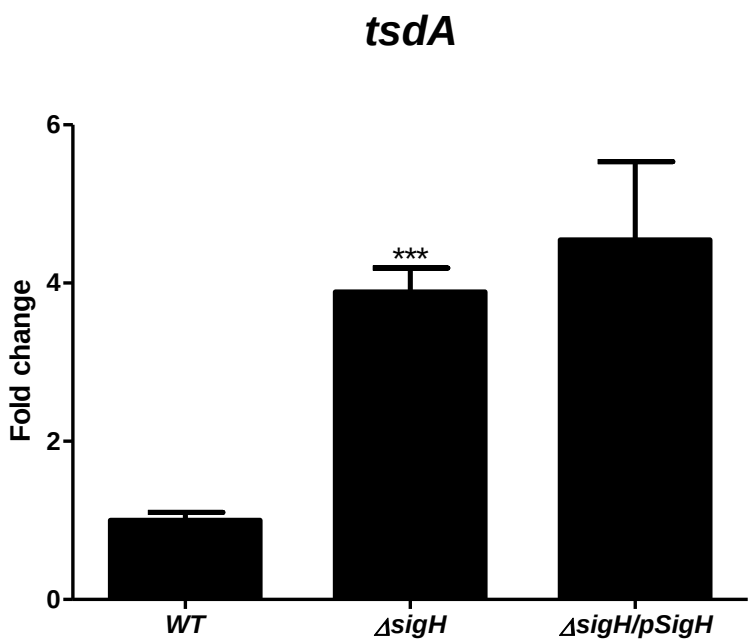

Figure 4.6. *tsdA* expression is induced in cells lacking the alternative sigma factor σ^H. Transcription of *tsdA* was determined by qRT-PCR. Average values of two experiments performed in triplicate are shown. ***p<0.0001 determined by unpaired two-tailed *t* test using GraphPad Prism.

bacterial growth (not shown), indicating that σ^H protein stoichiometry is important for its function. These data suggest that sigma factor σ^H is involved in regulation of *tsdA* expression, however further studies are necessary to elucidate its precise role in this process.

4.3. DISCUSSION

Bacterial gene expression is a tightly regulated process that is essential for cell adaptation to changing environments. This is especially critical for control of genes required by bacteria to cause infection. Gene expression can be regulated at the transcriptional, post-transcriptional or post-translational levels. Transcription is the first step in the gene expression process, and is controlled by binding of transcription factors to DNA regulatory regions, which can induce or block its initiation [174].

Here we report insights into the transcriptional regulation of a novel thiol-disulfide oxidoreductase named TsdA. The *tsdA* gene was identified in a screen for compensatory mutants lacking the MdbA disulfide bond forming machinery. Our X-ray crystallography analysis demonstrated that this gene codes for an alternate thiol-disulfide oxidoreductase named TsdA, which is structurally homologous to the main *C. diphtheriae* thiol-disulfide oxidoreductase MdbA but seems to have divergent functions.

Our group has previously demonstrated that wild-type *C. diphtheriae* expresses *tsdA* at very low levels; however, Δ*mdbA* compensatory mutants overexpress this gene. We investigated the remarkable effects of the single T-to-G

compensatory mutation resulting in an increase in *tsdA* transcription of over 30-fold. To initiate this analysis, we performed rapid amplification of cDNA ends and identified the precise transcriptional start site of *tsdA*. By scanning for conserved motifs upstream of the transcriptional start site, we determined the promoter region of this gene (Figure 4.1-B). Bacterial promoter regions are constituted by distinct motifs, including the -35 element, the -10 element, and the discriminator region, which are recognized by sigma factors to initiate transcription, and the UP element recognized by the α-subunits of the RNA polymerase. The sequences of these motifs determine the activity of a specific promoter [175]. The *tsdA* promoter has a weakly conserved sigma factor σ^A binding sequence (Figure 4.1-B). Sigma factor σ^A recruits RNA polymerase to housekeeping genes expressed during bacterial exponential growth phase [173]. A weakly conserved sigma factor σ^A promoter is expected to have low basal levels of expression, as promoters closely resembling consensus recognition sequences often have higher activities [175]. This is consistent with our transcriptional reporter analysis showing very low GFP reporter fluorescence when cells are grown to mid-exponential phase using standard laboratory growth conditions (Figure 4.5-A & B).

The T-to-G compensatory mutation occurred at position -14 of the *tsdA* promoter, resulting in a TG dinucleotide at positions -15 and -14. A TG dinucleotide at these positions results in an extended sigma σ^A promoter, lowering the thermal energy required to form an open RNA polymerase initiation complex [115, 160, 162, 163]. Extended sigma σ^A elements are common in non-canonical −10 regions, and they result in increased basal strength of the promoter and increased transcript levels

[161]. Because the wild-type *tsdA* promoter has low activity (Figure 4.5-A & B), a bias for selecting a mutation that enhances *tsdA* promoter strength confers a biological benefit to cells lacking the MdbA disulfide bond-forming machinery.

Surprisingly, compensatory mutations in genes that could be involved in regulation of *tsdA* expression have not been identified. Therefore, we used a bioinformatic approach to identify transcription factors that affect *tsdA* expression regulation. We identified a predicted DtxR binding site in the *tsdA* promoter region (Figure 4.3-A). DtxR is a global iron-dependent regulator which controls expression of an extensive number of genes in *C. diphtheriae* [115, 176]. DtxR has positive and negative effects over genes involved in iron homeostasis and virulence [176], including the potent diphtheria toxin. Experimental approaches did not provide evidence that *tsdA* expression is regulated by DtxR or iron-limiting conditions (Figure 4.3-B & C). This is in contrast to the diphtheria toxin positive control (Figure 4.3 & 4.4). Contrary to our bioinformatic analysis predictions, the experimental data indicate that *tsdA* is not regulated by DtxR.

Deletion of thiol-disulfide oxidoreductases often results in attenuation of bacterial pathogenicity [28]. In Actinobacteria, it also results in growth defects [67]. However, a deletion mutant of *tsdA* did not have any obvious phenotypic changes when grown under standard laboratory conditions [114]. To get insights into the physiological roles of this enzyme *in vivo,* we aimed at identifying the specific environmental conditions that affect its expression. Using our transcriptional reporter construct, we tested activity of *tsdA* promoter upon exposure to stress conditions. Conditions in which oxidoreductases are required for resistance to stress [52, 64], as

well as stress conditions encountered within the host, were tested [76]. We found that *tsdA* promoter activity is significantly increased when cells are exposed to heat stress (40°C); this was demonstrated using transcriptional reporter assays and quantitative RT-PCR of *tsdA*. To our knowledge, this is the first report of a thiol-disulfide oxidoreductase regulated by heat stress.

Development of fever is an important survival mechanism that vertebrates employ during infection to limit pathogens growth [177]. Elevated temperatures can affect virulence phenotypes and increase susceptibility to serum-induced bacterial lysis [178, 179]. Disulfide bonds are likely to confer stability to proteins facing high temperatures in extremophile bacteria [180, 181]. It is expected that bacterial groups secreting high levels of proteins predicted to contain disulfide bonds would be negatively affected by heat shock. About 60% of the secretome of Gram-positive Actinobacteria like *C. diphtheriae* are predicted to contain disulfide bonds [49]. The expression pattern of TsdA suggests a role for this enzyme in resistance to heat stress, which could be encountered by *C. diphtheriae* during presentation of fever in the host. Increased production of TsdA would be especially important to ensure stability and function of disulfide bond-containing substrates like cell division proteins, as well as critical virulence factors such as diphtheria toxin and SpaA pilus.

During our analysis of the *tsdA* promoter region, we identified a DNA binding motif for alternative sigma factor σ^H (Figure 4.1-B), which regulates gene expression of heat shock genes [160]. Since *tsdA* expression is induced under heat stress, we aimed at elucidating if this alternative sigma factor is involved in transcriptional regulation of *tsdA.* To answer this question, we created a deletion mutant of the *sigH*

gene, encoding alternative sigma factor σ^H, and determined *tsdA* expression in this strain. We observed increased expression of *tsdA* compared to the wild-type strain in cells lacking *sigH*, indicating that the alternative sigma factor σ^H is involved in *tsdA* transcriptional regulation. Bacterial sigma factors typically function as positive regulators of gene expression. The observation that *tsdA* expression is increased in Δ*sigH* under non-stress conditions was unexpected and suggests indirect regulation of *tsdA* by sigma factor σ^H. Sigma factors guide positioning of RNA polymerase at promoters and mediate transcription initiation, however the transition from transcriptional initiation to elongation can be blocked, so that RNA polymerase activity is induced only under specific environmental changes [175, 182]. It is possible that deletion of *sigH* removes blockage of *tsdA* transcriptional elongation, allowing other sigma factors to recognize the *tsdA* promoter region and mediate *tsdA* expression. Alternatively, sigma factor σ^H could regulate a repressor of *tsdA* expression, so that in the absence of *sigH,* this negative regulation is abrogated. Future studies are warranted to dissect the specific mechanism of *tsdA* transcriptional regulation.

CHAPTER 5. Oxidative Folding is Required for Stability of Penicillin Binding Proteins in *Corynebacterium diphtheriae.*

5.1. INTRODUCTION

Accurate disulfide bond formation is essential for proper folding, stability, resistance to protease degradation, and function of exported proteins [27]. Even though disulfide bonds can form spontaneously, this reaction occurs slowly and with a high error rate [183]. To overcome this, eukaryotic and prokaryotic cells encode specialized machineries that efficiently catalyze disulfide bond formation [27]. The oxidative protein folding machinery in the Gram-positive Actinobacterium *C. diphtheriae* is constituted by the thiol-disulfide oxidoreductase MdbA (Monoderm disulfide bond-forming) [56]. Corynebacterial MdbA is a transmembrane protein, and harbors a thioredoxin-like fold, an extended α-helical domain, and a CxxC motif in its active site, which are common features of thiol-disulfide oxidoreductases [56-58].

MdbA is required for growth, adhesive pilus assembly, toxin assembly, and virulence in *C. diphtheriae.* This indicates that MdbA has broad substrate specificity and constitutes the major disulfide bond-forming machinery in *C. diphtheriae* [56]. Proteomic analysis of Actinobacteria determined that over 60% of their secretome contains even numbers of cysteines, suggesting a bias for proteins that contain disulfide bonds [49]. Therefore, it is not surprising that deletion of *mdbA* causes pleotropic effects. Unlike Gram-negative bacteria where disulfide bond-forming pathways are dispensable for growth [67], absence of MdbA causes a significant temperature sensitive growth defect in *C. diphtheriae,* suggesting that MdbA catalyzes folding of growth factors essential for cell division [56]. Similarly, MdbA is essential for growth in *A. oris* and *C. matruchotii* [52, 55].

The bacterial cell wall is constituted by a peptidoglycan mesh that maintains cell shape, and keeps the cell from lysing due to turgor pressures [184, 185]. In prokaryotes, penicillin binding proteins (PBPs) are involved in cell elongation and division, constituting the essential machine that builds bacterial peptidoglycan (Figure 5.1) [184, 185]. PBPs are transmembrane proteins that can have transglycosylation and/or transpeptidation activity, and are responsible for polymerization and cross-linking of the glycan chains connected by short peptides that comprise the peptidoglycan mesh [186]. A bioinformatics analysis demonstrated that many corynebacterial PBPs contain multiple cysteine residues [114]. *mdbA* deletion in *C. diphtheriae* disrupts the rod shape, causes abnormal nascent peptidoglycan distribution, and increases sensitivity to PBP-targeting β-lactam antibiotics [56]. Even though single PBPs are not essential for cell viability, as shown in *C. glutamicum,* double deletion of *pbp* genes encoding PBP1A and PBP1B, as well as PBP1A and PBP2A results in chains of smaller, round cells [187].

In *Corynebacteria*, insertion of new peptidoglycan into the cell wall occurs at the poles and at the midpoint of growing cells [188]. Nascent peptidoglycan synthesis and distribution can be analyzed using a fluorescent antibiotic, fluorescent vancomycin (Van-Fl), which binds to the D-Ala, D-Ala moiety of unmodified nascent peptidoglycan, denoting active cell wall biosynthesis [189]. Staining by Van-FL showed absence of nascent peptidoglycan synthesis at the cell poles, and mislocalized fluorescence around *C. glutamicum pbp* mutant cells [187]. These phenotypes are strikingly similar to the *mdbA* mutant [56], and support the hypothesis that PBPs are substrates of MdbA. In agreement, round shape morphology has also

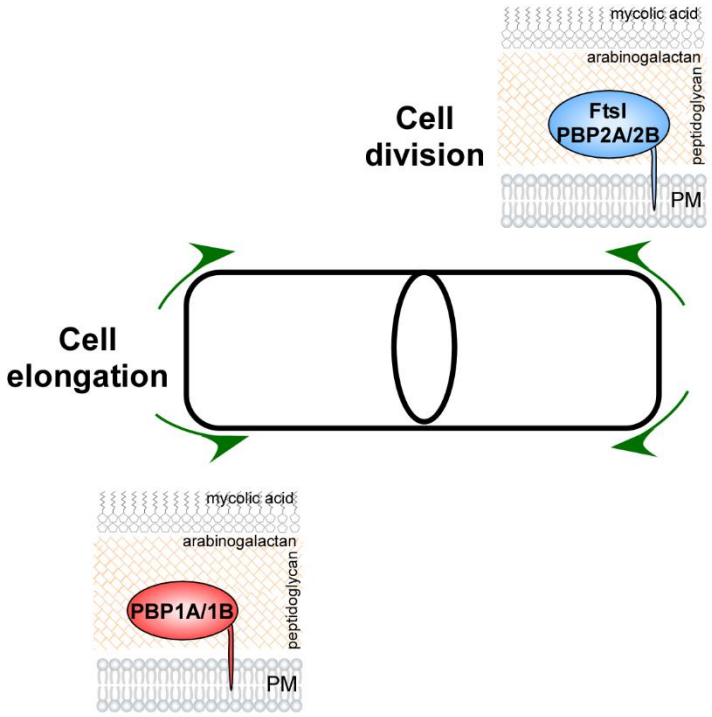

Figure 5.1. Localization of Penicillin binding proteins in *Corynebacterium.* Depicted are penicillin binding proteins (PBPs) involved in insertion of nascent peptidoglycan at the cell poles (PBP1A/1B) and mid-cell (FtsI, PBP2A/2B), resulting in cell elongation and septum formation, respectively. Modified from Letek, *et al*. 2008 [192].

been observed in *E. coli* and *Bacillus subtillis* upon alteration of cell wall biosynthesis [190, 191]. Given that the essentiality of the disulfide bond-forming machinery for growth in Actinobacteria is not completely understood, an analysis of putative substrates of MdbA involved in peptidoglycan biosynthesis will reveal novel aspects of the oxidative folding pathways. In this chapter, I demonstrate that in the absence of *mdbA*, stability and function of multiple PBPs is affected. As it has been observed with other MdbA substrates, protein levels of PBP1A and PBP1B are significantly lower in the *mdbA* mutant.

5.2. RESULTS

5.2.1. Analysis of cell division proteins containing multiple cysteine residues

To initiate our analysis of the essentiality of the disulfide bond forming machinery in *C. diphtheriae* we employed a bioinformatic approach to identify putative cell division proteins that could form disulfide bonds *in vivo.* Since MdbA catalyzes oxidative folding of substrates as they are exported outside of the cell, I focused my analysis on proteins that contained signal peptides as determined by the SignalP 4.1 server [193]. I identified a list of Cys-containing putative cell division proteins predicted to be involved in both cell division and elongation (Table 5.1). Of 11 secreted cell division candidates identified, 7 (64%) contained more than 2 cysteine residues and 4 (36%) were predicted to form disulfide bonds by Dianna 1.1 and Cyscon web servers [194].

Noticeably, both class A high molecular weight (HMW) PBPs, PBP1A and PBP1B, which present transglycosylase and transpeptidase domains, were predicted

Table 5.1. *C. diphtheriae* cell division proteins predicted to be exported

Cell division protein	Predicted activity	Cys Residues	Predicted Disulfide bonds
PBP1A	Transpeptidase/Transglycosilase Cell elongation	2	1
PBP1B	Transpeptidase/Transglycosilase Cell elongation	9	4
PBP2A	Transpeptidase/Cell division	2	0
PBP2B	Transpeptidase/Cell division	4	2
PBP3 (FtsI)	Transpeptidase/Cell division	0	0
D-Ala-D-Ala carboxypepidase	D-Ala-D-Ala carboxypepidase	2	0
D-Ala-D-Ala carboxypeptidase	D-Ala-D-Ala carboxypepidase	0	0
FtsK	Cell division	12	6
FtsW	Cell division	2	0
FtsQ	Cell division	1	0
RodA	Apical lipid II flipase Cell elongation	1	0

Sources: *C. diphtheriae* NCTC13129 genome (See https://www.genome.jp/); [114, 187, 192, 200, 201]. Predicted secreted proteins were identified using the SignalP 4.1 server. Number of predicted disulfide bonds were determined using the Dianna 1.1 and Cyscon web servers.

to form at least one disulfide bond. Class A HMW PBPs are proposed to be involved in apical peptidoglycan insertion and are required for cell elongation [187]. Of the class B HMW PBPs (PBP2A, PBP2B, PBP3) presenting only a transpeptidase domain, exclusively PBP2B was predicted to form 2 disulfide bonds. Class B HMW PBPs are proposed to be involved in septal peptidoglycan insertion and are required for cell division [187]. It is important to note that both class A and class B HMW PBPS localize at the poles and midcell in *C. glutamicum,* with the exception of PBP3 (FtsI) which is exclusively found at the septum [195]. FtsK, a complex multi-domain component of the divisome [196], presented the highest number of cysteine residues and predicted disulfide bonds among identified cell division proteins. FtsK is a DNA translocase and is involved in assembly of the cell division apparatus [197, 198]. Notably, the FtsK N-terminal domain, which is essential for cell viability in *E. coli*, is localized within the membrane and in the reducing environment of the cytoplasm [199].

5.2.2. PBP1A and PBP1B are not redundant in *C. diphtheriae*

In *C. glutamicum* PBP1B and PBP2B are synthetically lethal and a PBP1A/1B double mutant is phenotypically similar to the *C. diphtheriae mdbA* mutant [56, 187]. We chose to focus on the class A HMW PBPs, PBP1A and PBP1B for further characterizations, as they are also predicted to form the maximum and minimum number of disulfide bonds in *C. diphtheriae* PBPs, respectively (Table 5.1). Bioinformatic analysis employing the Dianna 1.1 and Cyscon web servers [194] predicts that one disulfide bond is formed in PBP1A and 4 disulfide bonds are formed

in PBP1B (Table 5.1 and Figure 5.2A). The primary amino acid sequence and structural modeling of both PBP1A and PBP1B reveals that predicted disulfide bonds in the transpeptidase domains are conserved and localize near the active site of these enzymes (Figure 5.2A-C). To examine the role of these proteins in *C. diphtheriae*, I generated non-polar, in-frame deletions of *pbp1a* and *pbp1b* using a previously described method [19]. *C. diphtheriae* mutants lacking *pbp1a* or *pbp1b* were unable to divide correctly, becoming chained and clumped independently of the growth temperature (Figure 5.3). The *pbp1A* mutant showed abundant cell clumps, but partially maintained the rod shape morphology. However, Δ*pbp1A* cells looked wider compared to the wild-type strain. These phenotypes suggest a role for PBP1A in insertion of peptidoglycan at the mid-cell and septum formation. This is in contrast to the proposed role of PBP1A in *C. glutamicum* cell elongation [187]. The *pbp1B* mutant showed chains and round morphology, which suggested a defect in cell elongation. Since nascent peptidoglycan insertion at the cell poles is responsible for cell elongation in *C. diphtheriae* [188], these data suggests that similar to *C. glutamicum* PBP1B [187], *C. diphtheriae* PBP1B localizes to the cell poles and is involved in peptidoglycan insertion at this site. Deletion of multiple PBPs is required to affect cell shape and viability in *C. glutamicum, E. coli* and *B. subtillis* [187, 202, 203]. Because *C. diphtheriae* cells lacking single PBPs present a strong cell division defect, our findings suggest that these proteins have non-redundant functions. Attempts to complement the *pbp* mutants *in trans* by electroporating a multi-copy plasmid expressing wild-type PBP1A and PBP1B into the respective deletion strains failed, despite multiple attempts. Nevertheless, the same plasmids successfully replicated

A

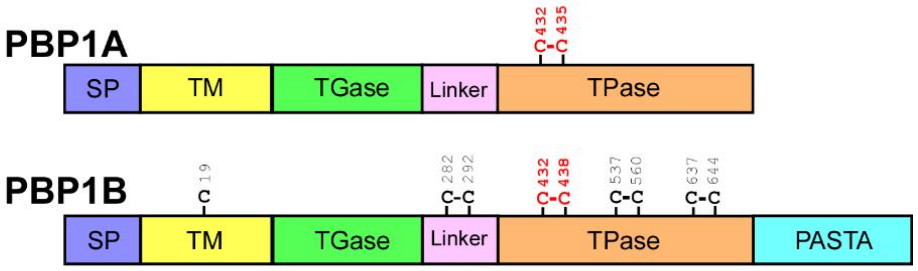
PBP1A
C 432
C 435
SP
TM
TGase
Linker
TPase
PBP1B
19
C
282
292
C-C
C 432
C 438
537
560
C-C
637
644
C-C
SP
TM
TGase
Linker
TPase
PASTA

B

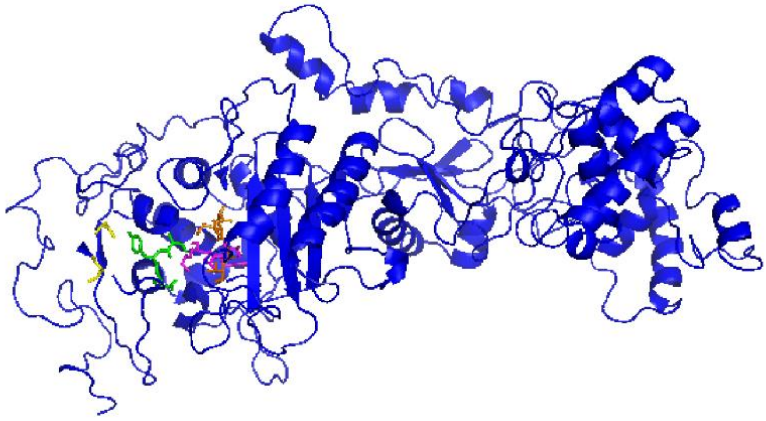

C

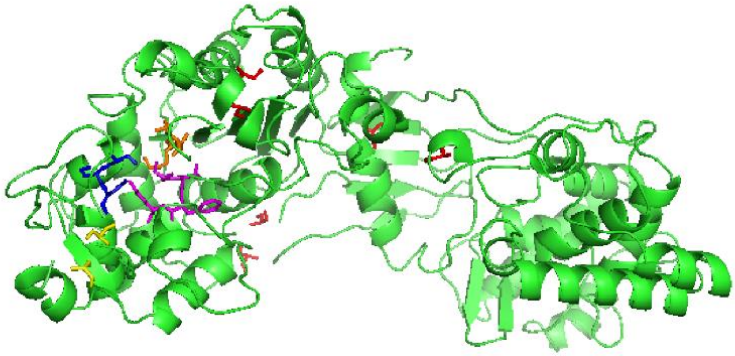

Figure 5.2. Class A HMW Penicillin Binding Proteins in *C. diphtheriae.* (A) The *C. diphtheriae* PBP1A and PBP1B primary amino acid schematic based on BLAST search. SP: signal peptide, TM: transmembrane domain, TGase: transglycosilase domain, TPase: transpeptidase domain. Predicted disulfide bonds determined by Dianna 1.1 and Cyscon servers are shown. Conserved Cys residues adjacent to the TPase active site are denoted in red. **(B-C)** Structural models of the PBP1A **(B)** and PBP1B **(C)** proteins determined by the Phyre2 server. Red: Cys residues. Pink, green/blue and orange: S*TFK, SYN and KTGT signature sequences that contribute to the catalytic site of the TPase domain. The conserved Cys residues adjacent to the TPase active site are denoted in yellow sticks.

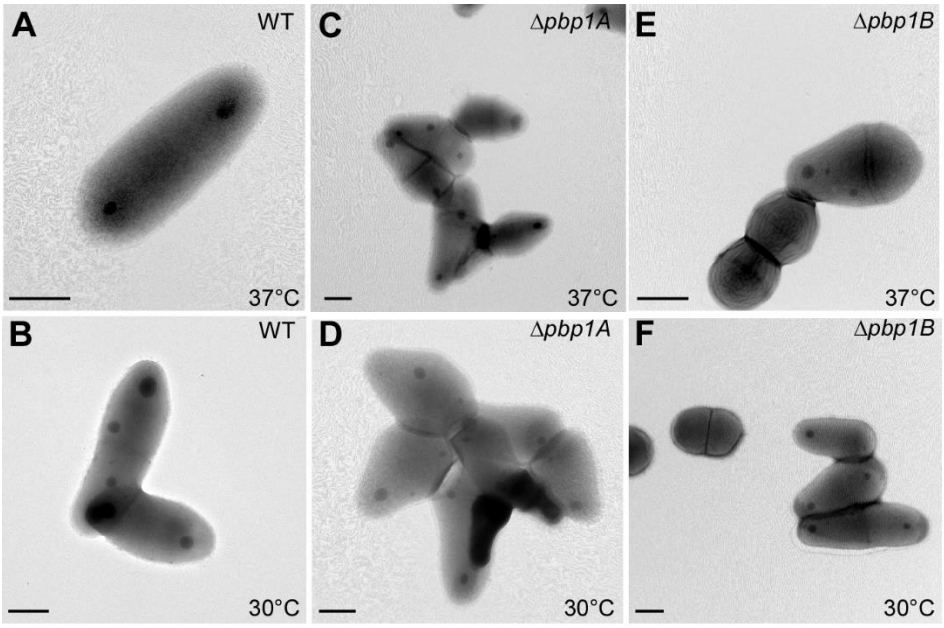

Figure 5.3. *pbp1A* and *pbp1B* are required for normal cell morphology in *C. diphtheriae.* (A-F) Stationary cultures of C*. diphtheriae* strains grown at 30°C in HIB were diluted into fresh media and incubated at 30°C or 37°C for 5 hours. Cells were harvested and immobilized on carbon-coated nickel grids. Samples were stained with 1% uranyl acetate and analyzed by transmission electron microscopy. Scale bars indicate 0.5 µm.

in the *mdbA* mutant (See section 5.2.3). These results suggest that overexpression of PBPs from a multi-copy plasmid is lethal to *C. diphtheriae*.

5.2.3. Overexpression of PBP1A/1B/2B rescues the defects of the Δ*mdbA* mutant

Studies in *B. subtillis* and *E. coli* showed that some PBPs are substrates of oxidoreductase enzymes, and disulfide bond formation and breakage is important for their function [39, 80, 204]. Deletion of *mdbA* causes a cell division defect and abnormal nascent peptidoglycan distribution in *C. diphtheriae* [56]. Furthermore, the remarkable similarity of the *pbp* mutant phenotypes (Figure 5.4) to the *C. diphtheriae mdbA* mutant grown at the non-permissive temperature supports the proposal that PBPs are substrates of MdbA. To begin to test this hypothesis, recombinant plasmids expressing individual or multiple combinations of PBPs predicted to form disulfide bonds *in vivo* (PBP1A, PBP1B and PBP2B) were electroporated into the *C. diphtheriae* Δ*mdbA* mutant. The cell morphology of the resulting strains was examined by transmission electron microscopy. Simultaneous overexpression of all PBPs predicted to form disulfide bonds *in vivo* rescued the cell morphology defect of the Δ*mdbA* mutant grown at the non-permissive temperature (37°C). However, expression of individual proteins or a combination of PBP1A and PBP1B did not. The results suggest that in the absence of *mdbA*, oxidative folding and function of multiple PBPs predicted to form disulfide bonds is disrupted. Additionally, this data is consistent with my previous results indicating that PBP1A and PBP1B have non-redundant functions.

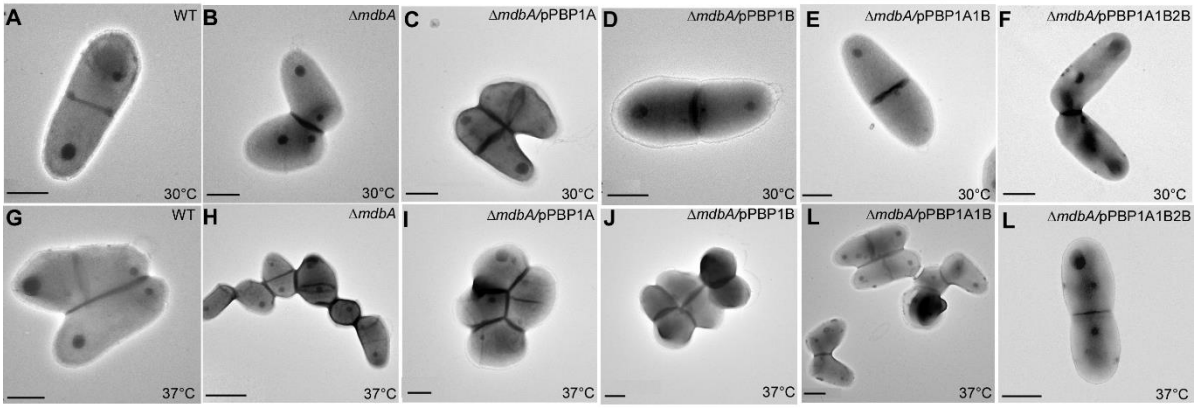

Figure 5.4. Ectopic expression of multiple Cys-containing PBPs rescues the Δ*mdbA* temperature-sensitive phenotype. (A-L) Stationary cultures of *C. diphtheriae* strains grown at 30°C in HIB were diluted into fresh media and incubated at 30°C or 37°C for 5 hours. Cells were harvested and immobilized on carbon-coated nickel grids. Samples were stained with 1% uranyl acetate and analyzed by transmission electron microscopy. Scale bars indicate 0.5 µm.

5.2.4. The disulfide bond forming machinery is required to maintain basal PBP protein levels

Disulfide bonds are important for proper folding and stability of secreted proteins [27]. Unfolded proteins are more sensitive to proteolysis degradation than proteins in their native state [205, 206]. Since overexpression of multiple Cys-containing PBPs rescues the cell division defect of Δ*mdbA*, I propose that in the absence of MdbA, PBPs fail to form native disulfide bonds. This likely leads to PBPs misfolding and subsequent degradation by proteases [27]. If disulfide bond formation is required for folding and stability of PBPs *in vivo,* I anticipated that decreased quantities of PBPs will be detected in Δ*mdbA* cells compared to the wild-type strain.

I employed Western blot analysis of *C. diphtheriae* protoplasts using affinity-purified antibodies specific for PBP1A (α-PBP1A) and PBP1B (α-PBP1B), to assess stability of PBPs *in vivo*. *pbp1A* is predicted to encode a 77.25 kDa transmembrane protein. Similarly, *pbp1B* is predicted to encode a 83.46 kDa transmembrane protein. Immunoblotting with α-PBP1A and α-PBP1B antibodies detected bands that migrated at the expected molecular masses in the wild-type strain, but that were absent in the corresponding deletion mutants (Figure 5.5A and B). PBP1A protein levels in the *mdbA* mutant were comparable to that of the wild-type strain (Figure 5.5A). However, a reduction in the PBP1A signal was observed in Δ*mdbA* cells expressing a catalytically inactive MdbA protein, where cysteine 91 within the active site was replaced with alanine (pCxxA). Deletion of *mdbA* caused a significant decrease in PBP1B protein levels of cells grown at the permissive temperature (30°C), as compared to the wild-type strain (Figure 5.5B). PBP1B protein levels were restored

by expression of *mdbA in trans* (pMdbA). However, expression of the catalytically inactive MdbA variant (pCxxA) failed to restore the wild-type phenotype. Furthermore, PBP1B protein levels were restored in the Δ*mdbA* compensatory mutant (Δ*mdbA*-S1) that overexpress the thiol-disulfide oxidoreductase TsdA described in chapter 4. These data suggest that in absence of active MdbA, oxidative folding of PBPs is disrupted and PBP proteins are unstable. This results in a decreased amount of PBPs that are successfully folded and embedded in the cell membrane to perform their function, which agrees with the cell division defect observed in *mdbA* mutant cells (See Figure 5.4H).

To ensure that the decreased amount of PBP proteins detected in the *mdbA* mutant was due to the oxidative folding defect of this strain, I determined expression of *pbp1A* and *pbp1B* by quantitative RT-PCR. Remarkably, the quantitative RT-PCR analysis demonstrated that the Δ*mdbA* strain significantly overexpresses both *pbp1A* and *pbp1B* compared to the wild-type strain (Figure 5.5C and D). Overexpression of these genes did not result in increased levels of PBP1B protein, but could explain the wild-type levels of PBP1A protein detected in the *mdbA* mutant strain. Furthermore, expression of *pbps* in the Δ*mdbA* compensatory mutant was comparable to the wild-type strain, confirming that restoration of PBP protein levels is likely due to oxidative folding of PBPs by the alternate oxidoreductase TsdA and not the result of increased expression of these genes.

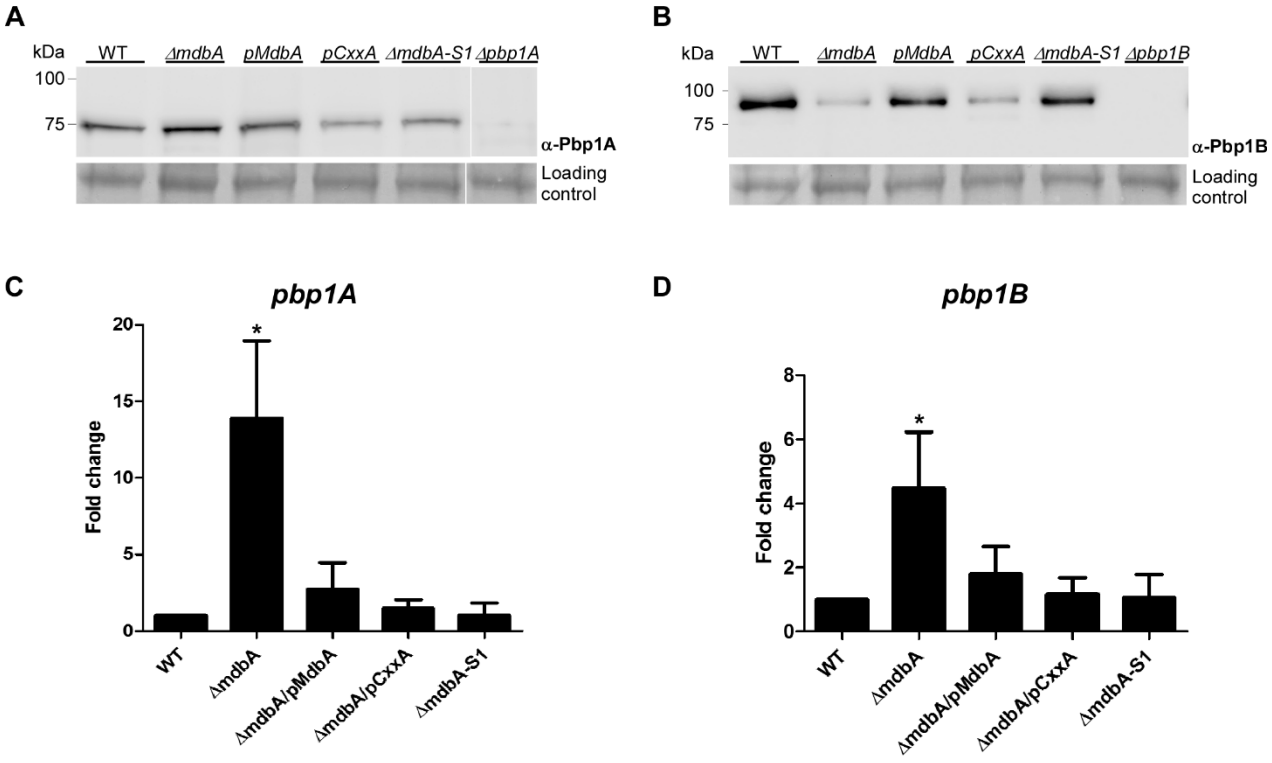

Figure 5.5. Cells lacking active MdbA present reduced PBP stability. (A-B) Equal amounts of protein samples from *C. diphtheriae* strains were subjected to SDS-PAGE, followed by immunoblotting with α-PBP1A and α-PBP1B. Molecular mass markers (kDa) are indicated. Coomassie blue staining of protein samples was used as loading control. A representative image of three experiments is shown. **(C-D)** Expression of *pbp1A* and *pbp1B* in *C. diphtheriae* strains was determined by qRT-PCR analysis. Average values of two experiments performed in triplicate are shown. *p<0.05 determined by unpaired two-tailed *t* test using GraphPad Prism. Δ*mdbA*-S1 indicates Δ*mdbA* suppressor mutant 1.

5.2.5. Growth in synthetic minimal media rescues the Δ*mdbA* cell division defect

The temperature sensitive phenotype of the *mdbA* mutant was puzzling. Since *mdbA* is dispensable for growth of *C. diphtheriae* at 30°C but not at 37°C, it was postulated that additional oxidoreductase enzymes compensate for the loss of MdbA at low replication rates. In agreement, the Δ*mdbA* compensatory mutant S1, which overexpresses the alternate oxidoreductase TsdA, presented wild-type levels of PBP1A and PBP1B (See section 5.2.4). To test this hypothesis, I examined cell morphology in low replication rate conditions by growing cells in synthetic minimal media. Overnight cultures in rich media (HIB) incubated at 30°C were diluted into fresh synthetic minimal media or rich media and incubated at 37°C for 5 hours. Bacterial cultures were then processed for transmission electron microscopy analysis. Remarkably, the Δ*mdbA* strain grown in synthetic minimal media at 37°C maintained a cell morphology similar to the wild-type strain (Figure 5.6A and D). In addition to forming the characteristic clumps and chains, and losing the rod shape morphology (See Figure 5.4H); a higher number (29%) of Δ*mdbA* cells grown in rich media died when cultures were incubated at 37°C (Figure 5.6C). This is demonstrated by increased staining with uranyl acetate of dead cells (denoted by arrow heads in Figure 5.6C). These data suggests that at low replication rates achieved by incubation in rich media at 30°C (See figure 5.4B) or in synthetic minimal media at 37°C (Figure 5.6D), *mdbA* mutant cells are capable of folding enough disulfide bond-containing cell division proteins (for example PBPs) to maintain a cell morphology similar to the wild-type strain.

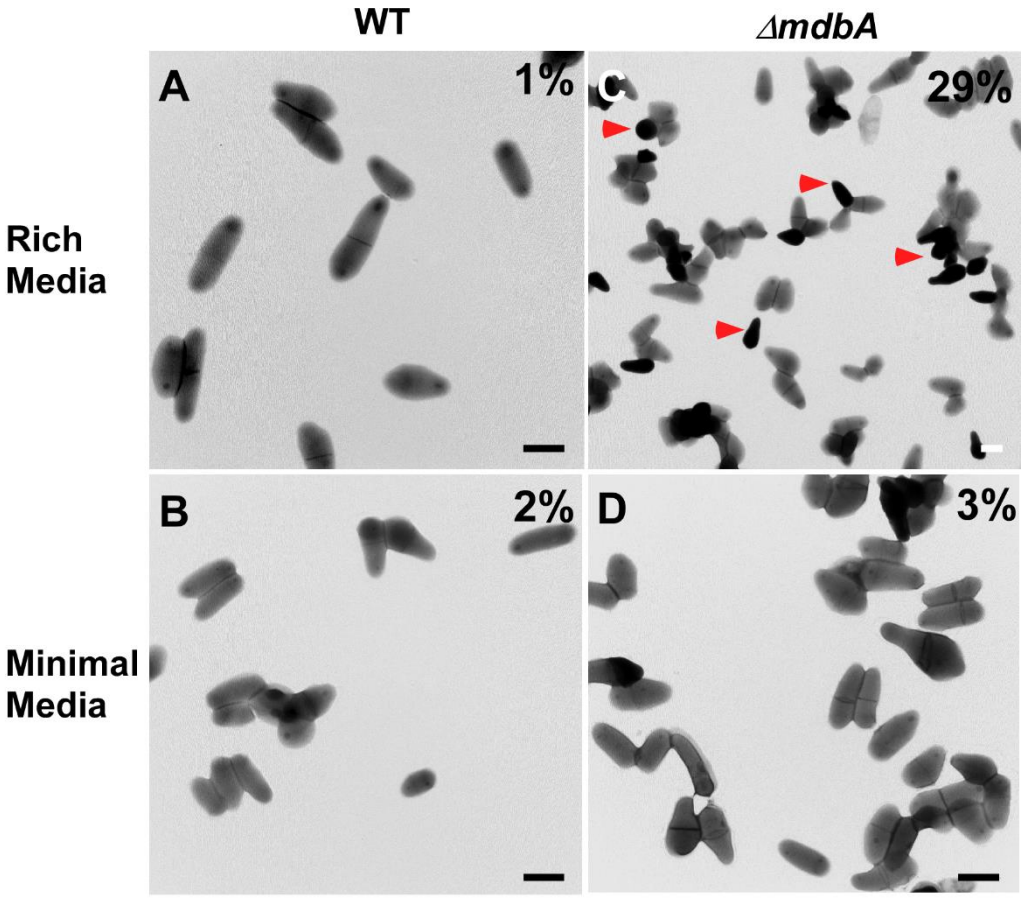

Figure 5.6. Growth in synthetic minimal media rescues the Δ*mdbA* cell division defect. (A-D) Stationary cultures of C*. diphtheriae* strains grown at 30°C in rich media were diluted into fresh rich or minimal media and then incubated at 37°C for 5 hours. Cells were harvested and immobilized on carbon-coated nickel grids. Samples were stained with 1% uranyl acetate and analyzed by Transmission electron microscopy. Dead cells show increased staining with uranyl acetate and are denoted by red arrowheads. The percentage of dead cells per sample is indicated in the upper right corner of each representative micrograph. Scale bars indicate 0.5 µm.

5.3. DISCUSSION

The requirement of the disulfide bond forming machinery for growth in Actinobacteria has not been previously studied. Results discussed in this chapter provide insights into the dependence on disulfide bond formation for cell division. The major oxidoreductase MdbA is essential for cell viability in *A. oris* and *C. matruchotii* [52, 55], but deletion of *mdbA* results in a temperature-sensitive growth defect in *C. diphtheriae* [56]. This makes *C. diphtheriae* a more suitable model system to study the requirement of the disulfide bond forming machinery for viability. The cell division and peptidoglycan distribution defects observed in a Δ*mdbA* mutant grown at the non-permissive temperature lead to the logical hypothesis that cell division proteins are substrates of MdbA. I employed a bioinformatic approach to identify putative MbdA substrates involved in cell division, by evaluating their predicted location within the cell, as well as the number of cysteine residues and predicted disulfide bonds. My bioinformatic analysis identified PBP1A, PBP1B, PBP2B and FtsK as prospective candidates to be MdbA substrates involved in cell division *in vivo.* By genetically and biochemically characterizing two representative putative substrates, PBP1A and PBP1B, I have established that these two components of the cell wall biosynthesis machinery require the major disulfide bond-forming machine MdbA for stability and function.

In *B. subtillis*, a sporulation-specific HMW class B PBP contains two conserved cysteine residues near the catalytic site of the transpeptidase domain, that are important for protein stability and peptidoglycan synthesis during sporulation [82]. These cysteine residues form a disulfide bond that is required for redox regulation of

PBP enzymatic activity [80, 81, 207]. Similarly, a disulfide bond forms between corresponding conserved cysteine residues in the homologous PBPA of *M. tuberculosis* [208, 209]. I have shown that both class A PBPs in *C. diphtheriae* have a conserved predicted disulfide bond close to the active site of the transpeptidase domain. The conservation and positioning of these cysteine residues suggest they might play a role for transpeptidase enzymatic activity. Even though a role for cell elongation has been proposed for PBP1A and PBP1B homologs in *C. glutamicum* [187], my data indicate that PBP functions are not completely conserved between *C. diphtheriae* and *C. glutamicum.* By electron microscopy, both Δ*pbp1A* and Δ*pbp1b*, present strong but divergent cell division defects (Figure 5.3). Divergent cell morphology phenotypes observed in Δ*pbp1A* and Δ*pbp1b* could be due to a C-terminal PASTA (penicillin-binding protein and serine/ threonine kinase associated domain) domain that is present in PBP1B but absent in PBP1A (Figure 5.2A). PASTA domains are found at the C-terminus of some PBPs and eukaryotic-like protein serine/ threonine kinases (PSTKs) in a variety of bacteria [210]. PASTA domains have been proposed to have a sensory function and to bind β-lactam antibiotics and peptidoglycan [211, 212]. Since recognition of peptidoglycan precursors has been proposed to determine localization of PASTA kinases involved in cell division [213, 214], it is possible that the presence of the PASTA domain in PBP1B could differentially affect localization and the role of this protein in cell division with respect to PBP1A.

I argued that the cell division defect of the *mdbA* mutant is due to reduced folding and activity of PBPs. Therefore, I tested if overexpression of PBPs could

compensate for the loss of MdbA. I found that simultaneous expression of multiple PBPs rescued the morphology defect of the *mdbA* mutant grown at the non-permissive temperature (37°C). Background oxidation of exported proteins can occur in the presence of oxygen [183]. *E. coli* mutants of the DsbAB machinery can grow aerobically, but not anaerobically [36, 63]. This has been attributed in part to spontaneous oxidative folding of the cell division protein FtsN when cells grow in presence of oxygen [215]. I believe that a similar mechanism of background oxidative folding allows viability at 37°C of *mdbA* mutants overexpressing PBPs. Because background oxidation of exported proteins is less efficient and more error prone than oxidation catalyzed by a dedicated disulfide bond-forming enzyme [183], overexpression of PBPs increases the number of PBP molecules that are properly folded and functional.

As unfolded proteins are more susceptible to protease degradation, I detected decreased quantities of PBPs in the membranes of cells lacking an active MdbA (Figure 5.5A & B). This data agrees with a requirement of disulfide bonds for PBP structural integrity and therefore function, and explains the growth defect observed in Δ*mdbA* cells. Interestingly, PBP1A protein levels observed in the *mdbA* mutant strain were not as decreased as PBP1B protein levels. This is probably due to the lower number of cysteine residues in this protein (2 vs. 9 in PBP1B), which makes PBP1A less susceptible to misfolding in the absence of MdbA, compared to PBP1B. Additionally, overexpression of *pbp1A* was much higher than *pbp1B* in the *mdbA* mutant strain, which likely contributes to a higher number of PBP1A molecules that are correctly folded in this strain (Figure 5.5C and D). In agreement, the *mdbA* mutant

strain expressing a catalytically inactive MdbA (pCxxA), which did not overexpress *pbp1A,* presented lower levels of PBP1A protein (Figure 5.5A). Overexpression of *pbps* in the *mdbA* mutant is potentially a compensatory mechanism that *C. diphtheriae* employs to ensure that more PBP molecules are correctly folded and to catalyze cell wall biosynthesis ensuring cell viability when oxidative folding is disrupted. The relationship between the disulfide bond forming machinery and mechanisms governing regulation of *pbps* in *C. diphtheriae* should be the focus of further studies.

Finally, I have also demonstrated that oxidative folding of PBPs can be mediated by the alternate oxidoreductase TsdA (Characterized in chapter 4). Overexpression of TsdA by the Δ*mdbA* compensatory mutant S1 restored PBP protein levels (Figure 5.5A and B). Additionally, when I induced low replicative rates by growing cells in synthetic minimal media (Figure 5.6), Δ*mdbA* maintained a morphology similar to the wild-type strain upon incubation of bacterial cultures at the non-permissive temperature (37°C). Overall, these results indicate that basal levels of TsdA mediate oxidative folding of sufficient amounts of PBPs to allow viability of Δ*mdbA* at low replicative rates, for example when cells are incubated at 30°C or grow in synthetic minimal media.

CHAPTER 6. Concluding Remarks and Future Implications

Traditionally, disulfide bond forming pathways in prokaryotes were assumed to be confined to the periplasm of Gram-negative bacteria, due to the oxidative nature of this compartment. Because Gram-positive bacteria lack an outer membrane and a conventional periplasmic space, it was believed that they avoid exporting proteins containing disulfide bonds. However, a very important study by Daniels and colleagues [49] demonstrated that in contrast to Gram-positive Firmicutes, Gram-positive Actinobacteria secrete a high number of proteins containing two or more cysteine residues. In fact, secreted proteins in Actinobacteria have a bias for containing an even number of cysteine residues, which suggested that they form disulfide bonds *in vivo.* Genes encoding oxidoreductase orthologues have also been found in the genomes of many Actinobacteria [68]. Moreover, it is believed that the complex cell wall of Gram-positive Actinobacteria, constituted by a thick peptidoglycan-arabinogalactan and mycolic acid layers, contributes to formation of a periplasmic-like space in the cell envelope [216, 217], which might in part explain why Actinobacteria favor secretion of cysteine-containing proteins. Studies in different bacterial species have demonstrated that although similarities with the classical Dsb system of *E. coli* exist, oxidative protein folding pathways are exceptionally diverse and current knowledge of the *E. coli* Dsb system cannot be assumed to be a universal paradigm for disulfide bond formation [50, 67, 68]. Recently, disulfide bond forming enzymes in Actinobacteria such as *Actinomyces, Corynebacterium* and *Mycobacterium* have been characterized [52, 55, 56, 59, 60, 218, 219]. However, many aspects of the oxidative protein folding pathways in Actinobacteria remain poorly understood.

The first part of this dissertation (**Chapter 3**), focused on the characterization of novel factors involved in the reoxidation of the primary thiol-disulfide oxidoreductase MdbA in *A. oris*. Using adhesive pilus assembly as a marker for correct disulfide bond formation we identified the *nuo* operon, encoding subunits of the NADH dehydrogenase, and *ubiE*, encoding a menaquinone C-methyltransferase involved in menaquinone biosynthesis, to be required for proper oxidative protein folding. Analyses of the representative *nuoA* and *ubiE* mutants, showed that these genes are required for display of wild-type levels of the disulfide bond-containing pilin subunits FimA and CafA, which constitute type 2 pili. The fact that pilus assembly was rescued by overexpression of MdbA from a plasmid, strongly suggested that this defect is related to disruption of disulfide bond formation. My results agree with previous studies from our lab indicating that the disulfide bond forming machinery is required for pilus assembly, coaggregation and biofilm formation in *A. oris* [55, 60].

The bacterial electron transport chain provides the oxidizing power to maintain the *E. coli* DsbAB in an oxidized state [40, 43]. In *E. coli* DsbB transfers electrons from DsbA to ubiquinone or menaquinone [40], therefore maintaining DsbA in an oxidized active state. DsbB has a quinone binding site, and crystallography studies determined this site is occupied by quinones *in vivo* [220]. Our studies indicate that menaquinone, the main quinone utilized in the electron transport chain of Gram-positive Actinobacteria [142], is required for reoxidation of MdbA. Deletion of the *ubiE* gene, encoding an enzyme catalyzing the last step of menaquinone biosynthesis [221], disrupts MdbA reoxidation and results in accumulation of the reduced form of MdbA. Furthermore, addition of exogenous menaquinone-4 to the growth media

rescued the pilus assembly and growth phenotypes observed in the *ubiE* mutant strain. Similar to the DsbAB system [41], we argue that in *A. oris* electrons resulting from reoxidation of MdbA are transferred from VKOR to menaquinone (Figure 6.1). Therefore, the electron transport chain provides the oxidative power that maintains the MdbA/VKOR system in an oxidized and active state. Structural studies of *A. oris* VKOR would be crucial to elucidate if similar to DsbB, VKOR directly interacts with quinones. Furthermore, *in vitro* reconstitution of the *A. oris* oxidative folding pathway using menaquinone as electron acceptor would shed light into the electron transfer process that takes place during reoxidation of MdbA. Monitoring of the menaquinone reduction status would specifically determine if this process is menaquinone-dependent [41].

The *nuoA* locus, encoding a subunit of the NADH dehydrogenase complex I, was also found necessary for MdbA reoxidation. A role for the NADH dehydrogenase in disulfide bond formation has not been described before. Because of the activity of the complex I as NADH:quinone oxidoreductase [134, 222, 223], it is possible that deletion of *nuo* genes affects the general electron flow of the electron transport chain, indirectly affecting MdbA reoxidation. Due to its large size and complexity, and its role in energy metabolism, dissecting the contributions of the NADH Complex I in MdbA reoxidation might result challenging. Nonetheless, the fact that a role for the NADH dehydrogenase complex I in oxidative protein folding has not been described before, make this a very interesting avenue for future research.

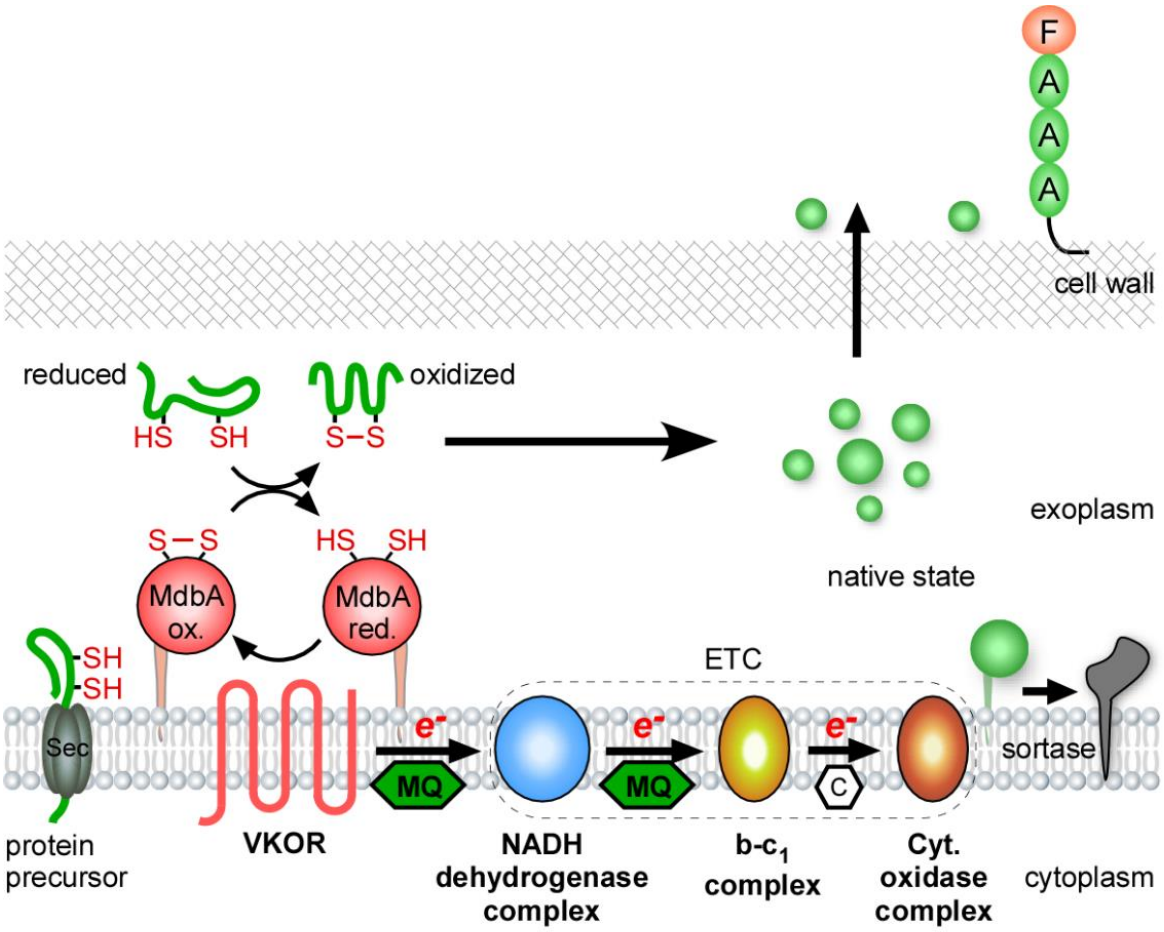

Figure 6.1. A model for MdbA/VKOR reoxidation in *A. oris.* *A. oris* VKOR catalyzes reoxidation of MdbA after disulfide bond formation. It is proposed that VKOR transfer electrons resulting from the reoxidation reaction to menaquinone. The electron carrier menaquinone can potentially transfer electrons to other electron acceptors within the electron transport chain (ETC). (see text for details).

Overall, part I of this dissertation discovered novel factors involved in disulfide bond formation in *A. oris*, and contributes to our understating of the mechanisms involved in reactivation of the oxidative folding machinery. Because disruption of the disulfide bond forming machinery results in pathogenicity and growth phenotypes in Actinobacteria*,* it seems a promising target for novel antimicrobial therapies. For example, it would be interesting to investigate the effects of compounds targeting menaquinone in *A. oris.* Studies in *M. tuberculosis* showed that inhibition of the menaquinone biosynthesis pathway significantly reduces growth of drug-resistant strains *in vitro* [138]. Interestingly, a small chemical compound directly interacting with menaquinone has bactericidal activity and reduces mortality in a murine model of systemic *Staphylococcus aureus* infection [224]. Since menaquinone is not found in mammalian cell membranes [138], antimicrobial targeting of menaquinone potentially encompasses advantages over other therapies that might have off target effects in humans.

For the second part of this dissertation (**chapter 4** and **chapter 5**), I focused on dissecting different aspects of the oxidative folding pathways in *C. diphtheriae*. In **chapter 4**, I characterized the regulation of an alternate oxidoreductase that seems to be responsible for viability of the Δ*mdbA* strain at the non-permissive temperature. In **chapter 5**, I characterized MdbA substrates involved in cell division in an effort to elucidate the essentiality of this machinery for bacterial growth.

Previous reports from our lab identified a putative oxidoreductase in *C. diphtheriae* named TsdA [56]*.* Our structural analysis of a TsdA CxxS mutant

confirmed that TsdA has DsbA protein family conserved features including a thioredoxin-like domain and an extended α-helical domain, and supports that TsdA is a thiol-disulfide oxidoreductase enzyme. Regulation of this novel oxidoreductase was puzzling because it is expressed at low levels in the wild-type strain, and its deletion did not result in any obvious phenotypes under standard laboratory growth conditions. Here, I have elucidated that the promoter driving *tsdA* expression is dependent on the housekeeping sigma factor σ^A. Because the σ^A binding sequence is weakly conserved, *tsdA* is poorly expressed in cells in logarithmic growth phase. I determined that Δ*mdbA* compensatory mutants overexpressing *tsdA* carry a mutation that results in an extended sigma factor σ^A promoter sequence, which significantly increases the strength of the promoter. Even though it is possible that the Δ*mdbA* compensatory mutation affects regulation of *tsdA* by other regulatory factors, this is unlikely. Transcription factors that bind to DNA sequences that overlap with the -10 or adjacent regions of bacterial promoters often repress gene expression by steric hindrance caused by blockage of RNA polymerase access to the promoter [175]. On the other hand, transcription factors that positively regulate gene expression (activators) often bind to motifs upstream of the promoter or to a site in the promoter adjacent to (or overlapping with) the –35 element [175]. A TG dinucleotide at positions -14, -15 of bacterial promoters has been widely described to increase promoter activity [115, 160, 162, 163]. In this sense, it is logical to conclude that the T-to-G mutation located at position -14 enhances interaction with RNA polymerase sigma factor σ^A, especially because the wild-type *tsdA* promoter sequence is suboptimal. Nonetheless, because our bioinformatic approach identified a putative DtxR binding motif upstream of the

-10 *tsdA* promoter region, we were motivated to investigate if the T-to-G mutation disrupts DtxR repression resulting in increased *tsdA* gene expression. Our experimental approach found no evidence that DtxR is involved in regulation of *tsdA* expression.

Interestingly, I found that *tsdA* transcription was induced when cells were incubated at 40°C. To our knowledge, differential regulation of an oxidoreductase by temperature has not been reported before. The TsdA expression pattern suggests a role for this alternate oxidoreductase in resistance to heat stress and potentially virulence. A possible role for TsdA in *C. diphtheriae* pathogenesis is intriguing. Analysis of *tsdA* expression, as well as comparison of wild-type and Δ*tsdA* mutant replication and survival in human phagocytes [225], and animal models of infection such as *Caenorhabditis elegans* and guinea pig would provide insights into the role of TsdA in virulence [98, 225-227]. Sigma factor σ^H is the central regulator that mediates bacterial response to heat [228, 229]. Induction of *tsdA* expression by heat and the identification of a putative sigma factor σ^H promoter upstream of the *tsdA* transcriptional start site, prompted us to investigate the role of this alternative sigma factor in *tsdA* regulation. Surprisingly, I found that *tsdA* is upregulated in the absence of *sigH*, encoding alternative sigma factor σ^H. Overexpression of *tsdA* in the Δ*sigH* strain suggests that regulation of *tsdA* by sigma factor σ^H is indirect and it is likely that additional transcription factors play a role in expression of *tsdA*. Our P^{tsdA}-*gfp* transcriptional reporter vector could be used in a transposon mutant screen to identify additional genes involved in *tsdA* regulation.

Finally, in **chapter 5** I demonstrate that MdbA is required for structural stability and activity of PBPs, suggesting that PBPs are substrates of MdbA. An *in silico* approach identified four exported cell division proteins predicted to form disulfide bonds *in vivo*. The characterization of two representative proteins, PBP1A and PBP1B, showed that they contain conserved cysteine residues in the transpeptidase domain, and have distinct functions in cell division. Consistent with requirement of disulfide bonds for protein stability, cells lacking a catalytically active MdbA enzyme presented decreased amounts of PBPs. Furthermore, overexpression of multiple cysteine-containing PBPs rescued the morphology defect of Δ*mdbA*, confirming PBPs activity is disrupted in absence of *mdbA.* Studies demonstrating a direct interaction of PBPs with MdbA would unequivocally demonstrate that MdbA catalyzes oxidative folding of PBPs. In an effort to test whether MdbA directly interacts with PBP proteins *in vivo*, I performed a preliminary pulldown assay. Membrane lysates from Δ*mdbA* cells expressing His-tagged versions of MdbA or the MdbA-CxxA mutant, were incubated with a nickel super flow resin. The obtained eluates were reactive to antibodies specific for MdbA (α-MdbA) and PBP1B (α-PBP1B), indicating direct interaction of PBP1B with MdbA *in vivo*. Furthermore, a high molecular weight band (~110 kDa), consistent with the expected migration of an MdbA-PBP1B complex, was detected in the α-PBP1B immunoblot for the MdbA-CxxA mutant sample (Figure 6.2). I hypothesize that an MdbA-PBP1B intermediate formed via a mixed-disulfide bond during oxidative folding cannot be resolved in the MdbA-CxxA mutant. Complementary experiments to confirm these findings, such as elucidating the

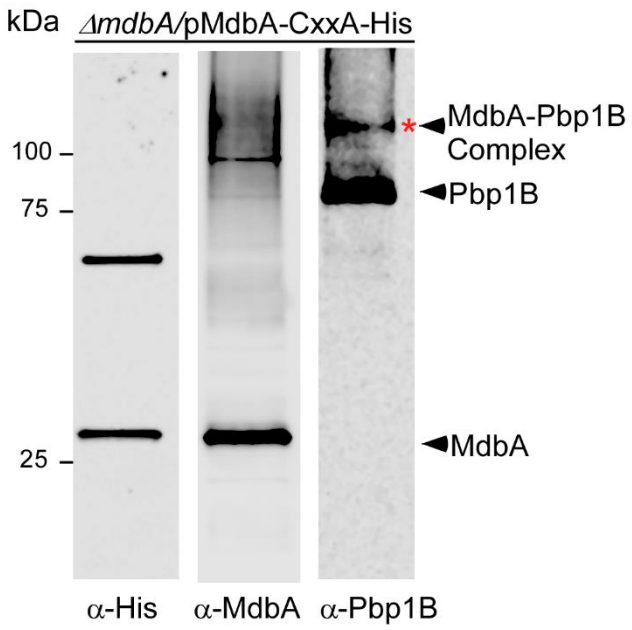

Figure 6.2. A putative mixed-disulfide MdbA-PBP1B intermediate is detected by a pull-down assay. Clear lysates obtained from membrane fractions of Δ*mdbA*/pMdbA-CxxC-His were incubated with anti-His agarose beads, followed by immunoblotting with α-His, α-MdbA or α-Pbp1B. MdbA, Pbp1B and MdbA-Pbp1B complex (black arrows) and molecular weight markers (kDa) are shown.

identity of the high molecular weight band by Mass-spectrometry analysis would provide further evidence that MdbA catalyzes disulfide bond formation in PBPs.

Our finding that cells lacking *mdbA* overexpress PBPs is intriguing. PBPs are usually constitutively expressed, however it has been argued that they can be differentially expressed in response to environmental conditions [162, 230]. In addition, increased PBP expression in response to stress exerted by cell wall active antibiotics has been reported in Gram-positive Firmicutes [162, 231, 232]. Since a relationship has been established between the Cpx-envelope stress response and oxidative protein folding in *E. coli* (discussed in chapter 1) [71], it is possible that cell envelope stress caused by disruption of peptidoglycan synthesis in the Δ*mdbA* strain induces PBP expression. Interestingly, I found that cells expressing the catalytically inactive MdbA-CxxA mutant do not overexpress PBPs. Therefore, potentially multiple unknown regulatory mechanisms play a role in regulation of PBP expression upon disruption of oxidative folding.

The studies in this dissertation indicate that the essentiality of the oxidative folding machinery in *C. diphtheriae* is related to disruption of disulfide bond formation in PBPs. Furthermore, our data indicates that survival of Δ*mdbA* at low replicative rates is due to basal expression of the alternate oxidoreductase TsdA. However, important questions regarding the essentiality of the disulfide bond forming machinery remain. Why does *C. diphtheriae* favor expression of PBPs containing cysteine residues? Does this provide a physiological advantage? Is this mechanism conserved in other bacterial groups? Since Actinobacteria secrete abundance of proteins

containing cysteine residues, one could argue that this is likely to be a general mechanism that provides protein stability in the corynebacterial natural niches, rather than a specific bias toward cell division proteins. Interestingly, in a survey of the *E. coli* secretome I found that of 11 PBPs identified, 3 are predicted to form disulfide bonds. However, disulfide bridges in these PBPs (PBP1A, PBP1B and PBP4) are dispensable for function [204, 233, 234]. Therefore, the requirement of disulfide bonds for PBPs activity does not seem to be universal. On the other hand, a survey of exported proteins in *A. oris* identified only 2 cell division proteins containing cysteine residues. Thus, the essentiality of MdbA for *A. oris* growth might be related to disruption of other systems. Whether oxidative folding is required for activity of cell division factors in other bacterial groups remains to be explored. Nonetheless, the results presented here are likely to lead to exciting future studies.

Previous reports from our group showed that overexpression of TsdA restored Diphtheria toxin and SpaA pilin protein levels in cells lacking *mdbA* [114]. Here I showed that PBP protein levels are also restored in the Δ*mdbA* compensatory mutant overexpressing TsdA. These data suggest that TsdA has a broad substrate specificity and might provide a compensatory mechanism of oxidative folding under unfavorable or stress conditions. I propose that under normal growth conditions expression of MdbA is sufficient to catalyze oxidative folding in *C. diphtheriae*. However, when bacterial cells are exposed to stresses encountered within the host, such as elevated temperatures, expression of the alternate oxidoreductase TsdA is induced by a yet unknown mechanism. In this situation, increased amounts of TsdA molecules aid in the oxidative folding of diverse substrates (Figure 6.3). Stimuli like temperature and

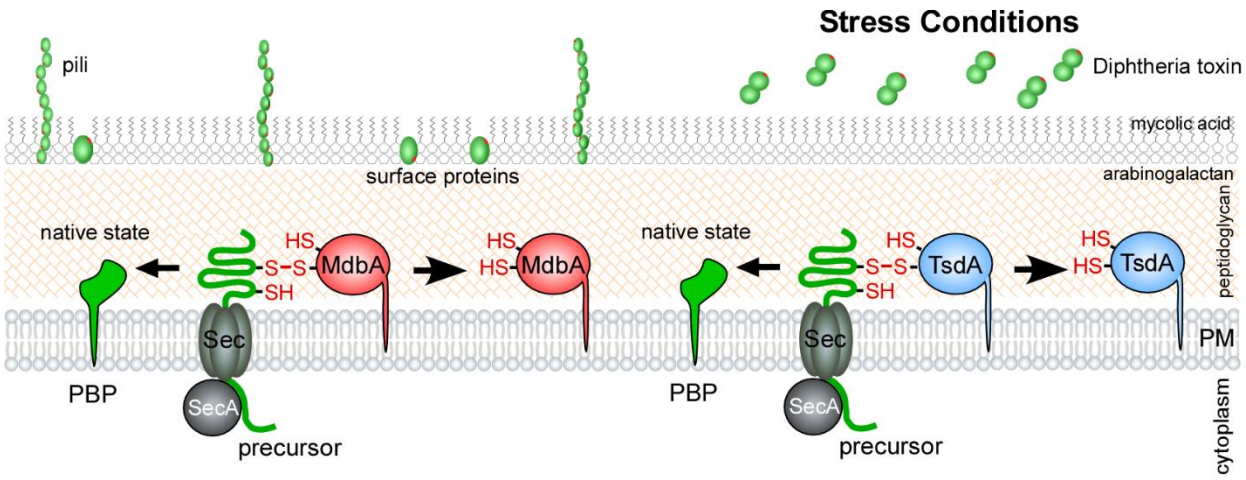

Figure 6.3. A model for oxidative protein folding pathways in *C. diphtheriae.* It is proposed that MdbA mediates oxidative folding of multiple PBPs required for cell division. Under stress conditions such as elevated temperatures, the alternate oxidoreductase TsdA is expressed and can aid in oxidative folding of diverse disulfide bond-containing substrates including PBPs, Diphtheria toxin and SpaA pilin subunits (see text for details).

iron concentrations indicate to pathogens they are within the host and have deep effects in bacterial gene regulation [74]. For example, expression of the disulfide bond-containing Diphtheria toxin is induced within the host [169]. Additionally, expression of the disulfide-bond containing SpaA-type pilus is highly prevalent among clinical isolates of *C. diphtheriae* [98]. Environmental stresses affecting protein stability together with high expression of disulfide bond-containing proteins, would exacerbate the necessity for an additional oxidoreductase like TsdA to help maintain protein homeostasis and ensure survival of *C. diphtheriae.*

Overall, the studies presented in this dissertation provide insights into diverse aspects of the oxidative folding pathways in Actinobacteria that have not been explored before. I showed that components of the electron transport chain are involved in MdbA reoxidation. Secondly, by characterizing regulation of TsdA by temperature I have discovered a novel stimulus controlling expression of a bacterial oxidoreductase. Finally, I determined that this alternate oxidoreductase is involved in survival of cells lacking *mdbA* and that the requirement of *mdbA* for cell division is related to incorrect folding of PBPs. Due to the impact of thiol-disulfide oxidoreductases in bacterial physiology, my work provides knowledge applicable not only to protein folding, but also to bacterial pathogenesis and potentially the discovery of novel antimicrobial therapies targeting bacterial viability and virulence.

REFERENCES

1. Willey JM, Sherwood, L.M., Woolverton, C.J.: **Prescott, Harley, and Klein's microbiology**, 7th edn: McGraw-Hill; 2008.
2. Kononen E, Wade WG: **Actinomyces and related organisms in human infections**. *Clin Microbiol Rev* 2015, **28**(2):419-442.
3. Mark Welch JL, Rossetti BJ, Rieken CW, Dewhirst FE, Borisy GG: **Biogeography of a human oral microbiome at the micron scale**. *Proc Natl Acad Sci U S A* 2016, **113**(6):E791-800.
4. Zijnge V, van Leeuwen MB, Degener JE, Abbas F, Thurnheer T, Gmur R, Harmsen HJ: **Oral biofilm architecture on natural teeth**. *PLoS One* 2010, **5**(2):e9321.
5. Brailsford SR, Tregaskis RB, Leftwich HS, Beighton D: **The predominant Actinomyces spp. isolated from infected dentin of active root caries lesions**. *J Dent Res* 1999, **78**(9):1525-1534.
6. Tanner AC, Mathney JM, Kent RL, Chalmers NI, Hughes CV, Loo CY, Pradhan N, Kanasi E, Hwang J, Dahlan MA *et al*: **Cultivable anaerobic microbiota of severe early childhood caries**. *J Clin Microbiol* 2011, **49**(4):1464-1474.
7. Bowden GH, Nolette N, Ryding H, Cleghorn BM: **The diversity and distribution of the predominant ribotypes of Actinomyces naeslundii genospecies 1 and 2 in samples from enamel and from healthy and carious root surfaces of teeth**. *J Dent Res* 1999, **78**(12):1800-1809.

8. Ximenez-Fyvie LA, Haffajee AD, Martin L, Tanner A, Macuch P, Socransky SS: **Identification of oral Actinomyces species using DNA probes**. *Oral Microbiol Immunol* 1999, **14**(4):257-265.

9. Gibbons RJ, Hay DI, Cisar JO, Clark WB: **Adsorbed salivary proline-rich protein 1 and statherin: receptors for type 1 fimbriae of Actinomyces viscosus T14V-J1 on apatitic surfaces**. *Infect Immun* 1988, **56**(11):2990-2993.

10. Kolenbrander PE, Palmer RJ, Jr., Periasamy S, Jakubovics NS: **Oral multispecies biofilm development and the key role of cell-cell distance**. *Nat Rev Microbiol* 2010, **8**(7):471-480.

11. Rickard AH, Gilbert P, High NJ, Kolenbrander PE, Handley PS: **Bacterial coaggregation: an integral process in the development of multi-species biofilms**. *Trends Microbiol* 2003, **11**(2):94-100.

12. Mishra A, Devarajan B, Reardon ME, Dwivedi P, Krishnan V, Cisar JO, Das A, Narayana SV, Ton-That H: **Two autonomous structural modules in the fimbrial shaft adhesin FimA mediate Actinomyces interactions with streptococci and host cells during oral biofilm development**. *Mol Microbiol* 2011, **81**(5):1205-1220.

13. Mishra A, Wu C, Yang J, Cisar JO, Das A, Ton-That H: **The Actinomyces oris type 2 fimbrial shaft FimA mediates co-aggregation with oral streptococci, adherence to red blood cells and biofilm development**. *Mol Microbiol* 2010.

14. Ammann TW, Belibasakis GN, Thurnheer T: **Impact of early colonizers on in vitro subgingival biofilm formation**. *PLoS One* 2013, **8**(12):e83090.

15. Petersen PE, Ogawa H: **Strengthening the prevention of periodontal disease: the WHO approach**. *J Periodontol* 2005, **76**(12):2187-2193.

16. Brown LJ, Johns BA, Wall TP: **The economics of periodontal diseases**. *Periodontol 2000* 2002, **29**:223-234.

17. Hadfield TL, McEvoy P, Polotsky Y, Tzinserling VA, Yakovlev AA: **The pathology of diphtheria**. *J Infect Dis* 2000, **181 Suppl 1**:S116-120.

18. Rogers EA, Das A, Ton-That H: **Adhesion by pathogenic corynebacteria**. *Adv Exp Med Biol*, **715**:91-103.

19. Ton-That H, Schneewind O: **Assembly of pili on the surface of Corynebacterium diphtheriae**. *Mol Microbiol* 2003, **50**(4):1429-1438.

20. Mandlik A, Swierczynski A, Das A, Ton-That H: **Pili in Gram-positive bacteria: assembly, involvement in colonization and biofilm development**. *Trends Microbiol* 2008, **16**(1):33-40.

21. Mandlik A, Swierczynski A, Das A, Ton-That H: **Corynebacterium diphtheriae employs specific minor pilins to target human pharyngeal epithelial cells**. *Mol Microbiol* 2007, **64**(1):111-124.

22. Barksdale L: **Corynebacterium diphtheriae and its relatives**. *Bacteriol Rev* 1970, **34**(4):378-422.

23. London E: **Diphtheria toxin: membrane interaction and membrane translocation**. *Biochim Biophys Acta* 1992, **1113**(1):25-51.

24. Naglich JG, Metherall JE, Russell DW, Eidels L: **Expression cloning of a diphtheria toxin receptor: identity with a heparin-binding EGF-like growth factor precursor**. *Cell* 1992, **69**(6):1051-1061.

25. Mitamura T, Higashiyama S, Taniguchi N, Klagsbrun M, Mekada E: **Diphtheria toxin binds to the epidermal growth factor (EGF)-like domain of human heparin-binding EGF-like growth factor/diphtheria toxin receptor and inhibits specifically its mitogenic activity**. *J Biol Chem* 1995, **270**(3):1015-1019.

26. Sangal V, Hoskisson PA: **Evolution, epidemiology and diversity of Corynebacterium diphtheriae: New perspectives on an old foe**. *Infect Genet Evol* 2016, **43**:364-370.

27. Mamathambika BS, Bardwell JC: **Disulfide-linked protein folding pathways**. *Annu Rev Cell Dev Biol* 2008, **24**:211-235.

28. Heras B, Shouldice SR, Totsika M, Scanlon MJ, Schembri MA, Martin JL: **DSB proteins and bacterial pathogenicity**. *Nat Rev Microbiol* 2009, **7**(3):215-225.

29. Frand AR, Kaiser CA: **The ERO1 gene of yeast is required for oxidation of protein dithiols in the endoplasmic reticulum**. *Mol Cell* 1998, **1**(2):161-170.

30. Anfinsen CB: **Principles that govern the folding of protein chains**. *Science* 1973, **181**(4096):223-230.

31. Goldberger RF, Epstein CJ, Anfinsen CB: **Acceleration of reactivation of reduced bovine pancreatic ribonuclease by a microsomal system from rat liver**. *J Biol Chem* 1963, **238**:628-635.

32. Bardwell JC, Lee JO, Jander G, Martin N, Belin D, Beckwith J: **A pathway for disulfide bond formation in vivo**. *Proc Natl Acad Sci U S A* 1993, **90**(3):1038-1042.

33. Peek JA, Taylor RK: **Characterization of a periplasmic thiol:disulfide interchange protein required for the functional maturation of secreted virulence factors of Vibrio cholerae**. *Proc Natl Acad Sci U S A* 1992, **89**(13):6210-6214.

34. Kadokura H, Beckwith J: **Detecting folding intermediates of a protein as it passes through the bacterial translocation channel**. *Cell* 2009, **138**(6):1164-1173.

35. Denoncin K, Collet JF: **Disulfide bond formation in the bacterial periplasm: major achievements and challenges ahead**. *Antioxid Redox Signal* 2013, **19**(1):63-71.

36. Bardwell JC, McGovern K, Beckwith J: **Identification of a protein required for disulfide bond formation in vivo**. *Cell* 1991, **67**(3):581-589.

37. Kadokura H, Tian H, Zander T, Bardwell JC, Beckwith J: **Snapshots of DsbA in action: detection of proteins in the process of oxidative folding**. *Science* 2004, **303**(5657):534-537.

38. Kadokura H, Katzen F, Beckwith J: **Protein disulfide bond formation in prokaryotes**. *Annu Rev Biochem* 2003, **72**:111-135.

39. Missiakas D, Georgopoulos C, Raina S: **Identification and characterization of the Escherichia coli gene dsbB, whose product is involved in the**

formation of disulfide bonds in vivo. *Proc Natl Acad Sci U S A* 1993, **90**(15):7084-7088.

40. Bader M, Muse W, Ballou DP, Gassner C, Bardwell JC: **Oxidative protein folding is driven by the electron transport system**. *Cell* 1999, **98**(2):217-227.

41. Bader MW, Xie T, Yu CA, Bardwell JC: **Disulfide bonds are generated by quinone reduction**. *J Biol Chem* 2000, **275**(34):26082-26088.

42. Kobayashi T, Ito K: **Respiratory chain strongly oxidizes the CXXC motif of DsbB in the Escherichia coli disulfide bond formation pathway**. *EMBO J* 1999, **18**(5):1192-1198.

43. Kobayashi T, Kishigami S, Sone M, Inokuchi H, Mogi T, Ito K: **Respiratory chain is required to maintain oxidized states of the DsbA-DsbB disulfide bond formation system in aerobically growing Escherichia coli cells**. *Proc Natl Acad Sci U S A* 1997, **94**(22):11857-11862.

44. Bader M, Muse W, Zander T, Bardwell J: **Reconstitution of a protein disulfide catalytic system**. *J Biol Chem* 1998, **273**(17):10302-10307.

45. Takahashi YH, Inaba K, Ito K: **Characterization of the menaquinone-dependent disulfide bond formation pathway of Escherichia coli**. *J Biol Chem* 2004, **279**(45):47057-47065.

46. Hatahet F, Boyd D, Beckwith J: **Disulfide bond formation in prokaryotes: history, diversity and design**. *Biochim Biophys Acta* 2014, **1844**(8):1402-1414.

47. Missiakas D, Georgopoulos C, Raina S: **The Escherichia coli dsbC (xprA) gene encodes a periplasmic protein involved in disulfide bond formation**. *EMBO J* 1994, **13**(8):2013-2020.

48. Missiakas D, Schwager F, Raina S: **Identification and characterization of a new disulfide isomerase-like protein (DsbD) in Escherichia coli**. *EMBO J* 1995, **14**(14):3415-3424.

49. Daniels R, Mellroth P, Bernsel A, Neiers F, Normark S, von Heijne G, Henriques-Normark B: **Disulfide bond formation and cysteine exclusion in gram-positive bacteria**. *J Biol Chem* 2010, **285**(5):3300-3309.

50. Davey L, Halperin SA, Lee SF: **Thiol-Disulfide Exchange in Gram-Positive Firmicutes**. *Trends Microbiol* 2016, **24**(11):902-915.

51. Kouwen TR, van der Goot A, Dorenbos R, Winter T, Antelmann H, Plaisier MC, Quax WJ, van Dijl JM, Dubois JY: **Thiol-disulphide oxidoreductase modules in the low-GC Gram-positive bacteria**. *Mol Microbiol* 2007, **64**(4):984-999.

52. Luong TT, Tirgar R, Reardon-Robinson ME, Joachimiak A, Osipiuk J, Ton-That H: **Structural Basis of a Thiol-Disulfide Oxidoreductase in the Hedgehog-Forming Actinobacterium Corynebacterium matruchotii**. *J Bacteriol* 2018, **200**(9).

53. Dutton RJ, Wayman A, Wei JR, Rubin EJ, Beckwith J, Boyd D: **Inhibition of bacterial disulfide bond formation by the anticoagulant warfarin**. *Proc Natl Acad Sci U S A* 2010, **107**(1):297-301.

54. Sassetti CM, Boyd DH, Rubin EJ: **Genes required for mycobacterial growth defined by high density mutagenesis**. *Mol Microbiol* 2003, **48**(1):77-84.

55. Reardon-Robinson ME, Osipiuk J, Chang C, Wu C, Jooya N, Joachimiak A, Das A, Ton-That H: **A Disulfide Bond-forming Machine Is Linked to the Sortase-mediated Pilus Assembly Pathway in the Gram-positive Bacterium Actinomyces oris**. *J Biol Chem* 2015, **290**(35):21393-21405.

56. Reardon-Robinson ME, Osipiuk J, Jooya N, Chang C, Joachimiak A, Das A, Ton-That H: **A thiol-disulfide oxidoreductase of the Gram-positive pathogen Corynebacterium diphtheriae is essential for viability, pilus assembly, toxin production and virulence**. *Mol Microbiol* 2015, **98**(6):1037-1050.

57. Martin JL, Bardwell JC, Kuriyan J: **Crystal structure of the DsbA protein required for disulphide bond formation in vivo**. *Nature* 1993, **365**(6445):464-468.

58. Shouldice SR, Heras B, Walden PM, Totsika M, Schembri MA, Martin JL: **Structure and function of DsbA, a key bacterial oxidative folding catalyst**. *Antioxid Redox Signal* 2011, **14**(9):1729-1760.

59. Premkumar L, Heras B, Duprez W, Walden P, Halili M, Kurth F, Fairlie DP, Martin JL: **Rv2969c, essential for optimal growth in Mycobacterium tuberculosis, is a DsbA-like enzyme that interacts with VKOR-derived peptides and has atypical features of DsbA-like disulfide oxidases**. *Acta Crystallogr D Biol Crystallogr* 2013, **69**(Pt 10):1981-1994.

60. Luong TT, Reardon-Robinson ME, Siegel SD, Ton-That H: **Reoxidation of the Thiol-Disulfide Oxidoreductase MdbA by a Bacterial Vitamin K Epoxide Reductase in the Biofilm-Forming Actinobacterium Actinomyces oris**. *J Bacteriol* 2017, **199**(10).

61. Vertommen D, Depuydt M, Pan J, Leverrier P, Knoops L, Szikora JP, Messens J, Bardwell JC, Collet JF: **The disulphide isomerase DsbC cooperates with the oxidase DsbA in a DsbD-independent manner**. *Mol Microbiol* 2008, **67**(2):336-349.

62. Bessette PH, Qiu J, Bardwell JC, Swartz JR, Georgiou G: **Effect of sequences of the active-site dipeptides of DsbA and DsbC on in vivo folding of multidisulfide proteins in Escherichia coli**. *J Bacteriol* 2001, **183**(3):980-988.

63. Meehan BM, Landeta C, Boyd D, Beckwith J: **The Disulfide Bond Formation Pathway Is Essential for Anaerobic Growth of Escherichia coli**. *J Bacteriol* 2017, **199**(16).

64. Hiniker A, Collet JF, Bardwell JC: **Copper stress causes an in vivo requirement for the Escherichia coli disulfide isomerase DsbC**. *J Biol Chem* 2005, **280**(40):33785-33791.

65. Yu J, Kroll JS: **DsbA: a protein-folding catalyst contributing to bacterial virulence**. *Microbes Infect* 1999, **1**(14):1221-1228.

66. Saleh M, Bartual SG, Abdullah MR, Jensch I, Asmat TM, Petruschka L, Pribyl T, Gellert M, Lillig CH, Antelmann H *et al*: **Molecular architecture of Streptococcus pneumoniae surface thioredoxin-fold lipoproteins crucial**

for extracellular oxidative stress resistance and maintenance of virulence. *EMBO Mol Med* 2013, **5**(12):1852-1870.

67. Reardon-Robinson ME, Ton-That H: **Disulfide-Bond-Forming Pathways in Gram-Positive Bacteria**. *J Bacteriol* 2015, **198**(5):746-754.

68. Landeta C, Boyd D, Beckwith J: **Disulfide bond formation in prokaryotes**. *Nat Microbiol* 2018, **3**(3):270-280.

69. Choe S, Bennett MJ, Fujii G, Curmi PM, Kantardjieff KA, Collier RJ, Eisenberg D: **The crystal structure of diphtheria toxin**. *Nature* 1992, **357**(6375):216-222.

70. Wilson AC, Hoch JA, Perego M: **Two small c-type cytochromes affect virulence gene expression in Bacillus anthracis**. *Mol Microbiol* 2009, **72**(1):109-123.

71. Pogliano J, Lynch AS, Belin D, Lin EC, Beckwith J: **Regulation of Escherichia coli cell envelope proteins involved in protein folding and degradation by the Cpx two-component system**. *Genes Dev* 1997, **11**(9):1169-1182.

72. Hunke S, Keller R, Muller VS: **Signal integration by the Cpx-envelope stress system**. *FEMS Microbiol Lett* 2012, **326**(1):12-22.

73. Slamti L, Waldor MK: **Genetic analysis of activation of the Vibrio cholerae Cpx pathway**. *J Bacteriol* 2009, **191**(16):5044-5056.

74. Fang FC, Frawley ER, Tapscott T, Vazquez-Torres A: **Bacterial Stress Responses during Host Infection**. *Cell Host Microbe* 2016, **20**(2):133-143.

75. Grabowska AD, Wandel MP, Lasica AM, Nesteruk M, Roszczenko P, Wyszynska A, Godlewska R, Jagusztyn-Krynicka EK: **Campylobacter jejuni**

dsb gene expression is regulated by iron in a Fur-dependent manner and by a translational coupling mechanism. *BMC Microbiol* 2011, **11**:166.

76. Bringer MA, Rolhion N, Glasser AL, Darfeuille-Michaud A: **The oxidoreductase DsbA plays a key role in the ability of the Crohn's disease-associated adherent-invasive Escherichia coli strain LF82 to resist macrophage killing**. *J Bacteriol* 2007, **189**(13):4860-4871.

77. Cassat JE, Skaar EP: **Iron in infection and immunity**. *Cell Host Microbe* 2013, **13**(5):509-519.

78. Andrews SC, Robinson AK, Rodriguez-Quinones F: **Bacterial iron homeostasis**. *FEMS Microbiol Rev* 2003, **27**(2-3):215-237.

79. Kpadeh ZZ, Jameson-Lee M, Yeh AJ, Chertihin O, Shumilin IA, Dey R, Day SR, Hoffman PS: **Disulfide bond oxidoreductase DsbA2 of Legionella pneumophila exhibits protein disulfide isomerase activity**. *J Bacteriol* 2013, **195**(8):1825-1833.

80. Liu Y, Carlsson Moller M, Petersen L, Soderberg CA, Hederstedt L: **Penicillin-binding protein SpoVD disulphide is a target for StoA in Bacillus subtilis forespores**. *Mol Microbiol* 2010, **75**(1):46-60.

81. Eichenberger P: **The red-ox status of a penicillin-binding protein is an on/off switch for spore peptidoglycan synthesis in Bacillus subtilis**. *Mol Microbiol* 2010, **75**(1):10-12.

82. Bukowska-Faniband E, Hederstedt L: **Transpeptidase activity of penicillin-binding protein SpoVD in peptidoglycan synthesis conditionally**

depends on the disulfide reductase StoA. *Mol Microbiol* 2017, **105**(1):98-114.

83. Eichenberger P, Jensen ST, Conlon EM, van Ooij C, Silvaggi J, Gonzalez-Pastor JE, Fujita M, Ben-Yehuda S, Stragier P, Liu JS *et al*: **The sigmaE regulon and the identification of additional sporulation genes in Bacillus subtilis**. *J Mol Biol* 2003, **327**(5):945-972.

84. Imamura D, Kobayashi K, Sekiguchi J, Ogasawara N, Takeuchi M, Sato T: **spoIVH (ykvV), a requisite cortex formation gene, is expressed in both sporulating compartments of Bacillus subtilis**. *J Bacteriol* 2004, **186**(16):5450-5459.

85. Zasada A: **Antimicrobial Susceptibility and Treatment**. In: *Corynebacterium diphtheriae and Related Toxigenic Species.* Edited by Burkovski A; 2014.

86. Manjelievskaia J, Erck D, Piracha S, Schrager L: **Drug-resistant TB: deadly, costly and in need of a vaccine**. *Trans R Soc Trop Med Hyg* 2016, **110**(3):186-191.

87. Siegel SD, Wu C, Ton-That H: **A Type I Signal Peptidase Is Required for Pilus Assembly in the Gram-Positive, Biofilm-Forming Bacterium Actinomyces oris**. *J Bacteriol* 2016, **198**(15):2064-2073.

88. Rohrschneider LR, Custodio JM, Anderson TA, Miller CP, Gu H: **The intron 5/6 promoter region of the ship1 gene regulates expression in stem/progenitor cells of the mouse embryo**. *Dev Biol* 2005, **283**(2):503-521.

89. Reyes O, Guyonvarch A, Bonamy C, Salti V, David F, Leblon G: **'Integron'-bearing vectors: a method suitable for stable chromosomal integration in highly restrictive corynebacteria**. *Gene* 1991, **107**(1):61-68.

90. Stols L, Gu M, Dieckman L, Raffen R, Collart FR, Donnelly MI: **A new vector for high-throughput, ligation-independent cloning encoding a tobacco etch virus protease cleavage site**. *Protein Expr Purif* 2002, **25**(1):8-15.

91. Wu C, Reardon-Robinson ME, Ton-That H: **Genetics and Cell Morphology Analyses of the Actinomyces oris srtA Mutant**. *Methods Mol Biol* 2016, **1440**:109-122.

92. Wu C, Huang IH, Chang C, Reardon-Robinson ME, Das A, Ton-That H: **Lethality of sortase depletion in Actinomyces oris caused by excessive membrane accumulation of a surface glycoprotein**. *Mol Microbiol* 2014, **94**(6):1227-1241.

93. Schafer A, Tauch A, Jager W, Kalinowski J, Thierbach G, Puhler A: **Small mobilizable multi-purpose cloning vectors derived from the Escherichia coli plasmids pK18 and pK19: selection of defined deletions in the chromosome of Corynebacterium glutamicum**. *Gene* 1994, **145**(1):69-73.

94. Cisar JO, Kolenbrander PE, McIntire FC: **Specificity of coaggregation reactions between human oral streptococci and strains of Actinomyces viscosus or Actinomyces naeslundii**. *Infect Immun* 1979, **24**(3):742-752.

95. Chang C, Huang IH, Hendrickx AP, Ton-That H: **Visualization of Gram-positive bacterial pili**. *Methods Mol Biol*, **966**:77-95.

96. Mishra A, Wu C, Yang J, Cisar JO, Das A, Ton-That H: **The Actinomyces oris type 2 fimbrial shaft FimA mediates co-aggregation with oral streptococci, adherence to red blood cells and biofilm development**. *Mol Microbiol* 2010, **77** (4):841–854.

97. Willey JM, Sherwood LM, Woolverton CJ: **Prescott, Harley, and Klein's Microbiology**, 7th edn. New York, NY: McGraw-Hill; 2008.

98. Broadway MM, Rogers EA, Chang C, Huang IH, Dwivedi P, Yildirim S, Schmitt MP, Das A, Ton-That H: **Pilus gene pool variation and the virulence of Corynebacterium diphtheriae clinical isolates during infection of a nematode**. *J Bacteriol* 2013, **195**(16):3774-3783.

99. Schmittgen TD, Livak KJ: **Analyzing real-time PCR data by the comparative C(T) method**. *Nat Protoc* 2008, **3**(6):1101-1108.

100. Gorrec F, Palmer CM, Lebon G, Warne T: **Pi sampling: a methodical and flexible approach to initial macromolecular crystallization screening**. *Acta Crystallogr D Biol Crystallogr* 2011, **67**(Pt 5):463-470.

101. Rosenbaum G, Alkire RW, Evans G, Rotella FJ, Lazarski K, Zhang RG, Ginell SL, Duke N, Naday I, Lazarz J *et al*: **The Structural Biology Center 19ID undulator beamline: facility specifications and protein crystallographic results**. *J Synchrotron Radiat* 2006, **13**(Pt 1):30-45.

102. Minor W, Cymborowski M, Otwinowski Z, Chruszcz M: **HKL-3000: the integration of data reduction and structure solution--from diffraction images to an initial model in minutes**. *Acta Crystallogr D Biol Crystallogr* 2006, **62**(Pt 8):859-866.

103. Vagin A, Teplyakov A: **MOLREP: an automated program for molecular replacement**. *Journal of Applied Crystallography* 1997, **30**:1022-1025.

104. Emsley P, Cowtan K: **Coot: model-building tools for molecular graphics**. *Acta Crystallogr D Biol Crystallogr* 2004, **60**(Pt 12 Pt 1):2126-2132.

105. Murshudov GN, Vagin AA, Dodson EJ: **Refinement of macromolecular structures by the maximum-likelihood method**. *Acta Crystallogr D Biol Crystallogr* 1997, **53**(Pt 3):240-255.

106. Collaborative Computational Project N: **The CCP4 suite: programs for protein crystallography**. *Acta Crystallogr D Biol Crystallogr* 1994, **50**(Pt 5):760-763.

107. Adams PD, Grosse-Kunstleve RW, Hung LW, Ioerger TR, McCoy AJ, Moriarty NW, Read RJ, Sacchettini JC, Sauter NK, Terwilliger TC: **PHENIX: building new software for automated crystallographic structure determination**. *Acta Crystallogr D Biol Crystallogr* 2002, **58**(Pt 11):1948-1954.

108. Davis IW, Murray LW, Richardson JS, Richardson DC: **MOLPROBITY: structure validation and all-atom contact analysis for nucleic acids and their complexes**. *Nucleic Acids Res* 2004, **32**(Web Server issue):W615-619.

109. Kabsch W, Sander C: **Dictionary of protein secondary structure: pattern recognition of hydrogen-bonded and geometrical features**. *Biopolymers* 1983, **22**(12):2577-2637.

110. Gouet P, Robert X, Courcelle E: **ESPript/ENDscript: Extracting and rendering sequence and 3D information from atomic structures of proteins**. *Nucleic Acids Res* 2003, **31**(13):3320-3323.

111. Reardon-Robinson ME, Wu C, Mishra A, Chang C, Bier N, Das A, Ton-That H: **Pilus hijacking by a bacterial coaggregation factor critical for oral biofilm development**. *Proc Natl Acad Sci U S A* 2014, **111**(10):3835-3840.

112. Sanchez BC, Chang C, Wu C, Tran B, Ton-That H: **Electron Transport Chain Is Biochemically Linked to Pilus Assembly Required for Polymicrobial Interactions and Biofilm Formation in the Gram-Positive Actinobacterium Actinomyces oris**. *MBio* 2017, **8**(3).

113. Wu C, Mishra A, Yang J, Cisar JO, Das A, Ton-That H: **Dual function of a tip fimbrillin of Actinomyces in fimbrial assembly and receptor binding**. *J Bacteriol* 2011, **193**(13):3197-3206.

114. Reardon-Robinson ME: **Oxidative Protein Folding Pathways in Gram-Positive Actinobacteria**. Houston, Texas: The University of Texas Health Science Center at Houston and The University of Texas M. D. Anderson Cancer Center; 2015.

115. Wittchen M, Busche T, Gaspar AH, Lee JH, Ton-That H, Kalinowski J, Tauch A: **Transcriptome sequencing of the human pathogen Corynebacterium diphtheriae NCTC 13129 provides detailed insights into its transcriptional landscape and into DtxR-mediated transcriptional regulation**. *BMC Genomics* 2018, **19**(1):82.

116. Mishra A, Das A, Cisar JO, Ton-That H: **Sortase-catalyzed assembly of distinct heteromeric fimbriae in Actinomyces naeslundii**. *J Bacteriol* 2007, **189**(8):3156-3165.

117. Proft T, Baker EN: **Pili in Gram-negative and Gram-positive bacteria - structure, assembly and their role in disease**. *Cell Mol Life Sci* 2009, **66**(4):613-635.

118. Spirig T, Weiner EM, Clubb RT: **Sortase enzymes in Gram-positive bacteria**. *Mol Microbiol* 2011, **82**(5):1044-1059.

119. Dramsi S, Trieu-Cuot P, Bierne H: **Sorting sortases: a nomenclature proposal for the various sortases of Gram-positive bacteria**. *Res Microbiol* 2005, **156**(3):289-297.

120. Swaminathan A, Mandlik A, Swierczynski A, Gaspar A, Das A, Ton-That H: **Housekeeping sortase facilitates the cell wall anchoring of pilus polymers in Corynebacterium diphtheriae**. *Mol Microbiol* 2007, **66**(4):961-974.

121. Budzik JM, Oh SY, Schneewind O: **Cell wall anchor structure of BcpA pili in Bacillus anthracis**. *J Biol Chem* 2008, **283**(52):36676-36686.

122. Nobbs AH, Rosini R, Rinaudo CD, Maione D, Grandi G, Telford JL: **Sortase A utilizes an ancillary protein anchor for efficient cell wall anchoring of pili in Streptococcus agalactiae**. *Infect Immun* 2008, **76**(8):3550-3560.

123. Kline KA, Kau AL, Chen SL, Lim A, Pinkner JS, Rosch J, Nallapareddy SR, Murray BE, Henriques-Normark B, Beatty W *et al*: **Mechanism for sortase localization and the role of sortase localization in efficient pilus assembly in Enterococcus faecalis**. *J Bacteriol* 2009, **191**(10):3237-3247.

124. Sillanpaa J, Chang C, Singh KV, Montealegre MC, Nallapareddy SR, Harvey BR, Ton-That H, Murray BE: **Contribution of Individual Ebp Pilus Subunits**

of Enterococcus faecalis OG1RF to Pilus Biogenesis, Biofilm Formation and Urinary Tract Infection. *PLoS One* 2013, **8**(7):e68813.

125. Mazmanian SK, Liu G, Ton-That H, Schneewind O: **Staphylococcus aureus sortase, an enzyme that anchors surface proteins to the cell wall**. *Science* 1999, **285**(5428):760-763.

126. Ton-That H, Liu G, Mazmanian SK, Faull KF, Schneewind O: **Purification and characterization of sortase, the transpeptidase that cleaves surface proteins of Staphylococcus aureus at the LPXTG motif**. *Proc Natl Acad Sci U S A* 1999, **96**(22):12424-12429.

127. Ellen RP, Walker DL, Chan KH: **Association of long surface appendages with adherence-related functions of the gram-positive species Actinomyces naeslundii**. *J Bacteriol* 1978, **134**(3):1171-1175.

128. Cisar JO, Vatter AE: **Surface fibrils (fimbriae) of Actinomyces viscosus T14V**. *Infect Immun* 1979, **24**(2):523-531.

129. Yeung MK: **Molecular and genetic analyses of Actinomyces spp**. *Crit Rev Oral Biol Med* 1999, **10**(2):120-138.

130. Henssge U, Do T, Radford DR, Gilbert SC, Clark D, Beighton D: **Emended description of Actinomyces naeslundii and descriptions of Actinomyces oris sp. nov. and Actinomyces johnsonii sp. nov., previously identified as Actinomyces naeslundii genospecies 1, 2 and WVA 963**. *Int J Syst Evol Microbiol* 2009, **59**(Pt 3):509-516.

131. Wang X, Dutton RJ, Beckwith J, Boyd D: **Membrane topology and mutational analysis of Mycobacterium tuberculosis VKOR, a protein**

involved in disulfide bond formation and a homologue of human vitamin K epoxide reductase. *Antioxid Redox Signal* 2011, **14**(8):1413-1420.

132. Reardon-Robinson ME, Ton-That H: **Disulfide-Bond-Forming Pathways in Gram-Positive Bacteria**. *J Bacteriol* 2016, **198**(5):746-754.

133. Cisar JO, Sandberg AL, Abeygunawardana C, Reddy GP, Bush CA: **Lectin recognition of host-like saccharide motifs in streptococcal cell wall polysaccharides**. *Glycobiology* 1995, **5**(7):655-662.

134. Friedrich T, Dekovic DK, Burschel S: **Assembly of the Escherichia coli NADH:ubiquinone oxidoreductase (respiratory complex I)**. *Biochim Biophys Acta* 2016, **1857**(3):214-223.

135. Virzintiene E, Trane M, Hagerhall C: **Revised transmembrane orientation of the NADH:quinone oxidoreductase subunit NuoA**. *FEBS Lett* 2011, **585**(20):3277-3283.

136. Lee PT, Hsu AY, Ha HT, Clarke CF: **A C-methyltransferase involved in both ubiquinone and menaquinone biosynthesis: isolation and identification of the Escherichia coli ubiE gene**. *J Bacteriol* 1997, **179**(5):1748-1754.

137. Clark WB, Wheeler TT, Cisar JO: **Specific inhibition of adsorption of Actinomyces viscosus T14V to saliva-treated hydroxyapatite by antibody against type 1 fimbriae**. *Infect Immun* 1984, **43**(2):497-501.

138. Kurosu M, Begari E: **Vitamin K2 in electron transport system: are enzymes involved in vitamin K2 biosynthesis promising drug targets?** *Molecules* 2010, **15**(3):1531-1553.

139. Dhiman RK, Mahapatra S, Slayden RA, Boyne ME, Lenaerts A, Hinshaw JC, Angala SK, Chatterjee D, Biswas K, Narayanasamy P *et al*: **Menaquinone synthesis is critical for maintaining mycobacterial viability during exponential growth and recovery from non-replicating persistence**. *Mol Microbiol* 2009, **72**(1):85-97.

140. Koike-Takeshita A, Koyama T, Ogura K: **Identification of a novel gene cluster participating in menaquinone (vitamin K2) biosynthesis. Cloning and sequence determination of the 2-heptaprenyl-1,4-naphthoquinone methyltransferase gene of Bacillus stearothermophilus**. *J Biol Chem* 1997, **272**(19):12380-12383.

141. Franza T, Delavenne E, Derre-Bobillot A, Juillard V, Boulay M, Demey E, Vinh J, Lamberet G, Gaudu P: **A partial metabolic pathway enables group b streptococcus to overcome quinone deficiency in a host bacterial community**. *Mol Microbiol* 2016, **102**(1):81-91.

142. Collins MD, Jones D: **Distribution of isoprenoid quinone structural types in bacteria and their taxonomic implication**. *Microbiol Rev* 1981, **45**(2):316-354.

143. Kamitani S, Akiyama Y, Ito K: **Identification and characterization of an Escherichia coli gene required for the formation of correctly folded alkaline phosphatase, a periplasmic enzyme**. *EMBO J* 1992, **11**(1):57-62.

144. Li W, Schulman S, Dutton RJ, Boyd D, Beckwith J, Rapoport TA: **Structure of a bacterial homologue of vitamin K epoxide reductase**. *Nature* 2010, **463**(7280):507-512.

145. Nakamaru-Ogiso E, Narayanan M, Sakyiama JA: **Roles of semiquinone species in proton pumping mechanism by complex I**. *J Bioenerg Biomembr* 2014, **46**(4):269-277.

146. Gong X, Xie T, Yu L, Hesterberg M, Scheide D, Friedrich T, Yu CA: **The ubiquinone-binding site in NADH:ubiquinone oxidoreductase from Escherichia coli**. *J Biol Chem* 2003, **278**(28):25731-25737.

147. Bott M, Niebisch A: **The respiratory chain of Corynebacterium glutamicum**. *J Biotechnol* 2003, **104**(1-3):129-153.

148. Bader MW, Hiniker A, Regeimbal J, Goldstone D, Haebel PW, Riemer J, Metcalf P, Bardwell JC: **Turning a disulfide isomerase into an oxidase: DsbC mutants that imitate DsbA**. *EMBO J* 2001, **20**(7):1555-1562.

149. Schmitt M: **Iron Acquisition and Iron-Dependent Gene Expression in *Corynebacterium diphtheriae***. In: *Corynebacterium diphtheriae and Related Toxigenic Species.* Edited by Burkovski A; 2014.

150. Alberts B JA, Lewis J, et al.: **Molecular Biology of the Cell**. New York: Garland Science; 2002.

151. Ott L BA: **Toxigenic Corynebacteria: Adhesion, Invasion and Host Response**. In: *Corynebacterium diphtheriae and Related Toxigenic Species.* Edited by Burkovski A; 2014.

152. Uribe-Querol E, Rosales C: **Control of Phagocytosis by Microbial Pathogens**. *Front Immunol* 2017, **8**:1368.

153. Yoon BY, Kim JS, Um SH, Jo I, Yoo JW, Lee K, Kim YH, Ha NC: **Periplasmic disulfide isomerase DsbC is involved in the reduction of copper binding**

protein CueP from Salmonella enterica serovar Typhimurium. *Biochem Biophys Res Commun* 2014, **446**(4):971-976.

154. Totsika M, Heras B, Wurpel DJ, Schembri MA: **Characterization of two homologous disulfide bond systems involved in virulence factor biogenesis in uropathogenic Escherichia coli CFT073**. *J Bacteriol* 2009, **191**(12):3901-3908.

155. Heras B, Totsika M, Jarrott R, Shouldice SR, Guncar G, Achard ME, Wells TJ, Argente MP, McEwan AG, Schembri MA: **Structural and functional characterization of three DsbA paralogues from Salmonella enterica serovar typhimurium**. *J Biol Chem* 2010, **285**(24):18423-18432.

156. Lafaye C, Iwema T, Carpentier P, Jullian-Binard C, Kroll JS, Collet JF, Serre L: **Biochemical and structural study of the homologues of the thiol-disulfide oxidoreductase DsbA in Neisseria meningitidis**. *J Mol Biol* 2009, **392**(4):952-966.

157. Um SH, Kim JS, Song S, Kim NA, Jeong SH, Ha NC: **Crystal Structure of DsbA from Corynebacterium diphtheriae and Its Functional Implications for CueP in Gram-Positive Bacteria**. *Mol Cells* 2015, **38**(8):715-722.

158. Rietsch A, Belin D, Martin N, Beckwith J: **An in vivo pathway for disulfide bond isomerization in Escherichia coli**. *Proc Natl Acad Sci U S A* 1996, **93**(23):13048-13053.

159. Kang HJ, Paterson NG, Gaspar AH, Ton-That H, Baker EN: **The Corynebacterium diphtheriae shaft pilin SpaA is built of tandem Ig-like**

modules with stabilizing isopeptide and disulfide bonds. *Proc Natl Acad Sci U S A* 2009, **106**(40):16967-16971.

160. Patek M, Nesvera J: **Sigma factors and promoters in Corynebacterium glutamicum**. *J Biotechnol* 2011, **154**(2-3):101-113.

161. Albersmeier A, Pfeifer-Sancar K, Ruckert C, Kalinowski J: **Genome-wide determination of transcription start sites reveals new insights into promoter structures in the actinomycete Corynebacterium glutamicum**. *J Biotechnol* 2017, **257**:99-109.

162. Haenni M, Moreillon P, Lazarevic V: **Promoter and transcription analysis of penicillin-binding protein genes in Streptococcus gordonii**. *Antimicrob Agents Chemother* 2007, **51**(8):2774-2783.

163. Helmann JD: **Compilation and analysis of Bacillus subtilis sigma A-dependent promoter sequences: evidence for extended contact between RNA polymerase and upstream promoter DNA**. *Nucleic Acids Res* 1995, **23**(13):2351-2360.

164. Raman S, Song T, Puyang X, Bardarov S, Jacobs WR, Jr., Husson RN: **The alternative sigma factor SigH regulates major components of oxidative and heat stress responses in Mycobacterium tuberculosis**. *J Bacteriol* 2001, **183**(20):6119-6125.

165. Shouldice SR, Heras B, Walden PM, Totsika M, Schembri MA, Martin JL: **Structure and function of DsbA, a key bacterial oxidative folding catalyst**. *Antioxid Redox Signal*, **14**(9):1729-1760.

166. Holm L, Rosenstrom P: **Dali server: conservation mapping in 3D**. *Nucleic Acids Res* 2010, **38**(Web Server issue):W545-549.

167. Crow A, Lewin A, Hecht O, Carlsson Moller M, Moore GR, Hederstedt L, Le Brun NE: **Crystal structure and biophysical properties of Bacillus subtilis BdbD. An oxidizing thiol:disulfide oxidoreductase containing a novel metal site**. *J Biol Chem* 2009, **284**(35):23719-23733.

168. Shepherd M, Heras B, Achard ME, King GJ, Argente MP, Kurth F, Taylor SL, Howard MJ, King NP, Schembri MA *et al*: **Structural and functional characterization of ScsC, a periplasmic thioredoxin-like protein from Salmonella enterica serovar Typhimurium**. *Antioxid Redox Signal*, **19**(13):1494-1506.

169. Boyd J, Oza MN, Murphy JR: **Molecular cloning and DNA sequence analysis of a diphtheria tox iron-dependent regulatory element (dtxR) from Corynebacterium diphtheriae**. *Proc Natl Acad Sci U S A* 1990, **87**(15):5968-5972.

170. Kunkle CA, Schmitt MP: **Analysis of the Corynebacterium diphtheriae DtxR regulon: identification of a putative siderophore synthesis and transport system that is similar to the Yersinia high-pathogenicity island-encoded yersiniabactin synthesis and uptake system**. *J Bacteriol* 2003, **185**(23):6826-6840.

171. Qian Y, Lee JH, Holmes RK: **Identification of a DtxR-regulated operon that is essential for siderophore-dependent iron uptake in Corynebacterium diphtheriae**. *J Bacteriol* 2002, **184**(17):4846-4856.

172. Merchant AT, Spatafora GA: **A role for the DtxR family of metalloregulators in gram-positive pathogenesis**. *Mol Oral Microbiol* 2014, **29**(1):1-10.

173. Gruber TM, Gross CA: **Multiple sigma subunits and the partitioning of bacterial transcription space**. *Annu Rev Microbiol* 2003, **57**:441-466.

174. Balleza E, Alvarez-Buylla ER, Chaos A, Kauffman S, Shmulevich I, Aldana M: **Critical dynamics in genetic regulatory networks: examples from four kingdoms**. *PLoS One* 2008, **3**(6):e2456.

175. Browning DF, Busby SJ: **Local and global regulation of transcription initiation in bacteria**. *Nat Rev Microbiol* 2016, **14**(10):638-650.

176. Brune I, Werner H, Huser AT, Kalinowski J, Puhler A, Tauch A: **The DtxR protein acting as dual transcriptional regulator directs a global regulatory network involved in iron metabolism of Corynebacterium glutamicum**. *BMC Genomics* 2006, **7**:21.

177. Evans SS, Repasky EA, Fisher DT: **Fever and the thermal regulation of immunity: the immune system feels the heat**. *Nat Rev Immunol* 2015, **15**(6):335-349.

178. Elhadad D, McClelland M, Rahav G, Gal-Mor O: **Feverlike Temperature is a Virulence Regulatory Cue Controlling the Motility and Host Cell Entry of Typhoidal Salmonella**. *J Infect Dis* 2015, **212**(1):147-156.

179. Osawa EM, L.H.: **Studies relating to the serum resistance of certain Gram-negative bacteria**. *J Exp Med* 1964(119):41-51.

180. Ladenstein R, Ren B: **Reconsideration of an early dogma, saying "there is no evidence for disulfide bonds in proteins from archaea"**. *Extremophiles* 2008, **12**(1):29-38.

181. Beeby M, O'Connor BD, Ryttersgaard C, Boutz DR, Perry LJ, Yeates TO: **The genomics of disulfide bonding and protein stabilization in thermophiles**. *PLoS Biol* 2005, **3**(9):e309.

182. Reppas NB, Wade JT, Church GM, Struhl K: **The transition between transcriptional initiation and elongation in E. coli is highly variable and often rate limiting**. *Mol Cell* 2006, **24**(5):747-757.

183. Anfinsen CB, Haber E, Sela M, White FH, Jr.: **The kinetics of formation of native ribonuclease during oxidation of the reduced polypeptide chain**. *Proc Natl Acad Sci U S A* 1961, **47**:1309-1314.

184. Typas A, Banzhaf M, Gross CA, Vollmer W: **From the regulation of peptidoglycan synthesis to bacterial growth and morphology**. *Nat Rev Microbiol* 2012, **10**(2):123-136.

185. Egan AJ, Biboy J, van't Veer I, Breukink E, Vollmer W: **Activities and regulation of peptidoglycan synthases**. *Philos Trans R Soc Lond B Biol Sci* 2015, **370**(1679).

186. Sauvage E, Kerff F, Terrak M, Ayala JA, Charlier P: **The penicillin-binding proteins: structure and role in peptidoglycan biosynthesis**. *FEMS Microbiol Rev* 2008, **32**(2):234-258.

187. Valbuena N, Letek M, Ordonez E, Ayala J, Daniel RA, Gil JA, Mateos LM: **Characterization of HMW-PBPs from the rod-shaped actinomycete**

Corynebacterium glutamicum: peptidoglycan synthesis in cells lacking actin-like cytoskeletal structures. *Mol Microbiol* 2007, **66**(3):643-657.

188. Daniel RA, Errington J: **Control of cell morphogenesis in bacteria: two distinct ways to make a rod-shaped cell**. *Cell* 2003, **113**(6):767-776.

189. Tiyanont K, Doan T, Lazarus MB, Fang X, Rudner DZ, Walker S: **Imaging peptidoglycan biosynthesis in Bacillus subtilis with fluorescent antibiotics**. *Proc Natl Acad Sci U S A* 2006, **103**(29):11033-11038.

190. Botta GA, Park JT: **Evidence for involvement of penicillin-binding protein 3 in murein synthesis during septation but not during cell elongation**. *J Bacteriol* 1981, **145**(1):333-340.

191. Carballido-Lopez R, Formstone A: **Shape determination in Bacillus subtilis**. *Curr Opin Microbiol* 2007, **10**(6):611-616.

192. Letek M, Fiuza M, Ordonez E, Villadangos AF, Ramos A, Mateos LM, Gil JA: **Cell growth and cell division in the rod-shaped actinomycete Corynebacterium glutamicum**. *Antonie Van Leeuwenhoek* 2008, **94**(1):99-109.

193. Petersen TN, Brunak S, von Heijne G, Nielsen H: **SignalP 4.0: discriminating signal peptides from transmembrane regions**. *Nat Methods* 2011, **8**(10):785-786.

194. Yang J, He BJ, Jang R, Zhang Y, Shen HB: **Accurate disulfide-bonding network predictions improve ab initio structure prediction of cysteine-rich proteins**. *Bioinformatics* 2015, **31**(23):3773-3781.

195. Valbuena N, Letek M, Ramos A, Ayala J, Nakunst D, Kalinowski J, Mateos LM, Gil JA: **Morphological changes and proteome response of Corynebacterium glutamicum to a partial depletion of FtsI**. *Microbiology* 2006, **152**(Pt 8):2491-2503.

196. Lutkenhaus J, Pichoff S, Du S: **Bacterial cytokinesis: From Z ring to divisome**. *Cytoskeleton (Hoboken)* 2012, **69**(10):778-790.

197. Grainge I: **FtsK--a bacterial cell division checkpoint?** *Mol Microbiol* 2010, **78**(5):1055-1057.

198. Geissler B, Margolin W: **Evidence for functional overlap among multiple bacterial cell division proteins: compensating for the loss of FtsK**. *Mol Microbiol* 2005, **58**(2):596-612.

199. Dorazi R, Dewar SJ: **Membrane topology of the N-terminus of the Escherichia coli FtsK division protein**. *FEBS Lett* 2000, **478**(1-2):13-18.

200. Sieger B, Bramkamp M: **Interaction sites of DivIVA and RodA from Corynebacterium glutamicum**. *Front Microbiol* 2014, **5**:738.

201. Sieger B, Schubert K, Donovan C, Bramkamp M: **The lipid II flippase RodA determines morphology and growth in Corynebacterium glutamicum**. *Mol Microbiol* 2013, **90**(5):966-982.

202. Goffin C, Ghuysen JM: **Multimodular penicillin-binding proteins: an enigmatic family of orthologs and paralogs**. *Microbiol Mol Biol Rev* 1998, **62**(4):1079-1093.

203. Scheffers DJ, Jones LJ, Errington J: **Several distinct localization patterns for penicillin-binding proteins in Bacillus subtilis**. *Mol Microbiol* 2004, **51**(3):749-764.

204. Mottl H, Nieland P, de Kort G, Wierenga JJ, Keck W: **Deletion of an additional domain located between SXXK and SXN active-site fingerprints in penicillin-binding protein 4 from Escherichia coli**. *J Bacteriol* 1992, **174**(10):3261-3269.

205. Parsell DA, Sauer RT: **The structural stability of a protein is an important determinant of its proteolytic susceptibility in Escherichia coli**. *J Biol Chem* 1989, **264**(13):7590-7595.

206. Park C, Marqusee S: **Pulse proteolysis: a simple method for quantitative determination of protein stability and ligand binding**. *Nat Methods* 2005, **2**(3):207-212.

207. Aad G, Abajyan T, Abbott B, Abdallah J, Abdel Khalek S, Abdinov O, Aben R, Abi B, Abolins M, Abouzeid OS *et al*: **Search for quantum black hole production in high-invariant-mass lepton+jet final states using pp collisions at radicals=8 TeV and the ATLAS detector**. *Phys Rev Lett*, **112**(9):091804.

208. Fedarovich A, Nicholas RA, Davies C: **Unusual conformation of the SxN motif in the crystal structure of penicillin-binding protein A from Mycobacterium tuberculosis**. *J Mol Biol* 2010, **398**(1):54-65.

209. Fedarovich A, Nicholas RA, Davies C: **The role of the beta5-alpha11 loop in the active-site dynamics of acylated penicillin-binding protein A from Mycobacterium tuberculosis**. *J Mol Biol* 2012, **418**(5):316-330.

210. Pensinger DA, Schaenzer AJ, Sauer JD: **Do Shoot the Messenger: PASTA Kinases as Virulence Determinants and Antibiotic Targets**. *Trends Microbiol* 2018, **26**(1):56-69.

211. Gordon E, Mouz N, Duee E, Dideberg O: **The crystal structure of the penicillin-binding protein 2x from Streptococcus pneumoniae and its acyl-enzyme form: implication in drug resistance**. *J Mol Biol* 2000, **299**(2):477-485.

212. Maestro B, Novakova L, Hesek D, Lee M, Leyva E, Mobashery S, Sanz JM, Branny P: **Recognition of peptidoglycan and beta-lactam antibiotics by the extracellular domain of the Ser/Thr protein kinase StkP from Streptococcus pneumoniae**. *FEBS Lett* 2011, **585**(2):357-363.

213. Mir M, Asong J, Li X, Cardot J, Boons GJ, Husson RN: **The extracytoplasmic domain of the Mycobacterium tuberculosis Ser/Thr kinase PknB binds specific muropeptides and is required for PknB localization**. *PLoS Pathog* 2011, **7**(7):e1002182.

214. Morlot C, Bayle L, Jacq M, Fleurie A, Tourcier G, Galisson F, Vernet T, Grangeasse C, Di Guilmi AM: **Interaction of Penicillin-Binding Protein 2x and Ser/Thr protein kinase StkP, two key players in Streptococcus pneumoniae R6 morphogenesis**. *Mol Microbiol* 2013, **90**(1):88-102.

215. Meehan BM, Landeta C, Boyd D, Beckwith J: **The essential cell division protein FtsN contains a critical disulfide bond in a non-essential domain**. *Mol Microbiol* 2017, **103**(3):413-422.

216. Burkovski A: **Cell envelope of corynebacteria: structure and influence on pathogenicity**. *ISRN Microbiol* 2013, **2013**:935736.

217. Bayan N, Houssin C, Chami M, Leblon G: **Mycomembrane and S-layer: two important structures of Corynebacterium glutamicum cell envelope with promising biotechnology applications**. *J Biotechnol* 2003, **104**(1-3):55-67.

218. Chim N, Riley R, The J, Im S, Segelke B, Lekin T, Yu M, Hung LW, Terwilliger T, Whitelegge JP *et al*: **An extracellular disulfide bond forming protein (DsbF) from Mycobacterium tuberculosis: structural, biochemical, and gene expression analysis**. *J Mol Biol* 2010, **396**(5):1211-1226.

219. Goulding CW, Apostol MI, Gleiter S, Parseghian A, Bardwell J, Gennaro M, Eisenberg D: **Gram-positive DsbE proteins function differently from Gram-negative DsbE homologs. A structure to function analysis of DsbE from Mycobacterium tuberculosis**. *J Biol Chem* 2004, **279**(5):3516-3524.

220. Inaba K, Murakami S, Suzuki M, Nakagawa A, Yamashita E, Okada K, Ito K: **Crystal structure of the DsbB-DsbA complex reveals a mechanism of disulfide bond generation**. *Cell* 2006, **127**(4):789-801.

221. Nowicka B, Kruk J: **Occurrence, biosynthesis and function of isoprenoid quinones**. *Biochim Biophys Acta* 2010, **1797**(9):1587-1605.

222. Black PA, Warren RM, Louw GE, van Helden PD, Victor TC, Kana BD: **Energy metabolism and drug efflux in Mycobacterium tuberculosis**. *Antimicrob Agents Chemother* 2014, **58**(5):2491-2503.

223. Erhardt H, Steimle S, Muders V, Pohl T, Walter J, Friedrich T: **Disruption of individual nuo-genes leads to the formation of partially assembled NADH:ubiquinone oxidoreductase (complex I) in Escherichia coli**. *Biochim Biophys Acta* 2012, **1817**(6):863-871.

224. Hamamoto H, Urai M, Ishii K, Yasukawa J, Paudel A, Murai M, Kaji T, Kuranaga T, Hamase K, Katsu T *et al*: **Lysocin E is a new antibiotic that targets menaquinone in the bacterial membrane**. *Nat Chem Biol* 2015, **11**(2):127-133.

225. Ott L, Hacker E, Kunert T, Karrington I, Etschel P, Lang R, Wiesmann V, Wittenberg T, Singh A, Varela C *et al*: **Analysis of Corynebacterium diphtheriae macrophage interaction: Dispensability of corynomycolic acids for inhibition of phagolysosome maturation and identification of a new gene involved in synthesis of the corynomycolic acid layer**. *PLoS One* 2017, **12**(7):e0180105.

226. Young RM, Mood GM: **Effect of Penicillin on Infection of Guinea Pigs with Corynebacterium diphtheriae**. *J Bacteriol* 1945, **50**(2):205-212.

227. Pappenheimer AM, Jr., Uhr JW, Yoneda M: **Delayed hypersensitivity. I. Induction of hypersensitivity to diphtheria toxin in guinea pigs by infection with Corynebacterium diphtheriae**. *J Exp Med* 1957, **105**(1):1-9.

228. Flentie K, Garner AL, Stallings CL: **Mycobacterium tuberculosis Transcription Machinery: Ready To Respond to Host Attacks**. *J Bacteriol* 2016, **198**(9):1360-1373.

229. Toyoda K, Inui M: **Regulons of global transcription factors in Corynebacterium glutamicum**. *Appl Microbiol Biotechnol* 2016, **100**(1):45-60.

230. Peters K, Pipo J, Schweizer I, Hakenbeck R, Denapaite D: **Promoter Identification and Transcription Analysis of Penicillin-Binding Protein Genes in Streptococcus pneumoniae R6**. *Microb Drug Resist* 2016, **22**(6):487-498.

231. Cao M, Wang T, Ye R, Helmann JD: **Antibiotics that inhibit cell wall biosynthesis induce expression of the Bacillus subtilis sigma(W) and sigma(M) regulons**. *Mol Microbiol* 2002, **45**(5):1267-1276.

232. Utaida S, Dunman PM, Macapagal D, Murphy E, Projan SJ, Singh VK, Jayaswal RK, Wilkinson BJ: **Genome-wide transcriptional profiling of the response of Staphylococcus aureus to cell-wall-active antibiotics reveals a cell-wall-stress stimulon**. *Microbiology* 2003, **149**(Pt 10):2719-2732.

233. Chalut C, Remy MH, Masson JM: **Disulfide bridges are not involved in penicillin-binding protein 1b dimerization in Escherichia coli**. *J Bacteriol* 1999, **181**(9):2970-2972.

234. Charpentier X, Chalut C, Remy MH, Masson JM: **Penicillin-binding proteins 1a and 1b form independent dimers in Escherichia coli**. *J Bacteriol* 2002, **184**(13):3749-3752.

VITA

Belkys Cecilia Sánchez Martinez was born in Caracas, Venezuela, the daughter of Belkys Martinez Lopez and Nestor Sánchez Romero. She attended Universidad Central de Venezuela in Caracas, Venezuela and earned a Bachelor of Science with honors with a major in Bioanalysis in 2010. For the next two years she worked as a Clinical Laboratory Scientist at Hospital de Clinicas Caracas and Policlinica Metropolitana in Caracas, Venezuela. In August of 2012 she joined the Graduate School of Basic Medical Sciences at New York Medical College in Valhalla, New York where she obtained a Master of Science degree in Microbiology and Immunology in 2014. In August 2014, she joined the doctoral program in Microbiology and Infectious Diseases at The University of Texas MD Anderson Cancer Center UTHealth Graduate School of Biomedical Sciences.